Synthesis of Muramyl Dipeptide Analogues as Immunomodulatory Agents

A thesis submitted in partial fulfillment of the requirements for the degree of Master of Science

Department of Chemistry

Lakehead University

Thunder Bay, Ontario

Nouf Muhammad Almzene

July 2018

ABSTRACT

Peptidoglycan occurs naturally in cell wall structures of almost all types of bacteria. Muramyl dipeptide (MDP) is a fragment of peptidoglycan, which consists of *N*-acetylmuramic acid that is attached to a dipeptide of L-alanine and D-iso-glutamine. Peptidoglycan is a potent immunostimulant and MDP has been identified as the minimal structure required of peptidoglycan for activating the innate immune system. MDP engages the nucleotide-binding oligomerization domain-containing protein 2 (NOD2) receptor and activates the receptor. Importantly, MDP shows a promising vaccine adjuvant property. However, high toxicity, hydrophilicity, rapid elimination from the biological system, and other drawbacks associated with MDP prevent it from being used in clinics. In this study, novel MDP analogues have been designed and synthesized in order to improve the molecule's biological activity. The modification in these analogues was applied within the dipeptide component, that is, using an artificial aromatic amino acid residue in place of the D-iso-glutamine residue in natural MDP. *N*-acetylation of 4-amino-3-nitrobenzoic acid was the starting point of the synthesis pathway. Next, the nitro group was reduced and coupled with L-alanine to form the main building block **14**. The incorporation of different lengths of lipid chains at the C-terminal of the dipeptide mimic **14** resulted in lipophilic dipeptide analogues **11, 12** and **13**. The dipeptide mimics **11 - 14** were then coupled with an *N*-acetylmuramic acid derivative **36** to provide protected MDP analogues **37 - 40**. The first set of MDP analogues **4 - 6** were obtained by applying **37, 38**, and **39** under the global deprotection reaction using Pd/C as the catalyst in a hydrogen atmosphere to remove both benzyl and benzylidene groups. The second set of analogues **7 - 9** were formed by treating **37 - 39** with trifluoroacetic acid to

remove only the benzylidene group. Attempts at forming hydrophilic mimics **2** and **3** were not entirely successful due to a technical obstacle during the last step of the deprotection reactions. Ultimately, biological evaluation will determine the potential of these analogues to act as ligands for NOD2 and their immune-modulatory/stimulatory property.

ACKNOWLEDGMENTS

In the name of Allah, the Most Gracious and the Most Merciful, Alhamdulillah, all praises are given to Allah for the strengths and His blessing in completing this thesis.

I must first express my gratitude to my supervisor and mentor, Professor Zi-Hua Justin Jiang. Professor Jiang always welcomed all questions regarding my research and writing. This thesis would never have been completed without his support and encouragement.

I would also like to acknowledge Professor Marina Ulanova of the Faculty of Medicine and Professor Stephen Kinrade of the Faculty of Science and Environmental Studies at Lakehead University. I am indebted for their valuable comments on this thesis.

My thanks are also extended to my co-worker, Dr. Farooq-Ahmad Khan, who guided me in my lab work and provided me with *N*-acetylmuramic acid. Special appreciation goes to Debbie Puumala of the Department of Chemistry and Michael Sorokopud of the Instrumentation Laboratory for their assistance with NMR spectroscopy and polarimetry. Furthermore, I would like to thank Kristina Jurcic from University of Western Ontario for the MS analysis.

Financial support from the Natural Sciences and Engineering Research Council of Canada (NSERC) and Lakehead University are gratefully acknowledged. I also would like to acknowledge the Ministry of Education in Saudi Arabia for giving me the opportunity to complete my MSc degree and for their financial support. My thanks are also extended to the Saudi Arabian Cultural Bureau in Canada for helping me deal with various obstacles during my academic years.

Finally, I must express profound gratitude to my parents who have always believed in me. Moreover, I cannot forget to thank my brothers, Abdullah and Yousif, and my friends for their patience and for providing me with unfailing support and continuous encouragement throughout my years of study. This research would not have been completed without them.

ABBREVIATIONS

anal	analytical
approx	approximate
Ar	aryl
calcd	calculated
CSF	colony stimulating factor
COSY	correlated spectroscopy
CIAS1	cold induced autoinflammatory syndrome 1
d	doublet
DABA	3,4-di-aminobenzoic acid
DCC	N,N'-dicyclohexylcarbodiimide
DCM	dichloromethane
dd	double doublet
DEA	diethanolamine
DIPEA	diisopropylethylamine
DMF	*N*,*N*-dimethylformamide
Et_3N	triethylamine
EtOAc	ethyl acetate

HBTU	*O*-(benzotriazol-1-yl)-*N,N,N′,N′*-tetramethyluronium hexafluorophosphate
HEK293	human embryonic kidney
HOAc	acetic acid
iE-DAP	d-glutamyl-*meso*-DAP
IL-	interleukin
IFN-α	interferon
IKK	IkappaB kinase complex
IKKβ	IKKbeta of IKK complex
IKB	*IkB* kinase regulatory protein that inhibits NF-kappa-B
J	coupling constant
MAPK	mitogen-activated protein kinase
MB	murabutide
MDP	muramyldipeptide
MTS	(3-(4,5-dimethylthiazol-2-yl)-5-(3-carboxymethoxyphenyl)-2-(4-sulfophenyl)-2*H*-tetrazolium
MeOH	methanol

MHz	megahertz
MS	mass spectroscopy
MTP-PE	Muramyl tripeptide phosphatidylethanolamine
NALP3	NACHT, LRR and PYD domains-containing protein 3 also known as cryopyrin
NBS	N-bromosuccinimide
NHS	N-hydroxysuccinimide
NMR	nuclear magnetic resonance
NF-κB	nuclear factor κB
NLR	nucleotide-oligomerization-domain-like receptor
NLRP3	(NOD)-like receptor protein 3
NOD	nucleotide oligomerization domain
PAMP	pathogen-associated molecular pattern
PBMC	peripheral blood mononuclear cells
PGN	peptidoglycan
PMA	phorbol 12-myristate 13-acetate
PRR	pattern recognition receptor
RICK	receptor-interacting serine–threonine kinase

RIG	retinoic acid inducible gene
rt	room temperature
s	singlet
SAR	structure–activity relationship
SEAP	secreted embryonic alkaline phosphatase
t	triplet
TLC	thin layer chromatography
TBTU	2-(1*H*-benzotriazol-1-yl)-1,1,3,3-tetramethyluronium tetrafluoroborate
THF	tetrahydrofuran
TFA	trifluoroacetic acid
TLR	toll-like receptor
TNF-α	tumor necrosis factor α
Troc	2,2,2-trichloroethoxycarbonyl

Table of Contents

1 INTRODUCTION

1.1 Biological background

1.1.1 The immune system

The immune system, which comprises special cells, tissues, proteins, and organs, protects the body against disease-causing microorganisms. The system has two separate arms that collaborate with each other to protect the host. The immune system can either be innate or adaptive. An innate immune system is a non-specific defense mechanism which comes into play as a first line of defense in the body. Unlike innate immunity, adaptive immunity is specific to the antigen and, thus, it is more complex[1]. Moreover, the immune system follows a sequence of steps known as the immune response towards invading microorganisms and foreign substances that attack the body and cause disorders. The system begins its response by processing and recognizing an antigen. It then proceeds to generate an army of immune cells specifically designed to invade the antigen. An adaptive system is also responsible for generating a future response that is more efficacious with respect to the same antigen[2].

1.1.2 The innate immune system

The innate immune system acts as the first line of defense against invading pathogens. The mechanisms involved in this system include physical blocks such as the skin, chemicals within the blood, and immune cells that invade and destroy any foreign microorganisms in the body. The cells in an innate immune system include neutrophils,

macrophages, eosinophils, basophils, natural killer cells, and dendritic cells[3,4]. The innate immunity is responsible for detecting and responding to microbial invasion. It does that by using specific pattern recognition receptors (PRRs) which are activated by pathogen associated molecular patterns (PAMPs).

1.1.3 Recognition receptors of innate immunity

The chemical characteristics of a particular antigen are responsible for activating the response of an innate immune system. Specifically, the innate immune system uses a group of (PRRs) to identify pathogenic products by recognizing unique (PAMPs). PAMPs are preserved structures that are characterized by pathogenic structures. Bacterial products are examples of the common PAMPs such as peptidoglycan, lipoteichoic acid, lipopolysaccharide (LPS), as well as viral RNA[2,5]. Many PRRs of the innate immune system have been identified. Toll-like receptors (TLRs) are the oldest PRRs that have been identified and studied for decades[6]. Recently, PRRs have been classified into five families based on distinct genetic and functional differences, including: TLRs; nucleotide-binding and oligomerization domain (NOD)-like receptors (NLRs); retinoic acid inducible gene-I (RIG-I)-like receptors (RLRs); C-type lectins (CTLs); and absent-in-melanoma (AIM)-like receptors (ALRs)[7,8]. TLRs and CTLs are membrane-associated receptors, while the NLRs, RLRs, and ALRs are intracellular sensors[7].

1.1.4 NOD-like receptors as innate immune system receptors

NLRs are a special group of intracellular receptors which play a critical role in the innate immune system through the detection of intracellular PAMPs and 'danger-associated molecular patterns' (DAMPs)[9]. Recently, NLRs, namely a family of proteins, have been identified as a target for muramyl dipeptide (MDP) derivatives. NLRs are readily available in nonimmune cells, dendritic cells, macrophages, and lymphocytes. They contain a unique form of PRRs, which play a crucial role in the detection of dangerous components such as cytosolic microbial products. Receptors of this family share a general tripartite domains structure that consists of the following: a carboxy (C)-terminal leucine rich repeat (LRR) domain, a central NOD domain (also known as NACHT domain) that has ATPase activity; and an amino (N)-terminal domain which controls the protein-protein interaction cassettes such as CARD (caspase activity and recruitment domain) or pyrin (PYD). PYD is a protein domain, specifically a branch of protein motif known as the death fold; it allows a pyrin domain-containing protein to interact with other proteins that contain a pyrin domain. NOD1 and NOD2 are the most common NLRs[10]. NOD1 is composed of C-terminal LRR, a central NOD and N-terminal domain that consists of a single CARD, while NOD2 has a C-terminal LRR, a central NOD and a N-terminal domain that contains two CARDs[11,12] (Figure 1). The two CARD domains referd to the caspase activity and recruitment domain; the NOD domain[11] is the site for nucleotide-binding oligomerization; and the LRR domain is usually where ligand binding takes place.

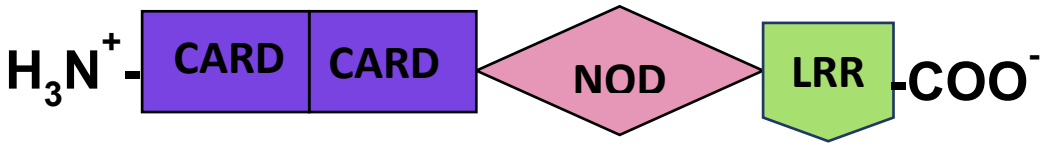

Figure 1: Structural domains in NOD2

1.1.5 NOD2 signaling pathway

The detection of the peptidoglycan fragment MDP activates the cytosolic recognition pattern receptor (NOD2) to produce an inflammatory immune response. The other effects of the activation include the release of cytokines, the generation of antimicrobial peptides such as defensins, the induction of autophagy, and the upregulation of interleukin 1β[13].

MDP is a critical player in the NOD2 signaling pathway since it acts as a ligand for NOD2. MDP enters a cell and binds itself to NOD2. After the activation of NOD2, it is ready to initiate the CARD-CARD interactions between NOD2 and receptor-interacting serine–threonine kinase RICK. Moreover, RICK polyubiquitination links to IKappaB kinase (IKK) complexes, a critical step in permitting polyubiquitylation of the NF-kB (IkB) kinase g (IKKg) inhibitors.

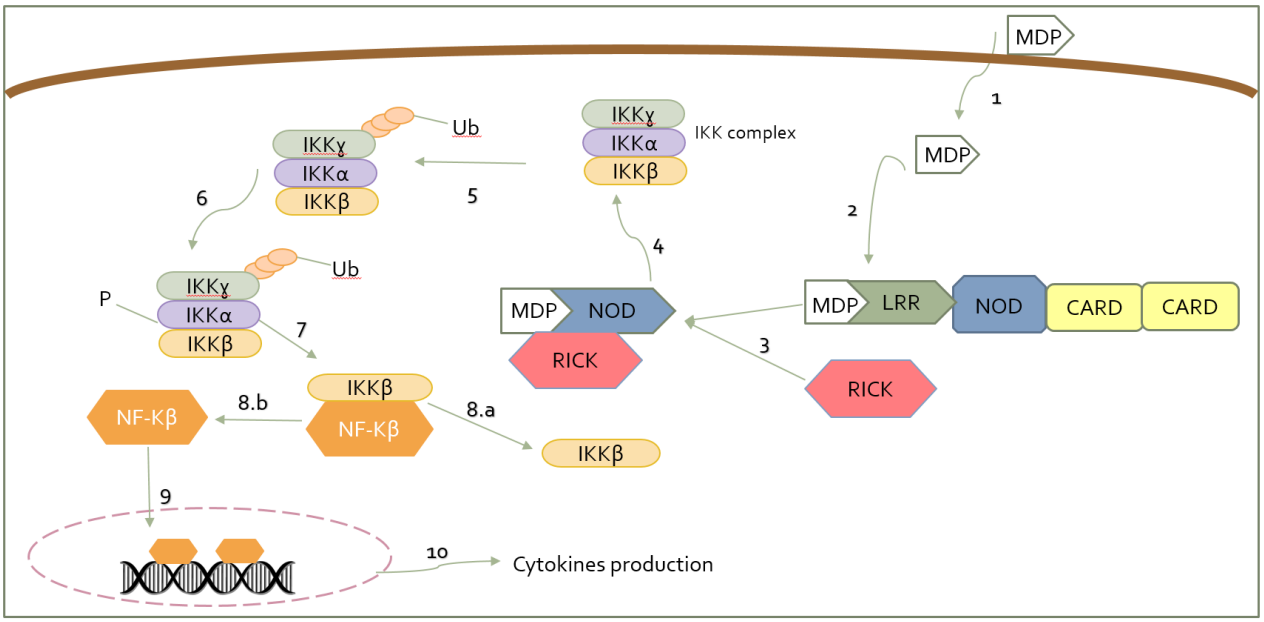

Figure 2: NOD2 signaling pathway. 1. MDP is introduced into this system. 2. Binds to NOD2 receptor via LRR. 3. NOD domain interacts with RICK mediator. 4. RICK joins the activated NOD2 receptor to activate IKK complex. 5. Simultaneous binding of the IKK complex to NOD2 through RICK/RIP2 results in ubiquitination of IKKɣ (NEMO). 6. NEMO degradation allows the IKKα and IKKβ subunits to phosphorylate IkBα. 7. This phosphorylation event leads to the dissociation of IκB from NF-κβ. 8a. IκB is degraded by the proteasome. 8.b the active form of NF-kβ is free. 9. NF-κβ translocases into the nucleus. 10. NF-kβ stimulate the production of pro-inflammatory cytokines.

The polyubiquitylation of the inhibitors causes a phosphorylation event of IKKβ, which in turn leads to the phosphorylation of IkB. The phosphorylation processes cause IkB to dissociate from NF-kB. NF-kB then translocates towards the nucleus. The translocation enhances the transcription of several anti-inflammatory and pro-inflammatory cytokines alongside defensins[12]. Some important cytokines include IL-10, IL-8, IL-1β, and TNF-α. Figure 2 is a schematic of the NOD2 signaling pathway.

1.2 Muramyl dipeptide

1.2.1 MDP as a trigger of the innate immune system

MDP is the smallest bioactive peptidoglycan motif (Figure 3) that occurs in all bacteria. MDP was discovered in 1974. Scientists believed that it was the minimal structure required for biological effects, including activity in Freund's complete adjuvant (FCA), one of the most potent and widely used adjuvants in experimental animal models to date[14]. MDP can be used for improving the adjuvant activities in vaccines. MDP consists of N-acetylmuramic acid connected to the N-terminal of an L-alanine D-isoglutamine dipeptide (Figure 3). The immune system recognizes MDP as a microorganism-associated molecular component that stimulates the NALP3 (NACHT, LRR and PYD domains-containing protein 3) inflammasome, which activates the production of cytokines, especially IL-1β and IL-1α[5].

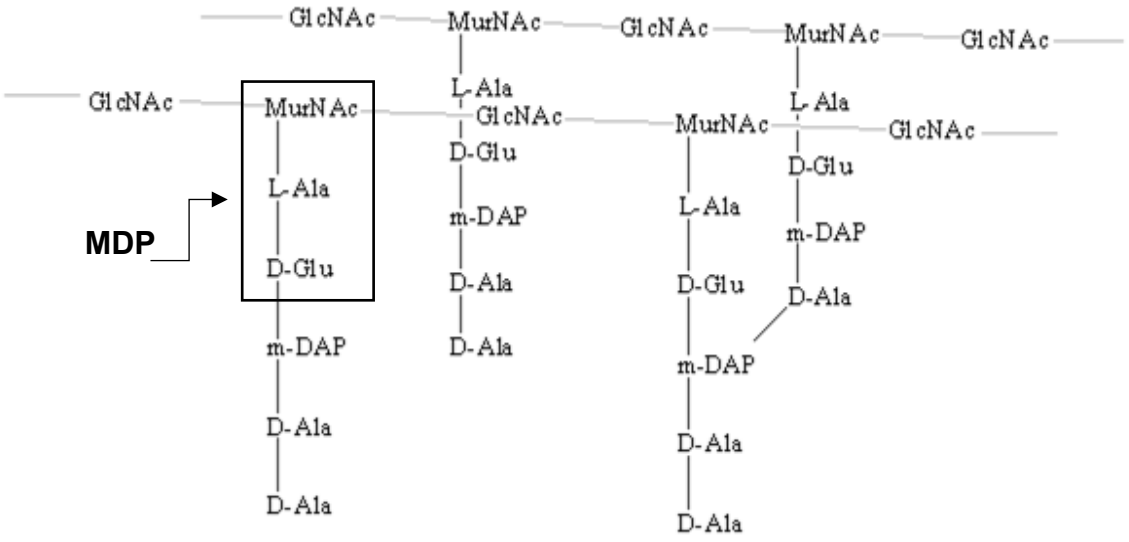

Figure 3: Structure of the peptidoglycan layer

Bacterial cell wall MDP and glucosaminyl-MDP (GMDP, Figure 4) are responsible for the activation of innate immunity. YB1 (Y box binding protein) and NOD2 are the two principal receptor targets in an innate immune system[15]. NOD2 targets are responsible for recognizing lignds such as MDP and all its derivatives. NOD2 plays a critical role in both innate and adaptive immunities by regulating chemokines, cytokines, and producing antimicrobial peptides[14].

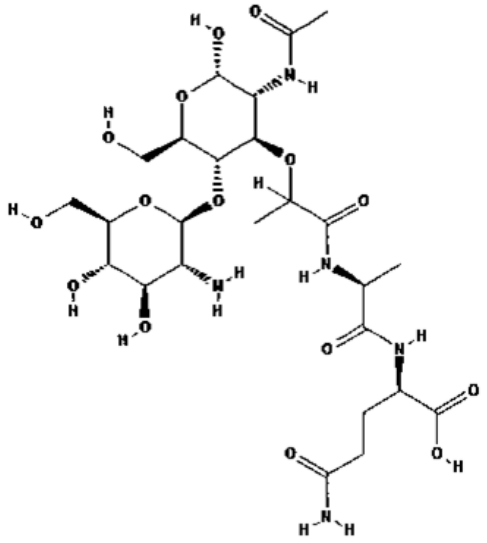

Figure 4: Glucosaminyl-MDP (GMDP)[16]

1.2.2 Structure-activity relationship of MDP

Girardin et al.[17] described MDP and its analogues as NOD2/CARD15 ligands. The recognition process of NOD2/CARD15 and its ligands is specific to the L-D isomer of the alanine-iso-glutamine dipeptide moiety, while analogues with L-L or D-D

configuration are not recognized. Researchers have linked MDP's potent adjuvant activity to CIAS1/NALP3/cryopyrin inflammasome activation[15].

However, until 2012, there was not enough detailed information about MDP-NOD2 interactions. Since then, some researchers reported that the first amino acid of MDP (L-alanine) is the most important component in the immunomodulatory activity of this compound[17]. Other scientists have indicated that the interaction between NOD2 and MDP required an intact MurNAc sugar group substituted in a peptide chain of MDP[18]. In fact, many studies have been done to further understanding the interaction between MDP and NOD2[19]. For instance, Mo et al. reported in 2012 that NOD2 is activated by MDP and ATP[20]. First, NOD2 binds and hydrolyzes ATP. Next, it binds itself directly to MDP and interacts with known NOD2-interacting proteins. As a result of this interaction, macrophages and other immune cells produce cytokines such as TNF-α, IL-1, IL-6, IL-8, along with secretion of nitric oxide (NO)[21]. These molecules are quite important not only in alerting the immune cells, but also in encouraging them to fight the rapidly multiplying bacteria.

1.2.3 Previous MDP analogues and their biological properties

There are many concepts that scientists focused on while designing and synthesizing MDP analogues. Solubility, lipophilicity, permeability and biological activity are the properties that are given most attention to when MDP analogues are examined. Reaching the balance between water solubility and lipophilicity helps to resolve issues

of rapid elimination and poor membrane penetration, which are the most significant drawbacks of a naturally occurring MDP structure.

Numerous studies have designed and synthesized lipophilic MDP derivatives through conjugating with carriers or modifying MDP structure. Lipophilic derivatives and lipophilic delivery carrier systems have shown an increase in the adjuvant activity compared to MDP[22]. This result indicates that having lipophilic characteristics in MDP analogues improves their pharmacological properties. Important examples of lipophilic MDP derivatives include romurtide and muramyl tripeptide phosphatidylethanolamine (MTP-PE, also known as Mafimuratide, Figure 5). Mafimuratide has similar immunostimulatory effects as the natural MDP[23]. Furthermore, Mafimuratide has entered clinical trials as a component of an influenza vaccine[24]. It has also been approved for the treatment of early stage osteosarcoma in combination with chemotherapy in Europe[23].

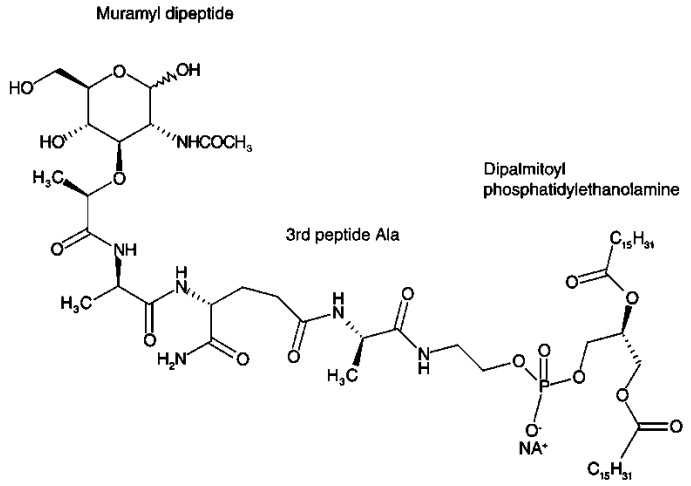

Figure 5. Mafimuratide (MTP-PE)[29]

Another well-known MDP analogue is called MDP-C (Figure 6). This analogue is free from pyrogenicity, allergenicity and toxicity. In addition, MDP-C presents a significant potential for immunotherapeutic prophylactic application in infectious diseases caused by Hepatitis B virus (HBV) and severe acute respiratory syndromes coronavirus (SARS)[25].

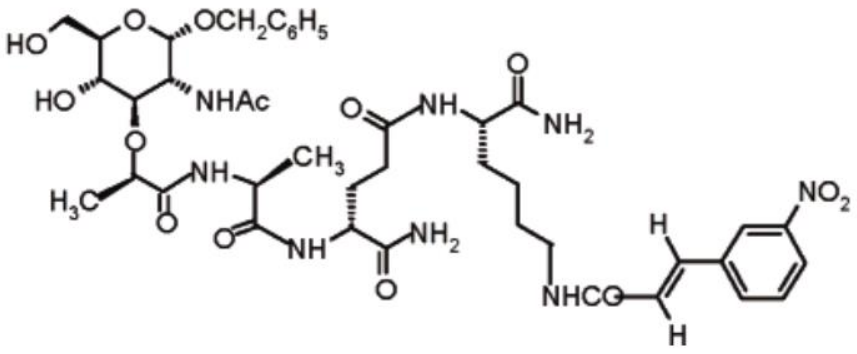

Figure 6. MDP-C structure

Perhaps one of the most notable modifications in all synthesized MDP analogues is the replacement of the MurNAc block. MDP derivatives which lack carbohydrate moiety are called desmuramyl peptides (DMPs)[11,26], for example, FK-565 (Figure 7) DMPs are less hydrophilic than the parent MDP molecule. Even though DMPs do not have carbohydrate residues, they are still recognized by the immune system receptors. Therefore, they are able to activate the innate immune system against microbial infections. They are also known to exhibit significant adjuvant activity and remarkable antitumor potency. Studies on DMPs prove that the sugar *N*-acetylmuramyl moiety (Mur*N*Ac) is not required for NOD2 activation[11,22].

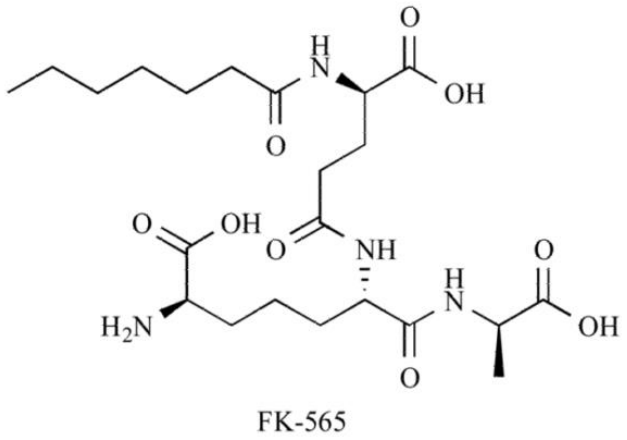

FK-565

Figure 7. Structure of FK-565, an example of DMPs[14]

Murabutide (MB), temurtide, nor-MDP and glucosaminyl-MDP (GMDP) are the hydrophilic analogues which have recently been selected for clinical development by researchers[11]. Nor-MDP does not have a methyl group in the same position as in MDP.

This modification helps to reduce the chirality effects in the lactic acid moiety. As a result, nor-MDP exhibits comparable stimulating activity and less toxicity. MB is also known as *N*-acetylmuramyl-L-alanyl-D-glutamine-n-butyl ester (Figure 8). Very simple modification is applied on MDP structure to form MB by having a butyl ester group in the dipeptide moiety, which is an apyroginic derivative of MDP[27]. MB enhances non-specific resistance to bacterial and viral infections[28]. A recent study found that MB is capable of boosting the antiviral and anti-inflammatory effects of IFN-α and it potentiates the antitumor activity of both IFN-α and IL-2 in vitro when it is combined with these cytokines[27]. In addition, MB is capable of inhibiting HIV-1 replication in acutely infected monocyte-derived macrophages (MDM) and dendritic cells[11].

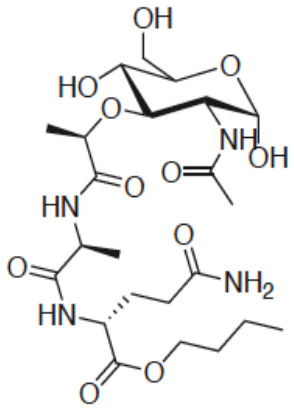

Figure 8. Structure of murabutide (MB)

1.2.4 The lipophilicity of MDP

Since the discovery of MDP, many MDP analogues have been designed and synthesized. One crucial property that affects the pharmacological properties of MDP is its lipophilicity[29]. Lipophilic modification of MDP helps eliminate the drawbacks of MDP such as the poor penetration through cell membrane and the rapid elimination from the biological system[24]. Many lipophilic analogues have been described in several previous research studies[14,15,21,30.] Biological studies showed that lipophilic MDP analogues present more favorable uptake profile than the relatively more polar MDP. Having lipophilic property would allow such MDP analogues to be incorporated into liposome, a favorable drug delivery system for both polar and non-polar small molecule drugs.

Muramyl tripeptide phosphatidylethanolamine (MTP-PE, Figure 5) is a synthetic lipophilic analogue of MDP. The lipophilic chains of the molecule give it a longer elimination half-life than the natural MDP molecule. MTP-PE (also known as Mifamurtide) has been developed for clinical use for the treatment of osteosarcoma, a kind of bone cancer mainly affecting children and young adults. The drug was approved in Europe in March 2009[29].

B30-MDP is another example of lipophilic MDP analogues. The molecule bears a lipophilic acyl chain with 30 carbon atoms at the 6-*O*-posiiton of the glucosaminyl sugar residue (Figure 9). The B30-MDP was evaluated for its adjuvant activity and found effective for the potentiation of the antigenicity of virus antigens[31].

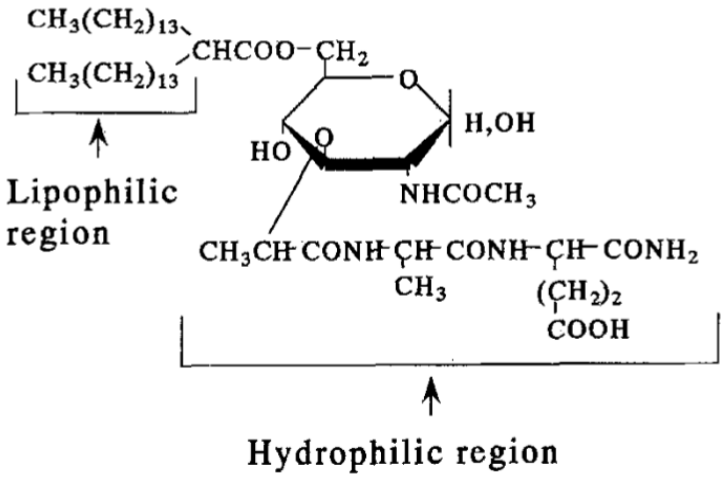

B30-MDP

Figure 9. Structure of B30-MDP[32].

Lipophilic MDP analogues enter the cell through passive diffusion across the cell membrane, which depends on the lipophilic character of these molecules[14,33,34]. Structure-activity relationship (SAR) studies of MDP analogues have shown that the introduction of lipophilic substituents into MDP may increase its adjuvant activity in the potentiation of immune responses to antigens and vaccines[35]. It is believed that hydrolyzing the lipophilic MDP analogues inside the cells is an essential step to produce a hydrophilic metabolite which activates NOD2[14]. These earlier findings clearly indicate that lipophilic modification is a viable strategy in creating novel lipophilic MDP analogues that are potentially effective molecules to activate NOD2 and display adjuvant activity.

1.3. The therapeutic potential of NOD2 signaling pathway

NOD-like receptors (NLRs) including NOD1 and NOD2 play critical roles in pathogen recognition and immune responses. For example, bacterial components such as peptidoglycan are sensed by NOD1 and NOD2 receptors. Therefore, NOD1 and NOD2 have been known to be responsible for the detection of bacteria and the production of pro-inflammatory cytokines by activating signaling pathways such as NF-kβ and Caspase 1. These pro-inflammatory cytokines promote the development of effective defense mechanisms which ultimately lead to the clearance of bacteria in the host[36].

NLRs also play important roles in mediating the immunostimulatory activity of adjuvant molecules, as NOD2 is able to bind to MDP. MDP or any other molecular adjuvants can enhance the adaptive immune responses toward antigens by influencing the innate immunity[37].

Modulating the innate immune response by blocking the binding site of NLRs or any central molecules in the signaling pathway is a developed therapeutic procedure for human autoimmune and chronic inflammatory diseases. One of the successful undertakings of modulation is using kinase inhibitors to block RIPK2, a serine/threonine protein kinase which is a component of signaling complexes in both the innate and adaptive immune pathways. Moreover, compounds capable of blocking NOD2 signaling, such as diterpene-based molecules, have been used as anti-inflammatory compounds[38]. For example, such molecules can be used to treat inflammatory diseases such as Crohn's

disease, asthma, and arthritis[37]. On the other hand, molecules capable of enhancing NOD2 signaling pathway can be useful to fight against bacterial/viral infections.

1.4 Vaccine adjuvant

Adjuvants are vaccine ingredients that facilitate the generation of a stronger response within the immune system in the body. As such, adjuvants enable vaccines to work better. Certain vaccines made from dead germs contain natural adjuvants[39]. Nonetheless, most contemporary vaccines contain only a small portion of germs, i.e., their proteins, instead of the entire bacteria or virus. Therefore, it's critical to include an adjuvant in a vaccine to not only stimulate the adaptive responses of the immune system, but also to activate the innate immune response to prevent unwanted side effects of the vaccine. Adjuvants have been used in both therapeutic and protective vaccines.

It is well recognized that PRRs of innate immunity such as TLRs and NLRs can modulate and control the generation of humoral and cellular immune responses. Therefore, PRR agonists can be strong vaccine adjuvants due to their ability to activate the innate immune responses mediated by these receptors. MDP has been well studied for its adjuvant property which enhances and directs the body's adaptive immune response towards vaccine antigens by triggering and activation of the NOD2 receptor[40].

Monocytes, macrophages and dendritic cells (DCs) are the antigen presenting cells (APCs) and responsible for innate-adaptive cross-function. Activation of NLRs initiates

the cellular defense mechanism which results in cytokine production as well as activation of APCs to modulate the adaptive responses. The stimulation of NLRs upregulates MHC class II on DCs. Specifically, NOD2 upregulates MHC class II $CD4^+$ T-cell response[39]. Two principal forms of lymphocytes (T and B cells) mediate this type of response[41]. Based on the T_H profiles such as T_H1, T_H17, and T_H2, humoral and/or cellular responses can be produced. With respect to humoral response, the generation of IgG2 and IgG1 antibodies is the primary target of the adaptive response in vaccination[41].

Researchers have recommended that the use of MDP as an adjuvant should remain restricted to the manufacture of veterinary vaccines, but not human vaccines. The reason is that MDP has proved to be extremely pyrogenic and unfit for human consumption[41]. The pyrogenic nature of MDP has inspired scientists to come up with less pyrogenic MDP derivatives that have high immunomodulatory potential and adjuvanticity. MDP(D-Glu^2)-OCH_3 and N-glycocyl-MDP (Figure 10) are some of the MDP derivatives with higher immunomodulatory potentials than the parent MDP and show vaccine adjuvant property[42,43].

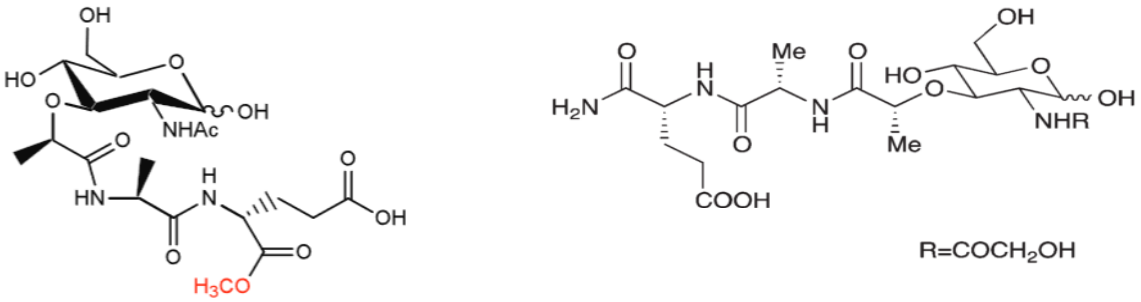

N-glycocyl-MDP

Figure 10. Structure of MDP(D-Glu[2])-OCH_3 and N-glycocyl-MDP[42,43]

1.5 Anticancer treatments by MDP analogues

Several anticancer treatment methods exist, and they are selected by physicians depending on the type of cancer and its stage. They include surgery, radiation therapy, chemotherapy, immunotherapy, targeted therapy, hormone therapy, and stem cell transplantation. Immunotherapy is a form of cancer treatment that boosts the immune system's ability to fight cancer.

The use of MDP to initiate NOD2 signaling is one of the many immunotherapies used to treat cancer[44]. In the last decade, researchers have diligently modified the structure of MDP to create various MDP derivatives to increase their immunodulatory property[14]. Studies have shown that some MDP derivatives are beneficial in treating cancer, as well as other disorders.

For example, murabutide (MB, Figure 8) increases the antiviral and antitumor impacts of cytokines, such as IFN-α and IL-2. Studies have discovered that injecting MB together with IL-2 causes significant tumor inhibition with total tumor regression in more than 70% of injected individuals[45]. Moreover, mifamurtide (Figure 5) is an example of many therapeutic drugs that require the collaboration of NOD2 to cure cancer[46]. The binding of mifamurtide to NOD2 activates white blood cells to fight against viral and bacterial infections[47]. In addition, mifamurtide has been used in combination with chemotherapy to treat osteosarcoma.

1.6 NOD2 therapeutic concerns

The NOD2 protein recognizes bacteria and stimulates the immune system to respond to an infection. When activated by certain substances released by bacteria, NOD2 activates a protein complex known as the nuclear factor-kappa-B (NF-κB). The protein complex is responsible for controlling the activation of many genes. Some of these genes include those that control the immune responses and ones that control the inflammatory responses[48]. NOD2 also plays a critical role in autophagy, a self-degradative process in which a cell eats its components. It is the primary catabolic mechanism that involves cell degradation through the action of lysosomes of unnecessary or unfunctional cellular components[49]. Therefore, the prime concern of stimulating NOD2 receptor is having over activating responses leading to unwanted effects. Over stimulating may lead to inflammatory disease such as arthritis.

2. OBJECTIVES OF THE PRESENT WORK

Although MDP and its derivatives represent potential therapeutic agents, they are still under clinical investigation due to their drawbacks. Some of the downsides are poor penetration of macrophages, pyrogenicity, and inflammatory reaction. In this study, considerable focus was placed on synthesizing novel MDP analogues by modifying the dipeptide moiety.

The MDP analogues are comprised of two building blocks: the carbohydrate moiety and the dipeptide moiety. In this research, a group of novel MDP analogues have been designed by (a) replacing the D-iso-glutamine (D-iso-Gln) with an aromatic amino acid, 3,4-di-aminobenzoic acid (DABA), and (b) attaching a lipophilic chain of different length at the C-terminal of the dipeptide moiety. The objectives of this thesis are to complete the synthesis of a group of such novel MDP analogues for future biological studies.

3 RESULTS AND DISCUSSION

3.1 Design of MDP analogues

As mentioned earlier, MDP is involved in a critical signaling pathway of the innate immune system against microbial infections. Studies show that it displays anticancer activity as well as vaccine adjuvant activity[50,51,52]. However, there are several drawbacks associated with MDP − such as toxicity, hydrophilicity, and rapid elimination from the biological system − which prevent this molecule from being used in the clinic. Previously reported MDP analogues have incorporated modifications to both sugar and dipeptide residues, mainly to increase their lipophilicity and, thus, intracellular delivery. In this research, unique mimics of MDP are proposed in which the dipeptide part is modified. In particular, the D-iso-glutamine (D-iso-Gln) is replaced with an aromatic amino acid, 3,4-di-aminobenzoic acid (DABA), and a lipophilic chain of different length is attached at the C-terminal of the dipeptide moiety. A significant advantage of these novel analogues is that DABA is structurally analogous to D-iso-Gln (Figure 11). Replacing D-iso-Gln is an attractive option for the synthesis of MDP analogues since D-iso-Gln is an expensive amino acid. Additionally, the aromatic ring in DABA enhances the stability of such MDP analogues (**1** and **2**, Figure 12) toward enzymes relative to the natural MDP bearing D-iso-Gln. A substituent group (R) on the 4-amino group of DABA can bring structural variation to these analogues. R could be an alkyl group (proposed structure **1**) or acyl substituent (structure **2**). In mimic **3**, the *N*-acetylmuramic acid moiety exists as the benzyl α-glycoside. According to Yang et al.[25], benzyl glycosides of MDP derivatives show significant immunomodulating activity. Therefore, these benzyl glycosides can

potentially interact with NOD2 and display agonistic or antagonistic activity. Finally, the lipid chains were presented in analogues **4** – **9** to increase the lipophilicity of these molecules (Figure 13).

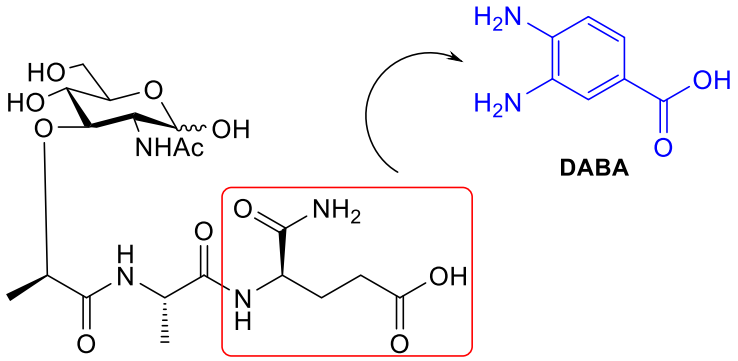

Figure 11. Structure of muramyl dipeptide (MDP).

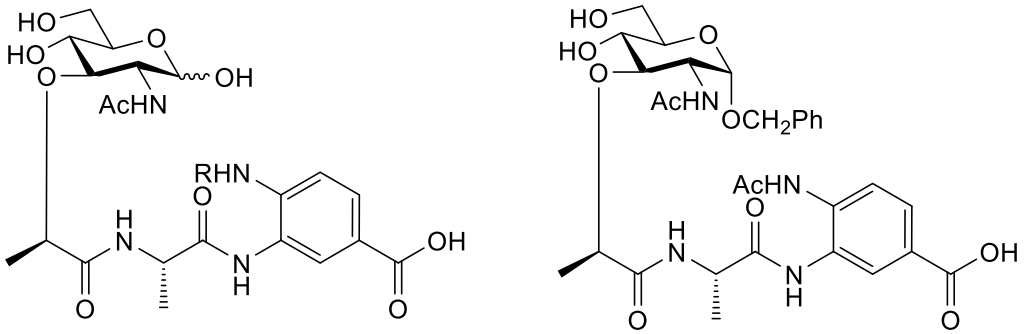

Figure 12. Structures of MDP mimics

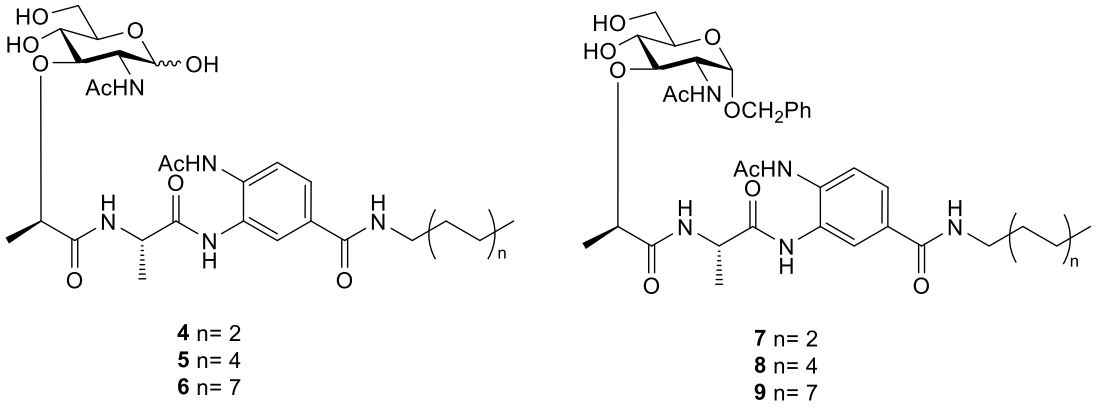

4 n= 2
5 n= 4
6 n= 7

7 n= 2
8 n= 4
9 n= 7

Figure 13. Target lipophilic MDP mimics

3.2. Retrosynthetic analysis for the lipophilic MDP analogues

Based on scheme 1, compounds **4 - 6** can be disconnected to give the sugar building block **10** and the dipeptide building blocks **11 - 13**. The synthesis of compound **10** has been reported in the literature[53,54,55]. The dipeptide building blocks **11 - 13** could be broken down to more simple molecules: alkyl amines and compound **14**. Furthermore, compound **14** can be disconnected to Boc-L-alanine and amino acid derivative **15** which can be prepared from the commercially available 4-amino-3-nitrobenzoic acid **16**.

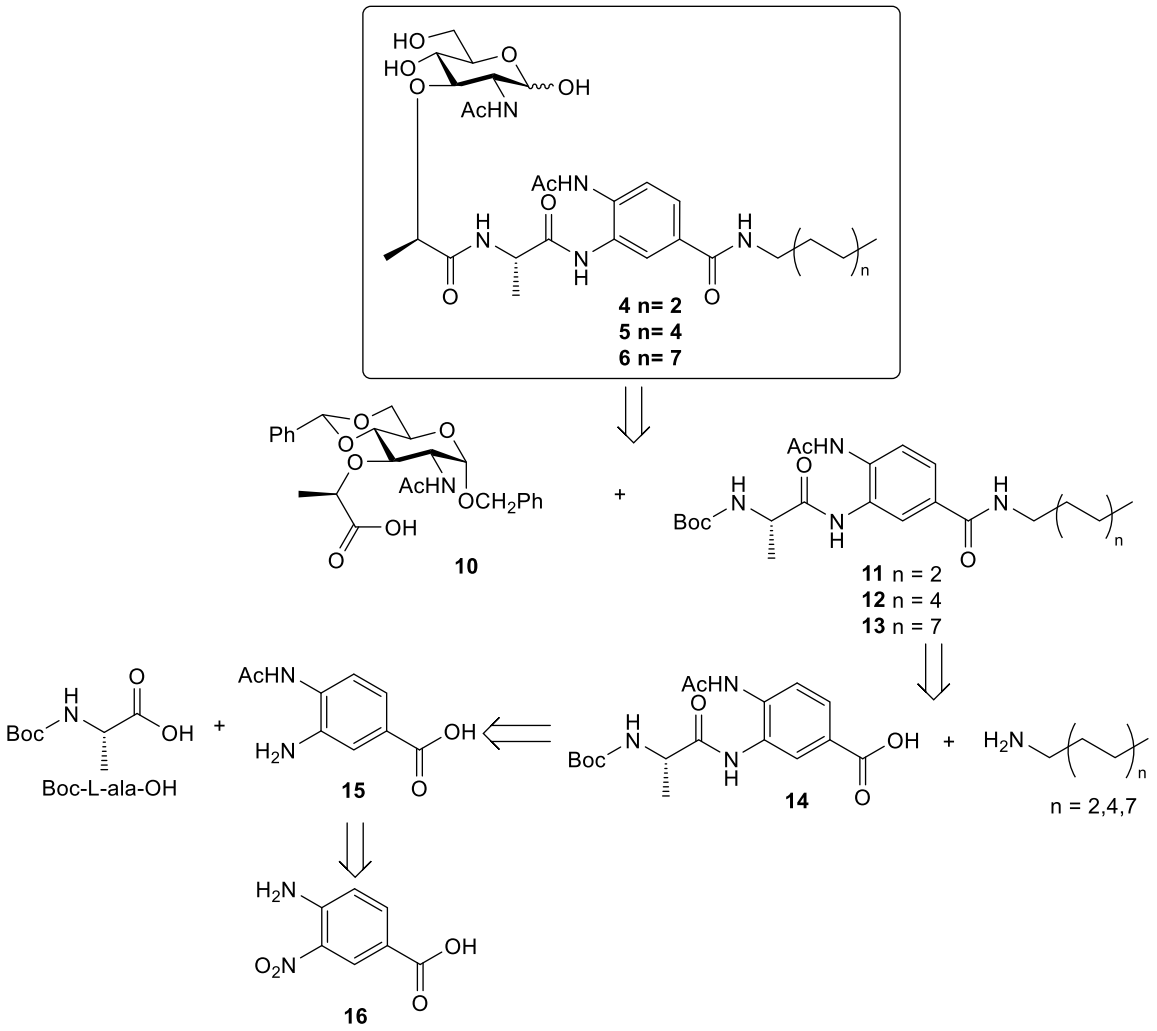

Scheme 1. Retrosynthetic analysis of the lipophilic analogues **4 – 6**.

3.3 Preparation of 4-amino-3-nitrobenzoic acid derivatives

3.3.1 Protecting amino group

3.2.1.1 Boc-group

4-Amino-3-nitrobenzoic acid **16** is the starting material for the preparation of 3,4-diaminobenzoic acid (DABA) building blocks. Forming an intermediate with a temporary protecting group at the 4-amino group of DABA is necessary in order to introduce a different R group at late stage of the synthesis. Therefore, different protecting groups were investigated. The tert-butyloxycarbonyl (Boc) is a general amino protecting group, and therefore **16** was first tried to react with Boc-anhydride in order to make **17** (Scheme 2). Compound **17** was not formed under various sets of reaction conditions, as indicated by the absence of a carbon signal at around δ = 28 ppm in the ^{13}C NMR spectrum of the isolated product. This carbon signal is indicative of the Boc-group. The results of these experiments indicate that the amino group in **16** is very unreactive.

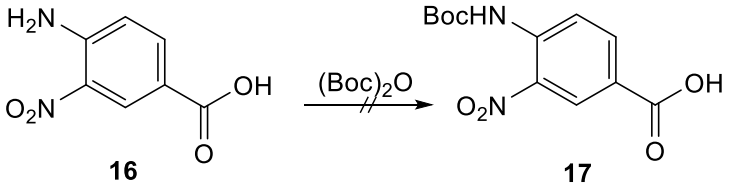

Conditions:
a. MeOH, Sulfuric acid, 60°C
b. THF, DMAP, 60°C
c. DMF, NaH, 0°C
d. THF, DMAP, MeOH, 40°C

Scheme 2. Attempted synthesis of **17**.

3.3.1.2 Troc-group

Another common protecting group for amines is the 2,2,2-trichloroethoxycarbonyl (Troc) group. Treating **16** with 2,2,2-trichloroethoxyl chloroformate (Troc-Cl) and diisopropylethylamine (DIPEA) in different solvents offered the desired product **18** in low yields (Scheme 3 and Table 1). TLC indicated the formation of other side products; structure such as **19** might be formed during the reaction since Troc-Cl can potentially react with a carboxylic acid. The structures of these side products were not established.

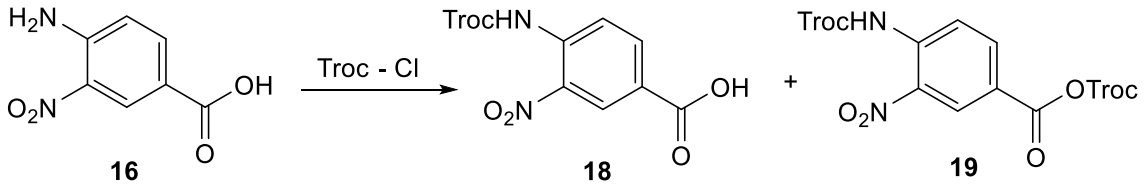

Scheme 3. Protecting the amine group on **16** by Troc-Cl.

Table 1. Conditions and yields for the Troc protection reaction

Solvents/ Reagents	Temperature (°C)	Yield: **18**
Acetone/ DIPEA	rt	10%
EtOAc/ DIPEA	80	28%
Toluene/ DIPEA	120	24%

According to the results of the reaction in Scheme 3, the carboxyl group in **16** should be protected first before protecting the amino group. This strategy would prevent Troc-Cl from attacking the carboxyl group. Thus, compound **16** was treated with phenacyl bromide and triethylamine in dioxane to give **20** in 93% yield. After that, compound **20**

was treated with Troc-Cl in the presence of DIPEA as an activator in toluene at 120 °C to give the desired protected product **21** in 71% yield. Reducing the nitro group in **21** by using Pd/C under H_2 in $CHCl_3$/MeOH (2:1) provided **22**. Compound **22** was structurally not confirmed due to its instability. An attempt was nevertheless made to couple the reaction product with Boc-L-alanine under the coupling condition of HBTU and DIPEA in DMF (Scheme 4), but the anticipated product **23** was not isolated. It is unclear whether **22** failed to form altogether or it was too short-lived to undergo coupling. Due to time constraint, the issues faced with this method were not further investigated. Instead, we switched our focus to preparing *N*-acetylated derivatives (See next section). However, putting a protecting group on the 4-amino group of **16** is still worth further study in order to prepare an advanced intermediate to access structures such as **1** (Figure 12) with a variable R group at that nitrogen atom.

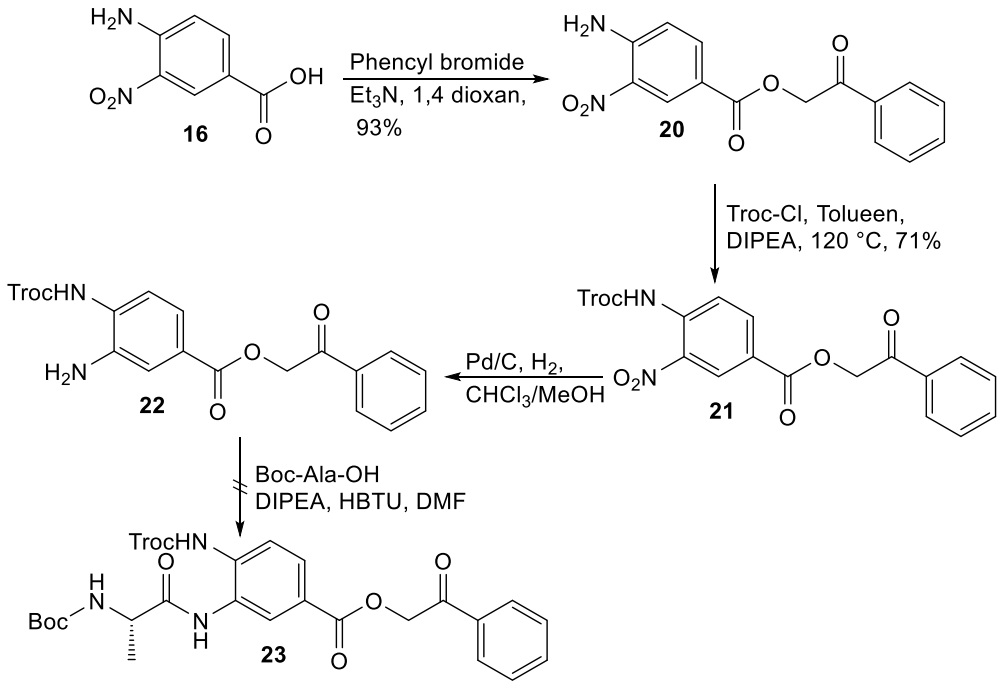

Scheme 4. Protecting strategy with Troc group

3.3.2 *N*-Acylation

Here, the acyl group was introduced directly in the initial step. Successfully, both acetyl and butyryl groups were added to the amino group in **16**. Compound **16** was treated with acetic anhydride in acetic acid and sulfuric acid at 100 °C to form **24** in 98% yield. Under the same conditions and by using butyric anhydride, compound **25** was obtained in quantitative yield (Scheme 5). The present work focused on the synthesis of MDP mimics bearing an *N*-acetyl substituted aromatic amino acid residue. Therefore, compound **24** was subsequently used to form our target molecules while compound **25** could be used in future studies to produce MDP mimics bearing an *N*-butyryl substituted aromatic amino acid residue.

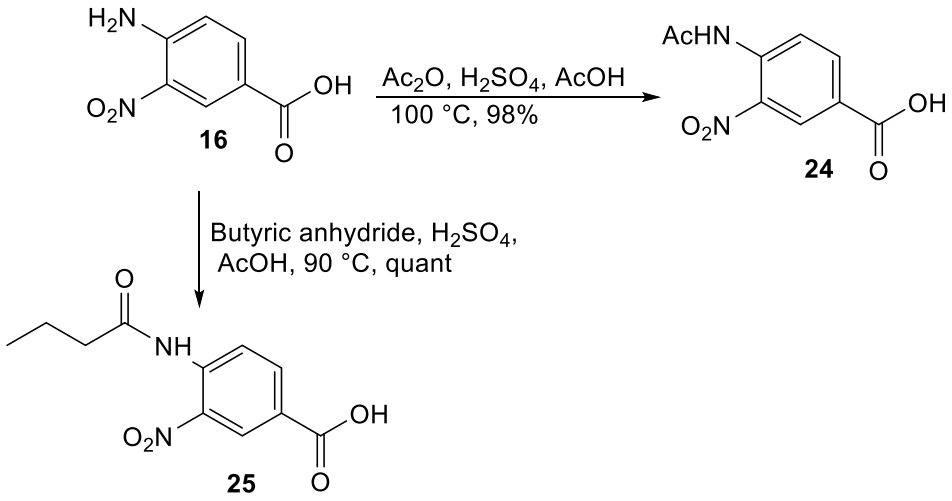

Scheme 5. Acylation of amino group in **16**.

3.3.3 Attachment of lipids

3.3.3.1 Lipidation of 16

In order to reduce the number of protecting groups required, an alternative pathway was investigated by which the lipid chain would be added early on, so that it would also serve to block the carboxyl group from interfering with formation of other amide bonds. Compound **26** was prepared with an 81% yield by coupling compound **16** with hexadecyl amine in the presence of DIPEA and HBTU in DMF (Scheme 6). Compound **26** was then treated with Troc-Cl and DIPEA in toluene to make **27** in 71% yield. Compound **27** could be used in the future to generate a general building block to access other MDP mimics with a variable R substituent on the amino group.

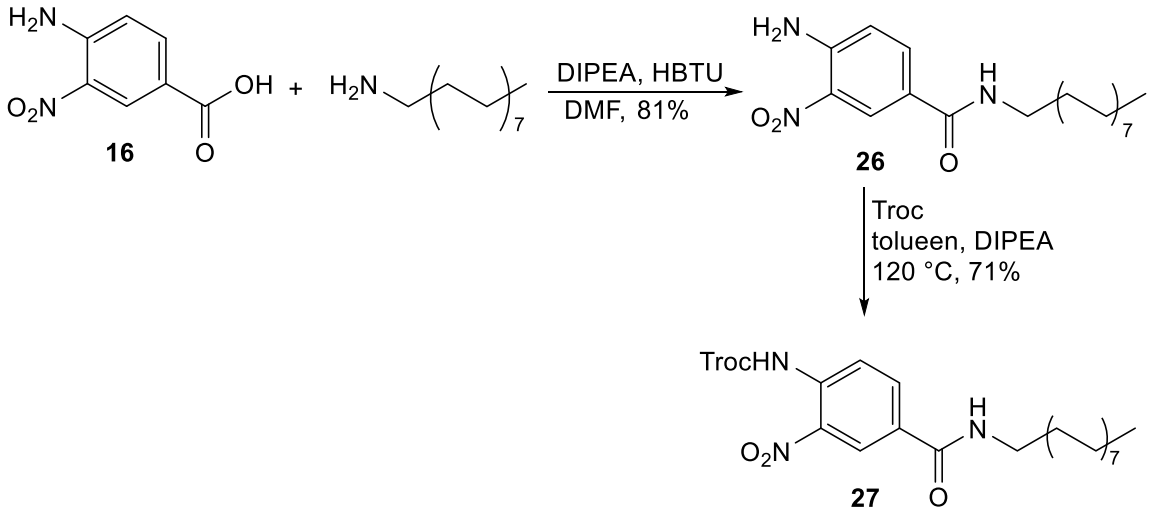

Scheme 6. Preparation of aromatic amino acid building block **27**.

3.3.3.2 Lipidation of 24

Since we chose to converge on the synthesis of MDP mimics bearing an *N*-acetyl substituent on the aromatic ring, a lipidation reaction was applied to **24** using the general coupling conditions (Scheme 7). As a result, compound **28** was achieved with 40% yield. Due to the solubility issue of compound **28**, the purification was not an easy procedure.

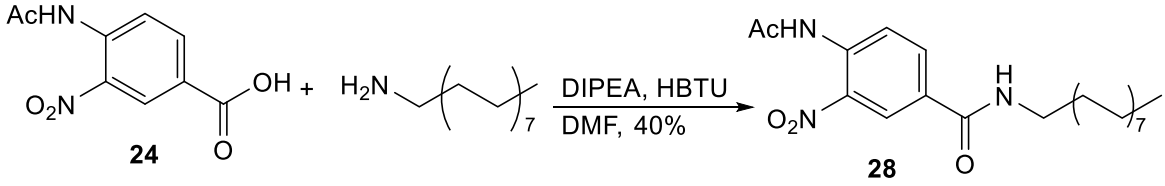

Scheme 7. Lipidation of compound **24**

3.4 Preparation of the dipeptide building blocks

3.4.1 Metallic reduction of the nitro group

The reduction of the nitro group in **28** was tried using two different sets of conditions. Compound **28** was treated with tin (Sn) in the HCl acidified MeOH and heated at 50 ^{o}C. TLC analysis of the reaction mixture indicated clear conversion of the starting material to a much more polar product, which was reasonably assumed to be the expected amine **29** in HCl salt form. A similar TLC profile was observed when the reaction was carried out using zinc powder (Zn) in ethanol and acetic acid at 70 ^{o}C. As the work-up procedure of these reactions, the reaction mixture was first treated with 1 M NaOH to adjust pH to ca. 5. Due to the chemical instability of **29** in free amine form and the large

amount of tin/zinc salt present in the reaction mixture, it was hard to isolate compound **29** in pure form; therefore, we proceeded with the coupling of **29** to Boc-L-Ala-OH (Scheme 8). The desired product **13**, however, was not obtained, possibly because a large amount of metal salts ($SnCl_2$ or $Zn(OAc)_2$) in the mixture interfered the reaction. Due to the complexity of the work-up procedure for the metal reduction of the nitro group, this reaction pathway was not continued.

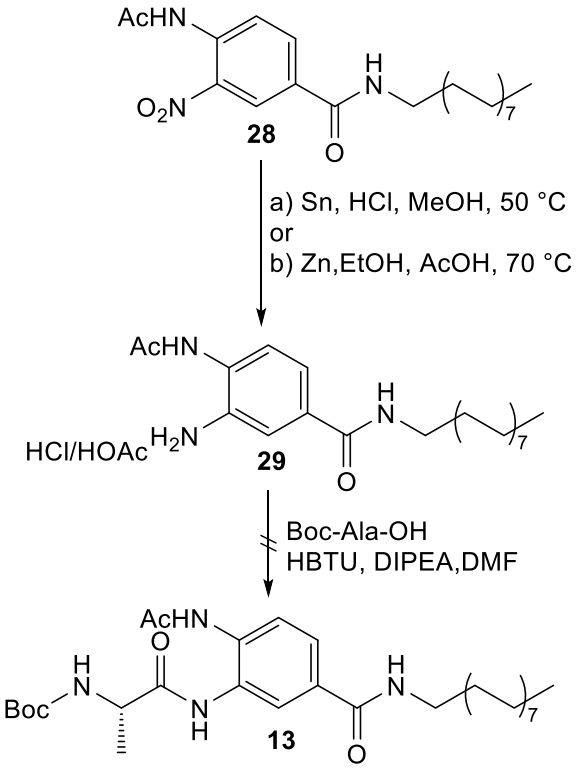

Scheme 8. Attempt to reduce the nitro group on **28** by metallic conditions.

3.4.2 Activating Boc-L-Ala-OH

An activated intermediate form of Boc-L-ala-OH (**30**) was prepared in quantitative yield by treating Boc-L-Ala-OH with *N*-hydroxy succinmide (NHS), *N,N'*-dicyclohexylcarbodiimide (DCC) and CH_2Cl_2 (Scheme 9).

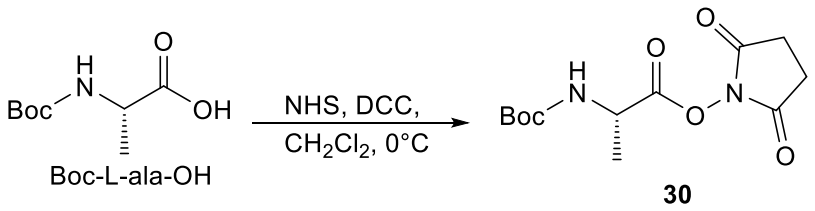

Scheme 9. Preparation of the active form of Boc-L-Ala-OH.

3.3.3 Preparation of building block 14

The nitro group in **24** was reduced through catalytic hydrogenation using palladium on activated carbon (Pd-C) in MeOH under hydrogen atmosphere in a Schlenk apparatus, resulting in compound **31** which presents sensitivity toward air (Scheme 10). Next, **31** was directly coupled to L-alanine in two approaches. As presented in Scheme 10, compound **31** and Boc-L-Ala-OH were dissolved in DMF along with coupling agents HBTU and DIPEA to form **14** in 35% yield over two steps. In the other approach, **31** and the activated alanine **30** were treated with DIPEA in DMF to generate **14** in 42% yield over two steps. So the reaction of **24** with the pre-activated alanine **30** provides slightly higher yield of the desired dipeptide mimic **14**.

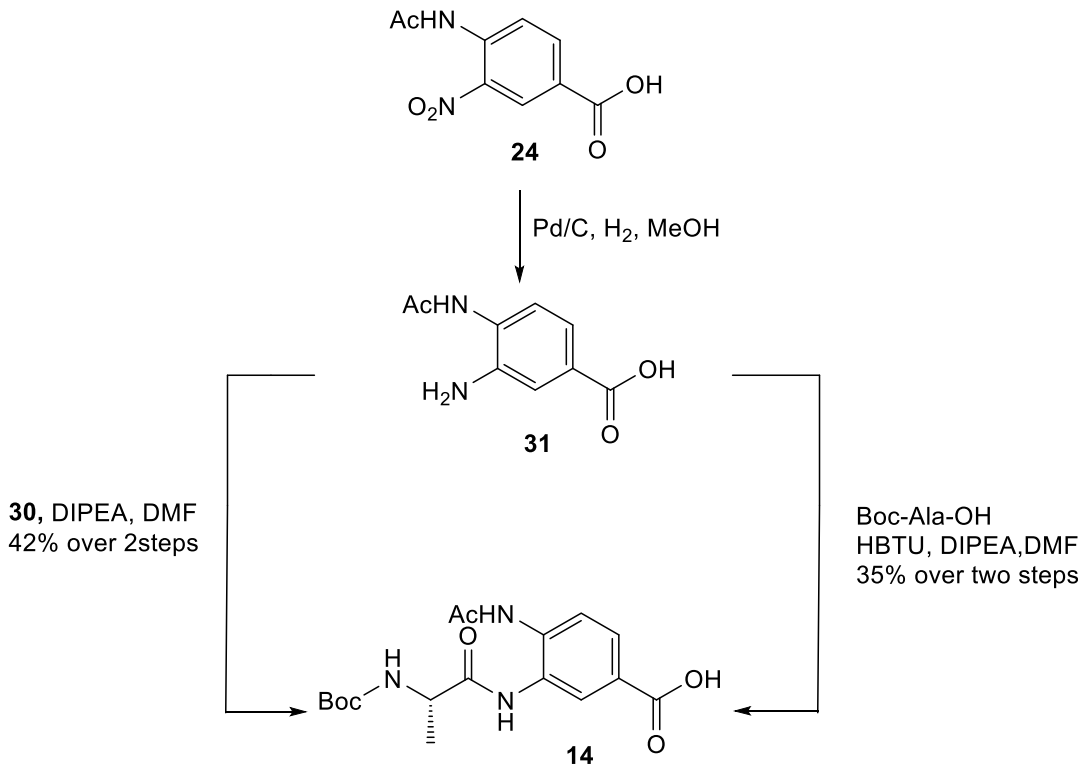

Scheme 10. Reducing the nitro group in **24** followed by coupling with L-alanine.

3.3.4 Lipidation of the dipeptide derivative 14

The lipid chains could be added to the dipeptide derivatives at this stage. Product **14** was coupled to hexyl amine, dodecyl amine, and hexadecyl amine by the coupling condition of HBTU and DIPEA in DMF to afford **11, 12**, and **13** in 83%, 59%, and 85% yield, respectively (Scheme 11).

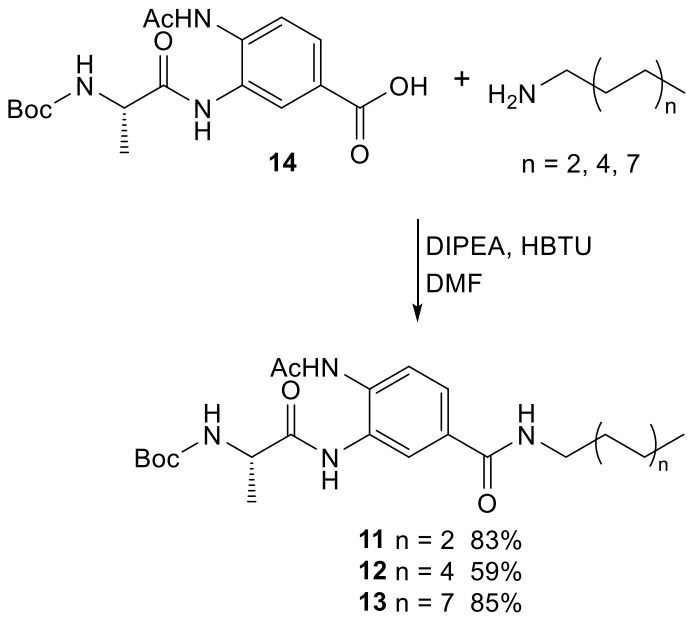

Scheme 11. Lipidation of the dipeptide derivative **14**

3.4 Preparation of MDP mimics

3.4.1 *N*-Boc deprotection

Following the general procedure to remove the protecting Boc-group, compounds **11** – **14** were treated individually with trifluoracetic acid (TFA)/dichloromethane/water (45:50:5) (Scheme 12) to give **32 – 35**, respectively, in quantitative yields. Compounds **32 – 35** were used for direct coupling with the carbohydrate moiety without further purification.

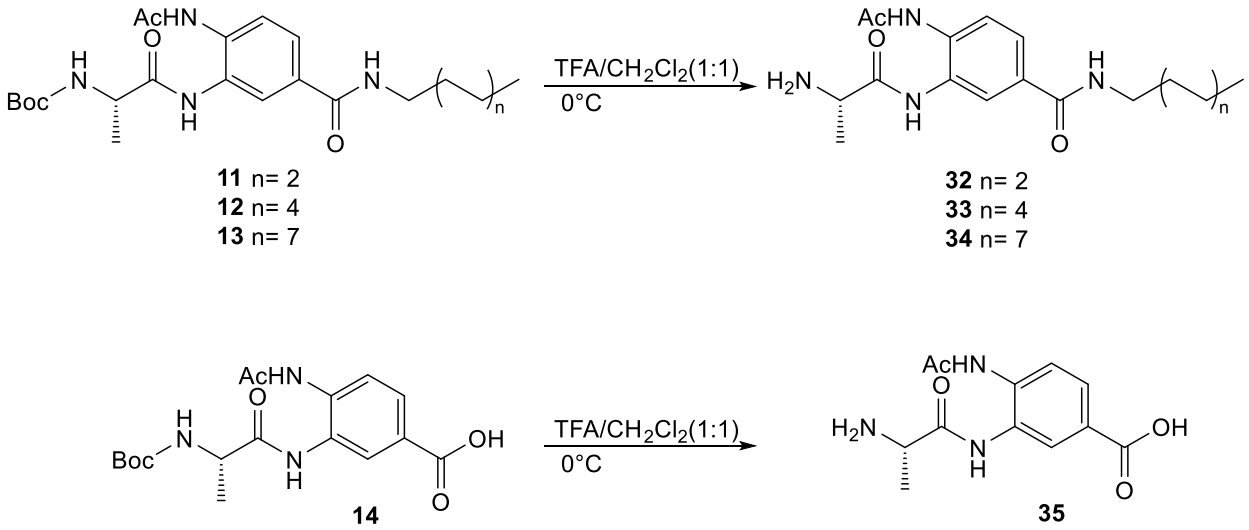

Scheme 12. The removal of the Boc-group.

3.4.2 Activating the *N*-acetylmuramic acid

Following known procedures[53,54,55], compound **10** was prepared by my coworker Dr. Farooq Khan. Compound **10** was reacted with NHS and DCC in dry CH_2Cl_2 at 0° C to make **36** in quantitative yield (Scheme 13).

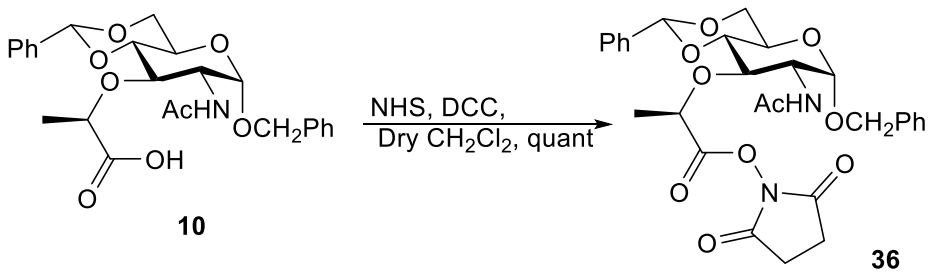

Scheme 13. Preparation of the activated sugar building block **36**

3.4.3 Linking the carbohydrate moiety to the peptide residue

The activated ester of *N*-acetylmuramic acid derivative **36** was dissolved in dry CH_2Cl_2 and treated with amines **32, 33** and **34** separately. Compounds **37**, **38** and **39** were obtained with 69%, 53%, and 71% yields, respectively (Scheme 14). The structures of **37** – **39** were confirmed by NMR and MS data.

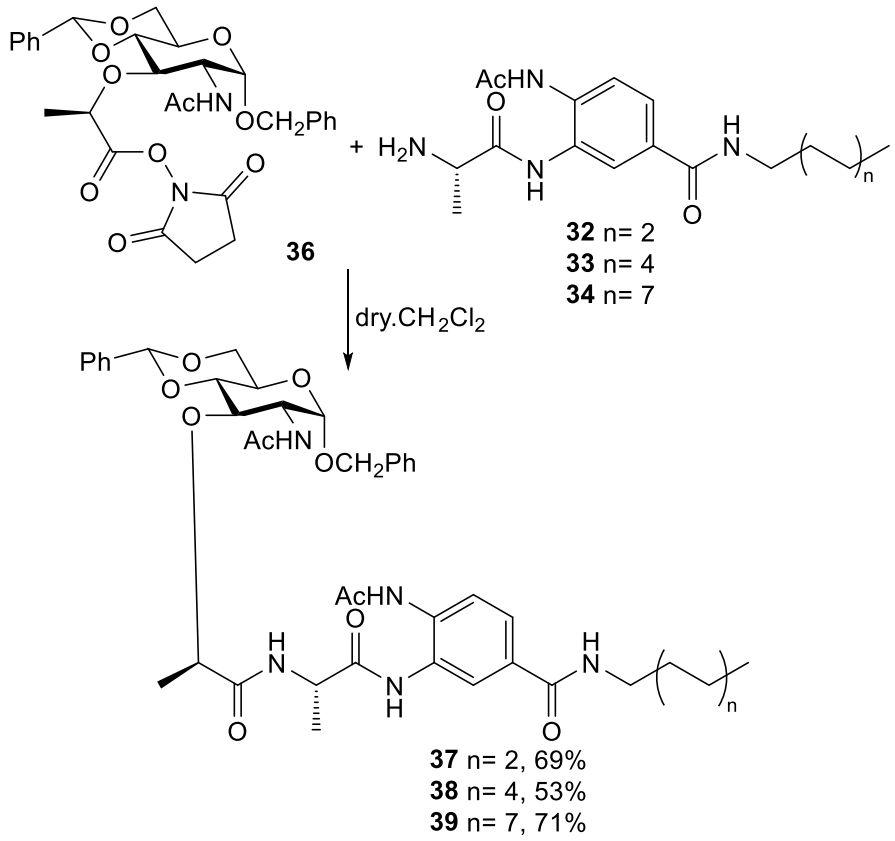

Scheme 14. The preparation of intermediates **37**, **38** and **39**

3.5 Synthesis of the target MDP analogues 4 – 9

Two different deprotection methods were employed in order to form the target analogues with lipid chains. The first group of analogues, **4** − **6**, were synthesized using the general deprotection method, that is, by treating **37**, **38** and **39** with Pd-C under hydrogen atmosphere in 1:1 THF/CH_3OH in 40 to 69% yield. The other group of analogues **7** − **9**, were obtained with 60–100% yield by dissolving, respectively, **37**,**38** and **39** in TFA/CH_2Cl_2/H_2O (45:50:5) at 0 °C to cleave the 4,6-*O*-benzylidene acetal group (Scheme 15). The structures of **4 – 9** were confirmed by NMR and MS spectral data.

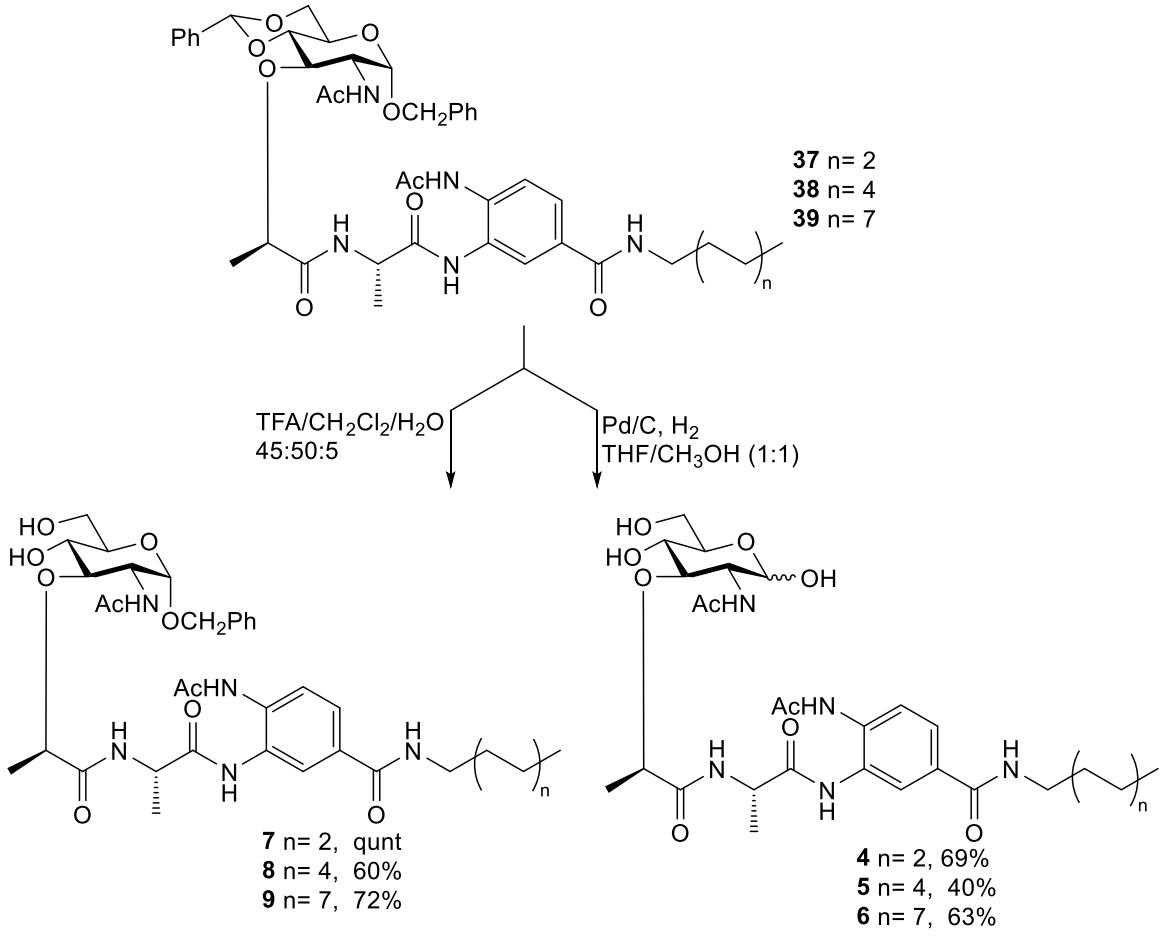

Scheme 15. Deprotection to yield target analogues.

3.6 Preparation of the hydrophilic MDP analogues

3.6.1 Retrosynthetic analysis of the hydrophilic MDP analogues

As described for the lipophilic analogues, compound **2** can be disconnected to give the sugar building block **10** and the dipeptide building block **14** (Scheme 16). The synthetic methods for **10** and **14** have been described in the previous Sections 3.3.3 and 3.4.2.

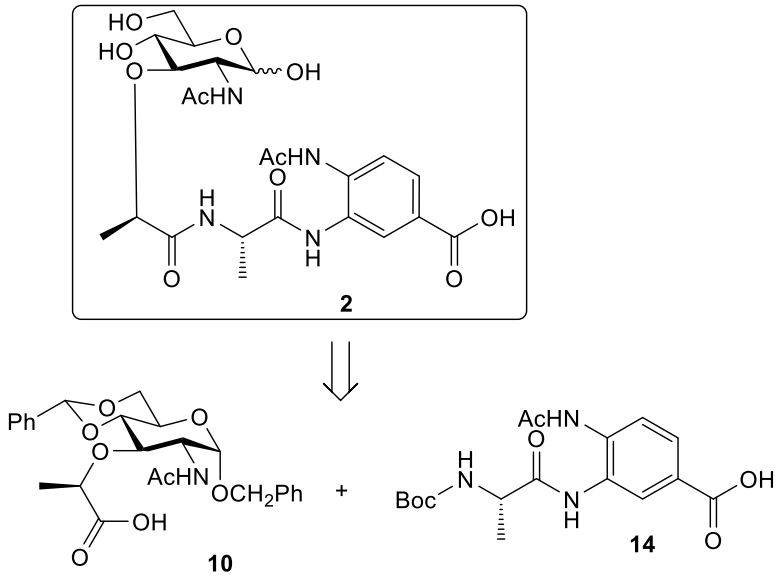

Scheme 16. The retrosynthetic analysis of mimic **2**

3.6.2 Linking the carbohydrate derivative 36 to the dipeptide derivatives 35

Compounds **35** and **36** were coupled in two different ways to give **40** (Scheme 17). In the first way, **40** was obtained by adding both **35** and **36** to DIPEA in dry CH_2Cl_2. In the second way, **40** was formed by employing sodium bicarbonate ($NaHCO_3$) in 1:1 H_2O/ dimethoxyethane (DME). Compound **40** was produced impurely through these two procedures and the subsequent purification procedure was very challenging according to TLC. For purification purpose, the carboxyl group of **40** was converted to a benzyl ester. In this step, the impure mixture of product **40** was reacted with benzyl bromide ($C_6H_5CH_2Br$) in the presence of DIPEA in acetonitrile (CH_3CN) to form **41** in 89% yield over two steps (Scheme 17).

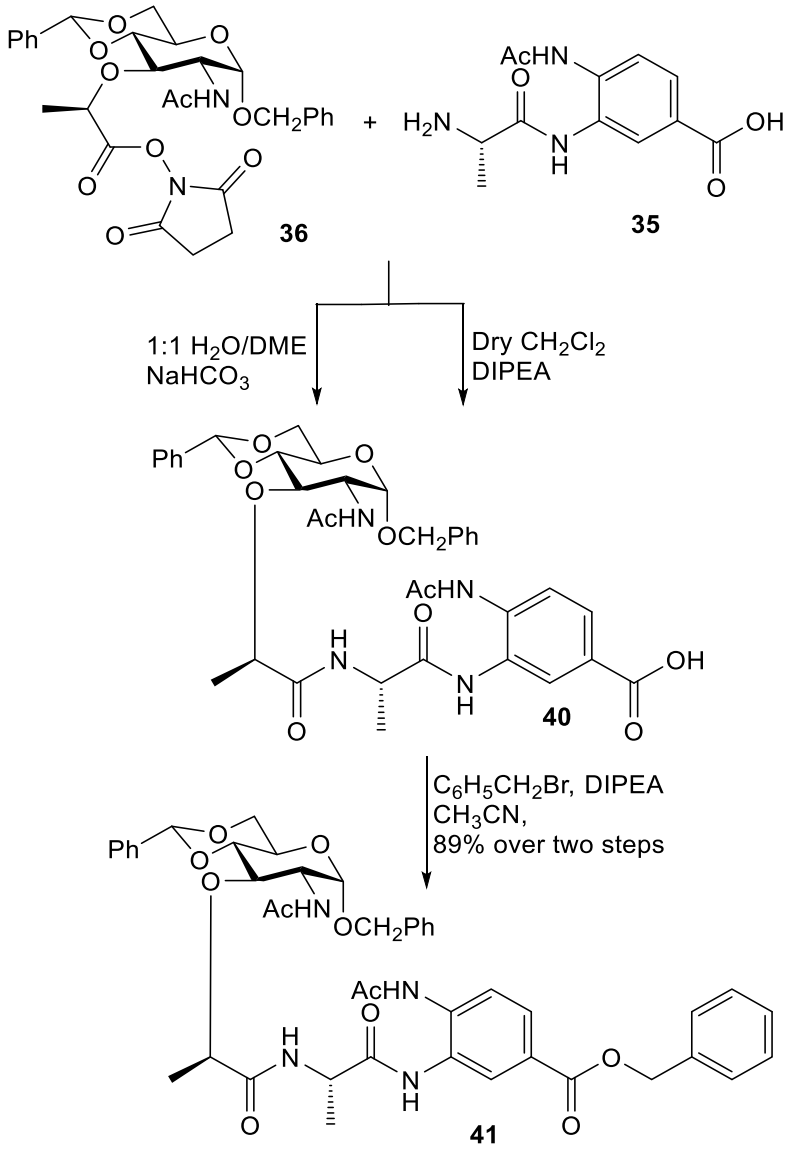

Scheme 17. Linking the carbohydrate derivative **36** to the dipeptide derivatives **35**

3.6.3 Attempt to synthesize the target analogues 2 and 3

To form products **2** and **3**, compound **41** was subjected, as a first try, to deprotection with Pd-C and H_2 in 1:1 tetrahydrofuran (THF)/acetic acid (HOAc) to afford the target

molecule **2** in an impure mixture (5 mg, 38%). Alternatively, dissolving compound **41** in TFA/CH_2Cl_2/H_2O (45:50:5) at 0 °C cleaved the 4,6-*O*-benzylidene acetal group and gave the intermediate **42** in 90% yield. Finally, the benzyl ester **42** was subjected to hydrolysis with 1 M lithium hydroxide (LiOH) and THF (1:2) (Scheme 18) to form **3** (5 mg, 63%). The structures of both **2** and **3** were not characterized. However, there was not enough material of compound **41** and **42** for a second attempt. These reactions need to be repeated in order to provide enough pure materials for the structural characterization of **2** and **3**, as well as for the planned biological studies.

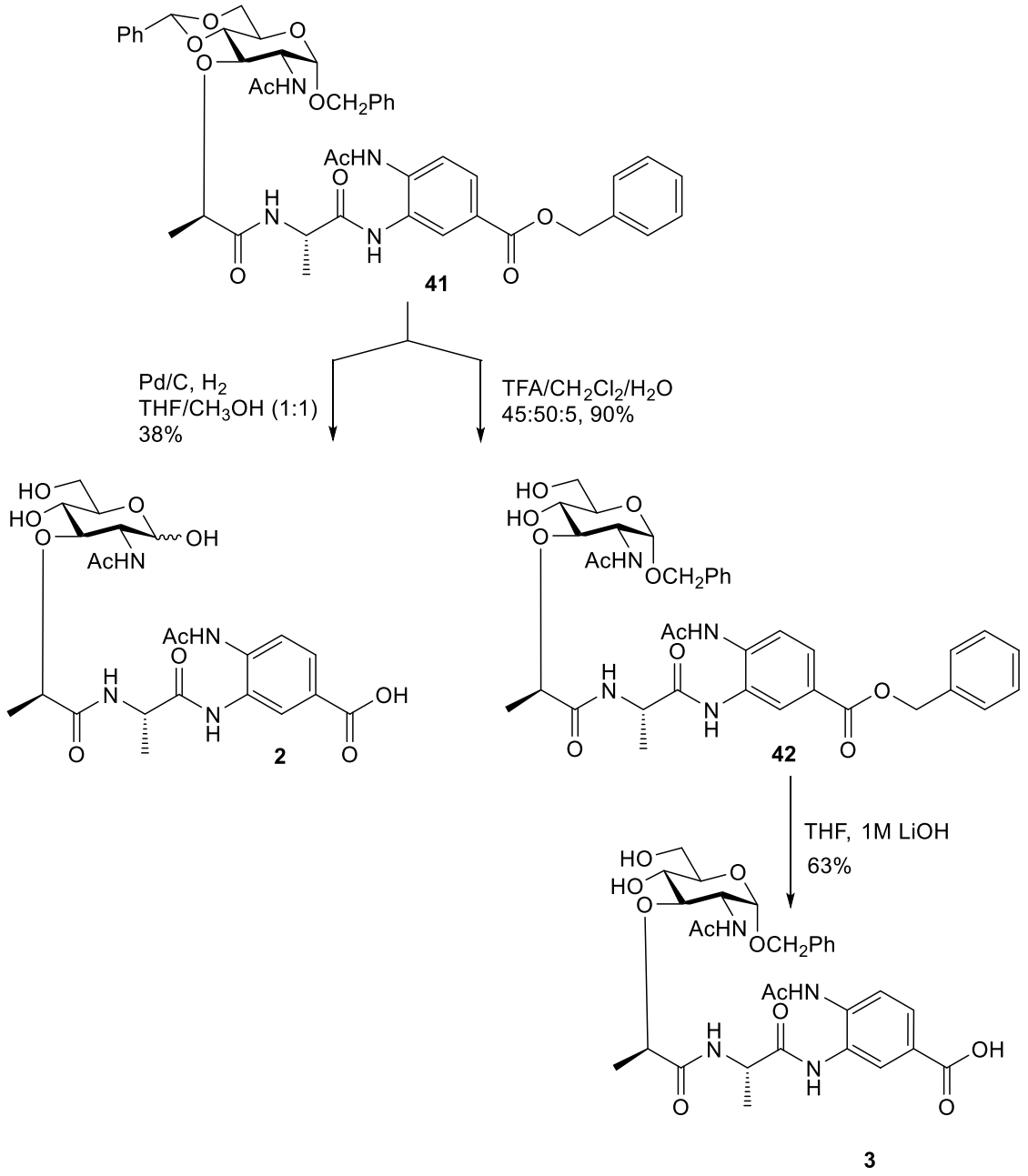

Scheme 18. Deprotection to target compounds **2** and **3**

4. CONCLUSION

Muramyl dipeptide is the smallest structure motif of peptidoglycan found in all types of bacteria. Scientists have discovered that muramyl dipeptide has immunostimulatory property that plays an important role as an adjuvant in vaccines. Muramyl dipeptide is a ligand for the NOD2 receptor, which activates innate immunity. The detection of the bioactive MDP activates the cytosolic pattern recognition receptor NOD2. NOD2 activation plays a critical role in both innate and adaptive immune systems by producing an inflammatory immune response and releasing cytokines. Numerous investigations have focused on the structure activity relationship of MDP for activating the NOD2 signaling pathway. Also, a great deal of work has been conducted with various synthetic MDP analogues. The goal of using these MDP analogues is not only to harness the beneficial immunostimulatory properties of MDP, but also to eliminate the toxic side effect associated with MDP.

In the present study, a novel group of MDP analogues have been synthesized. In this case, the D-iso-glutamine is replaced by an aromatic amino acid that is attached to a lipid chain. This modification is thought to offer advantages in terms of chemical and enzymatic stability, as well as membrane permeability. The synthesis of the dipeptide component was started with *N*-acetylation of the commercially available 4-amino-3-nitrobenzoic acid, which is followed by a reduction of the nitro group, and then coupling with L-alanine to yield the critical dipeptide building block **14**. Lipid chains of different length were coupled with **14** to form dipeptide building blocks **11** – **13**. The reaction between the *N*-acetylmuramic acid derivative **36** with the dipeptide analogues **11** – **14** provided protected

MDP analogues **37** – **40**. Global deprotection of **37** – **39** using Pd/C as the catalyst in a hydrogen atmosphere resulted in the removal of both benzyl and benzylidene groups, providing the first set of MDP analogues **4** – **6**. Treatment of **37** – **39** with TFA caused the cleavage of the 4,6-*O*-benzylidene group and gave the second set of MDP analogues **7 – 9** as benzyl α-glycosides of *N*-acetylmuramic acid derivatives. For the preparation of MDP analogues (**2** and **3**) without a lipid chain attached, compound **40** was converted to the benzyl ester **41**. Global deprotection of **41** under catalytic hydrogenation resulted in MDP mimic **2**, while treatment with TFA followed by LiOH provided MDP mimic **3**. The structures of the synthesized MDP analogues **4** – **9** were characterized by ^{1}H NMR, ^{13}C NMR and MS spectral data while that of **2** and **3** were not characterized.

5. FUTURE STUDIES

The biological evaluation of MDP analogues has been left for future study due to lack of time. Therefore, the first goal of future studies should be concentrated on testing the activity and the safety of the lipophilic analogues **4 - 9**. If these molecules work well as immunomodulatory agents, the use of muramyl peptide analogues at low and safe doses in combination with other drugs, including antibiotics and cytokines, might lead to another biological investigation. In terms of the biological studies, human monocyte cells (THP-1 monocytes) would be utilized to preliminarily test the immune stimulating ability of synthesized analogues. Cell counting would be performed using a hemocytometer, with viability being determined through the trypan blue cellular exclusion method. As preliminary studies, ICAM-1 induction and cytokines (including

TNF-α and IL-6) will be measured to determine the immune-stimulating activity of the synthesized MDP analogues.

From the synthesis point of view, adding protecting groups at the C- and N-terminals of the starting point (4-amino-3-nitobenzoic acid) in order to add a variety of R groups at these two positions is worth more investigation. For example, the preparation of building block **23** (Scheme 4) is worthy of reinvestigation. Compound **23** has an *N*-Troc protection group on the 4-amino group of the aromatic amino acid, which allows for the introduction of a variable substituent at that nitrogen at the late stage of the synthesis. In addition, the deprotection for getting the final hydrophilic mimics **2** and **3** needs to be repeated with different reaction conditions.

It could also be possible to design new MDP analogues by replacing amide-linked lipids with ester-linked lipid chains, which could be more favorable in biological metabolism. If the present modified analogues present high ability to activate innate immunity, that would confirm that the the employed 3,4-diaminobenzoic acid (DABA) is a good replacement for D-iso-glutamine. New MDP analogues based on DABA, perhaps without the carbohydrate moiety, can be designed and synthesized for future studies.

6 Experimental

6.1 General methods

TLC was performed on Silica Gel 60Å F_{254} (thickness 250 µm; Silicycle Inc., Canada) and detected by fluorescence (254 nm), followed by dipping into one of the staining reagents, 15% H_2SO_4 or Mostain reagent [ammonium molybdate ($(NH_4)_6Mo_7O_{24}.4H_2O$, 20 g) and cerium (IV) sulfate ($Ce(SO_4)_2$, 0.4 g) in 10% H_2SO_4 solution (400 ml)] and charring at ~ 120 °C.

Flash column chromatography was performed on Silica Gel 60 (40 - 63 µm; Silicycle Inc., Canada). ^1H NMR and ^{13}C NMR spectra were recorded on a Varian Unity Inova 500 MHz spectrometer. Tetramethylsilane (TMS, δ 0.00 ppm) or solvent peaks were used as internal standards for ^1H and ^{13}C NMR spectra. The chemical shifts were given in ppm and coupling contents in Hz. Multiplicity of proton signals is indicated as follows: s (singlet), d (doublet), dd (double doublet), t (triplet), q (quartet), m (multiplet), br (broad), and approx. (approximate).

All air and moisture sensitive reactions were performed under nitrogen atmosphere. All commercial reagents were used as supplied. Anhydrous solvents were dried according to literature procedures. Dichloromethane was distilled over calcium hydride, while THF was distilled over sodium. Anhydrous DMF was purchased from Sigma Aldrich. Optical rotations were measured with a PerkinElmer 241 Polarimeter at rt (20 - 22 °C). Mass spectra were obtained from a Biflex-IV MALDI linear/reflector instrument at Western University, ON, Canada.

6.2 2-Oxo-2-phenylethyl 4-amino-3-nitrobenzoate (**20**)

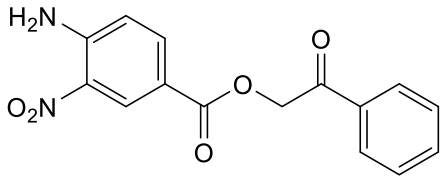

A solution of compound **16** (1.03 g, 5.49 mmol) and triethylamine Et_3N (0.76 ml, 7.51 mmol) in dioxane (6 ml) was stirred at rt for 30 min. After that, phenacyl bromide (1.12 g, 5.64 mmol) was added to the mixture and stirred at rt for 2 h. The solvent was removed in *vacuo* and the residue was dissolved with EtOAc (100 ml) and washed with H_2O (10 ml x 2). The organic layer was dried over anhydrous Na_2SO_4 and concentrated under vacuum to give product **20** (1.587 g, 93%) as a yellow solid. R_f 0.35 (hexane/ethyl acetate, 2:1). ^{1}H NMR (500 MHz, chloroform-*d*):δ 8.97 (d, *J* = 1.9 Hz, 1H), 8.07 (dd, *J* = 8.7, 1.9 Hz, 1H), 8.04 – 7.90 (m, 2H), 7.63 (d, *J* = 7.5 Hz, 1H), 7.52 (t, *J* = 7.5 Hz, 2H), 6.86 (d, *J* = 8.7 Hz, 1H), 5.58 (s, 2H). ^{13}C NMR (126 MHz, chloroform-*d*): δ 192.01, 164.38, 147.61, 136.11, 134.17, 134.02, 129.63, 128.94, 127.83, 118.57, 118.22, 66.50.

6.3 2-Oxo-2-phenylethyl 3-nitro-4-(2,2,2-trichloroethoxycarbonyl)aminobenzoate (**21**)

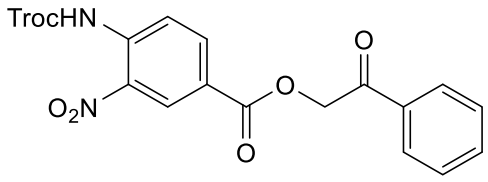

A solution of compound **20** (300 mg, 0.9997 mmol) and *N,N*-diisopropylethylamine (DIPEA, 0.68 ml, 5.261 mmol) in toluene (15 ml) was stirred at 120 °C. Then, 2,2,2-trichloroethyl chloroformate (Troc-Cl) (0.52 ml, 2.454 mmol) was diluted in toluene (5

ml) and added dropwise over 45 mins to the stirring mixture. After stirring for two days at 120 °C, the solvent was removed in *vacuo.* The residue was subjected to a dry loading flash column chromatography (CH_2Cl_2/Hexane, 5:2) to give **21** (330 mg, 71%) as light yellow solid. R_f 0.47 (CH_2Cl_2/hexane, 5:2). ^{1}H NMR (500 MHz, chloroform-*d*): δ 10.35 (s, 1H), 9.04 (d, *J* = 7.4 Hz, 1H), 8.72 (d, *J* = 7.4 Hz, 1H), 8.49 – 8.36 (m, 1H), 8.03 – 7.91 (m, 2H), 7.60 (d, *J* = 7.4 Hz, 1H), 7.64 – 7.52 (m, 2H), 4.90 (s, 2H), 4.76 (s, 2H).^{13}C NMR (126 MHz, chloroform-*d*): δ 191.39, 163.61, 153.15, 151.05, 138.28, 136.87, 135.80, 134.07, 129.01, 128.25, 127.82, 124.33, 120.59, 94.50, 74.95, 66.91.

6.4 4-Acetamido-3-nitrobenzoic acid (**24**)

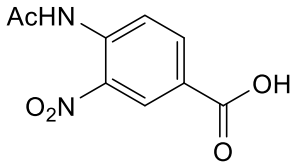

A solution of **16** (3.00 g, 16.471 mmol) in acetic anhydride (15.56 ml, 152.414 mmol) and acetic acid (20 ml) was stirred for 4 h at 110 °C. Then, sulfuric acid (3.5 ml) was added, and the solution was stirred for another 4 h at the same temperature. The mixture was then poured in a beaker containing ice. The precipitate was filtrated and washed three times with cold water to give **24** (3.68 g, 98%) as off-white to light yellow solid. R_f 0.25 (acetone/hexane, 4:3). ^{1}H NMR (500 MHz, DMSO-d_6): δ 13.46 (s, 1H), 10.54 (s, 1H), 8.37 (d, *J* = 2.0 Hz, 1H), 8.19 (dd, *J* = 8.5, 2.0 Hz, 1H), 7.82 (d, *J* = 8.5 Hz, 1H), 2.12 (s, 3H).^{13}C NMR (126 MHz, DMSO-d_6): δ 168.82, 165.38, 141.23, 135.09, 134.37, 126.78, 126.01, 124.56, 23.70. MS m/z calcd for $C_9H_8N_2O_5$: 224.043; found: 225.048 [M+H], 247.030 [M+Na] and 263.002 [M+K].

6.5 4-Butyrylamino-3-nitrobenzoic acid (**25**)

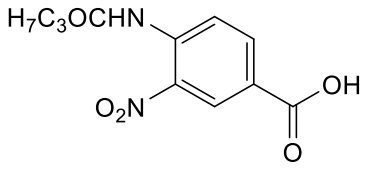

A solution of **16** (3.00 g, 16.471 mmol) in butyric anhydride (15.56 ml, 152.414 mmol) and acetic acid (20 ml) was stirred for 3 h at 90 °C. Then, sulfuric acid (3 ml) was added, and the solution was continued with stirring for 2 h at the same temperature. The mixture was then poured in a beaker containing ice. The precipitate was filtrated and washed three times with cold water to give **25** (3.68 g, quant.) as beige solid. R_f 0.18 (ethyl acetate/hexane/MeOH, 3:3:0.2). ^{1}H NMR (500 MHz, chloroform-*d*): δ 10.63 (s, 1H), 9.01 (d, *J* = 9.0 Hz, 1H), 8.98 (d, *J* = 2.1 Hz, 1H), 8.33 (dd, *J* = 9.0, 2.1 Hz, 1H), 2.53 (t, *J* = 7.4 Hz, 2H), 1.82 (t, *J* = 7.4 Hz, 2H), 1.05 (t, *J* = 7.4 Hz, 3H). ^{13}C NMR (126 MHz, chloroform-*d*): δ 172.76, 166.55, 138.39, 137.16, 135.91, 128.17, 125.83, 121.94, 30.02, 19.02, 13.93. MS m/z calcd for $C_{11}H_{12}N_2O_5$: 252.23; found: 253.065 [M+H], 275.055 [M+Na] and 291.030 [M+K].

6.6 4-Amino-*N*-hexadecyl-3-nitrobenzamide (**26**)

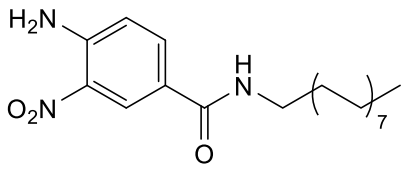

Compound **16** (1.00 g, 5.49 mmol) was dissolved with hexadecyl amine (1.32g, 5.49 mmol), HBTU (2.208 g, 5.819 mmol) and DIPEA (2.09 ml, 16.17 mmol) in DMF (10 ml) and the mixture was stirred at rt for 18 h. The solvent was removed in *vacuo,* and the residue was dissolved in 250 ml of CH_2Cl_2 and washed with $NaHCO_3$ (25 ml x 3), then with H_2O (50 ml x1). The organic layer was dried over anhydrous Na_2SO_4 and concentrated under vacuum. The resulting residue was subjected to flash column chromatography ($CHCl_3$/MeOH, 4.5:0.5) to give **26** as a yellow solid (1.8 g, 81%). R_f 0.8 ($CHCl_3$/MeOH, 4.5:0.5), ^{1}H NMR (500 MHz, chloroform-*d*): δ 8.47 (d, *J* = 2.1 Hz, 1H), 7.90 (dd, *J* = 8.7, 2.1 Hz, 1H), 6.85 (d, *J* = 8.7 Hz, 1H), 6.28 (s, 2H), 5.95 (s, 1H), 3.44 (td, *J* = 7.3, 5.7 Hz, 2H), 1.63 (m, 2H), 1.27 – 1.4 (m, 26H), 0.92 – 0.84 (m, 3H). ^{13}C NMR (126 MHz, chloroform-*d*): δ 165.23, 146.44, 134.62, 124.68, 124.04, 119.01, 45.14, 40.36, 31.99, 29.84, 29.74, 29.72, 29.70, 29.65, 29.60, 29.39, 27.11, 22.71, 14.04. MS m/z calcd for $C_{23}H_{39}N_3O_3$: 405.29; found: 406.298 [M+H], 428.27 [M+Na] and 444.247 [M+K].

6.7 *N*-Hexadecyl-3-nitro-4-(2,2,2-trichloroethoxycarbonyl)aminobenzamide (**27**)

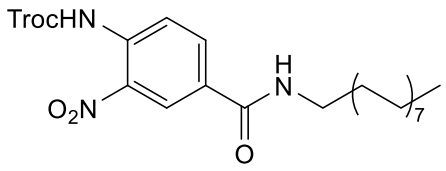

A solution of **26** (500 mg, 1.2318 mmol) and DIPEA (0.85 ml, 6.576 mmol) in toluene (10 ml) was stirred at 120 °C. Then, trichloroethyl chloroformate (Troc-Cl) (0.66 ml, 3.128 mmol) was added dropwise over 30 min. The mixture was stirred for 16 h and the solvent was removed in *vacuo.* The residue was diluted in EtOAc (100 ml) and washed with 0.1 M HCl (15 ml x 1), $NaHCO_3$ (20 ml x 1) and finally with H_2O (20 ml x 1). The organic layer was dried over anhydrous Na_2SO_4 and concentrated under *vacuum*. The resulting residue was subjected to flash column chromatography ($CHCl_3$: EtOAc/hexane,1:2) to give **27** (0.5 g, 71%) as a very light yellow solid. R_f 0.14 (CH_2Cl_2), ^{1}H NMR (500 MHz, chloroform-*d*): δ 10.22 (s, 1H), 8.69 – 8.63 (m, 2H), 8.09 (dd, *J* = 9.0, 2.2 Hz, 1H), 6.12 (s, 1H), 4.88 (s, 2H), 3.47 (q, *J* = 6.8 Hz, 2H), 1.65 (q, *J* = 7.2 Hz, 4H), 1.40 – 1.34 (m, 2H), 1.25 (s, 22H), 0.88 (t, *J* = 6.9 Hz, 3H). ^{13}C NMR (126 MHz, chloroform-*d*) δ 164.31, 151.15, 136.70, 135.78, 134.25, 129.55, 124.69, 120.87, 94.50, 74.92, 40.44, 31.93, 31.59 29.71, 29.70, 29.68, 29.67, 29.65, 29.61, 29.60, 29.54, 29.37, 29.31, 27.00, 22.70, 14.14. MS m/z calcd for $C_{26}H_{40}Cl_3N_3O_5$: 579.97; found: 580.232 [M+H], and 602.204 [M+Na].

6.8 4-Acetamido-*N*-hexadecyl-3-nitrobenzamide (**28**)

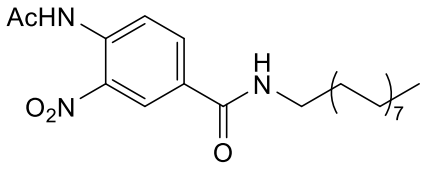

A solution of **27** (700 mg, 3.029 mmol), and hexadecyl amine (800 mg, 3.313mmol) with DIPEA (1.05 ml, 8.123 mmol), and HBTU (1.14g, 3.0289 mmol) in DMF (25 ml) was stirred at rt. After stirring for two days, the solvent was removed in *vacuo* and the residue was dissolved with $CHCl_3$ (70 ml) and washed with $NaHCO_3$ (10 ml x 3), then with H_2O (15 ml x1). The organic layer was dried over anhydrous Na_2SO_4 and concentrated under *vacuum* to give product **28** as a white solid (520 mg, 40 %). Another way to get compound **28** is to treat **26** in a similar procedure of forming **24.** This pathway gave **28** in 89%. R_f 0.5 (chloroform/MeOH, 9:0.5), ^{1}H NMR (500 MHz, chloroform-*d*): δ 10.47 (s, 1H), 8.89 (d, *J* = 8.9 Hz, 1H), 8.63 (d, *J* = 2.1 Hz, 1H), 8.03 (dd, *J* = 8.9, 2.1 Hz, 1H), 6.17 (br s, 1H), 3.46 (td, *J* = 7.3, 5.8 Hz, 2H), 2.32 (s, 3H), 1.71 – 1.58 (m, 2H), 1.25 (s, 26H), 0.88 (t, *J* = 6.9 Hz, 3H). ^{13}C NMR (126 MHz, chloroform-*d*): δ 169.15, 164.47, 137.04, 135.85 134.03, 129.47, 124.62, 121.99, 40.42, 31.94, 29.70, 29.68, 29.67, 29.66, 29.60, 29.55, 29.32, 28.3827.00, 25.76, 22.71, 14.14. MS m/z calcd for $C_{25}H_{41}N_3O_4$: 447.309; found: 448.317 [M+H], 470.288 [M+Na] and 486.262 [M+K].

6.9 2,5-Dioxopyrrolidin-1-yl (*S*)-2-*tert*-butoxycarbonylaminopropanoate (**30**)

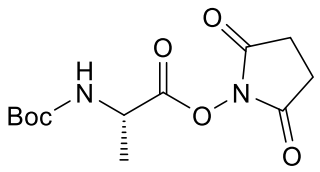

A mixture of Boc-L-Ala-OH (1 g), *N*-hydroxy succinimide NHS (608 mg, 5.282 mmol), and *N,N'*-dicyclohexylcarbodiimide DCC (1.09 g, 5.282 mmol) in dry dichloromethane (5 ml) was stirred at 0-21 °C for 16 h. The solids were filtered and washed with 2 ml of dry dichloromethane. The filtrate was concentrated under vacuum to yield **30** (1.48 g, 98%) as white solid. Compound **30** was used directly for the preparation of **14**.

6.10 4-Acetamido-3-aminobenzoic acid (**31**)

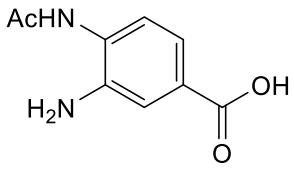

To a solution of **24** (800 mg, 4.015 mmol) in methanol (30 ml) in 100 ml Schlenk flask, palladium on activated carbon (5%, 40 mg) was added under argon atmosphere. The mixture was stirred under hydrogen gas (1 bar, using balloon) at rt for 20 h. The mixture was filtered, the solid washed with MeOH (10 ml), and the filtrate concentrated to afford **31** as a white solid (700 mg, crude). R_f 0.22 (diethyl ether/acetic acid, 2 : 0.15), ^{1}H NMR (500 MHz, chloroform-*d*): δ 7.33 (d, *J* = 1.9 Hz, 1H), 7.28 – 7.27 (m, 1H), 7.17 (d, *J* = 7.7 Hz, 1H), 2.03 (s, 3H). ^{13}C NMR (126 MHz, chloroform-*d*): δ 170.05, 168.41, 140.398,

128.88.128.17, 124.18, 120.33, 118.72, 22.53. This product presented sensitivity toward air, so it was proceeded to the following step directly.

6.11 4-Acetamido-3-[2-(*S*)- *tert*-butoxycarbonylamino]propamidobenzoic acid (**14**)

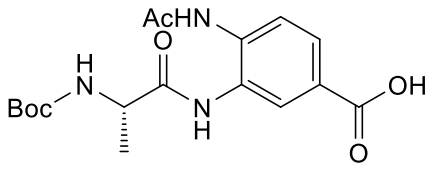

To a solution of **31** (700 mg, crude) and **30** (1.54 g, 5.379 mmol) in 10 ml of dry DMF, DIPEA (2.51 ml, 19.342 mmol) was added, and the mixture was stirred under argon atmosphere at 55°C for 2 days. The solvent was removed in *vacuo*, and the residue was diluted with dichloromethane (100 ml) and washed with 15% citric acid solution (20 ml x 3). The organic layer was dried over anhydrous Na_2SO_4, and concentrated under *vacuum*. The residue was subjected to flash column chromatography ($CHCl_3$/MeOH/AcOH, 5:0.5:0.1) to give compound **14** (550 mg, 42% over 2 steps) as a beige solid. R_f 0.43 ($CHCl_3$/MeOH/AcOH, 5:0.5:0.1), $[\alpha]_D^{22}$ -6.6° (C 1.0, MeOH). ^{1}H NMR (500 MHz, DMSO-d_6): δ 9.55 (s, 1H), 9.37 (s, 1H), 8.02 (s, 1H), 7.81 (d, *J* = 8.5 Hz, 1H), 7.76 – 7.71 (m, 1H), 7.35 (d, *J* = 8.5 Hz, 1H),4.10 (m, 1H) 2.13 (s, 3H), 1.40 (s, 9H), 1.29 (d, *J* = 7.1 Hz, 3H), ^{13}C NMR (126 MHz, DMSO-d_6): δ 172.88, 172.67, 169.59, 167.20, 156.16, 136.16, 129.45, 127.20, 127.12, 123.41, 79.01, 51.09, 45.00, 28.63, 24.14, 21.52, 17.72. MS m/z calcd for $C_{17}H_{23}N_3O_6$: 365.158; found: 366.158 [M+H], 388.150 [M+Na] and 404.129 [M+K].

6.12 4-Acetamido-3-[2-(*S*)-*tert*-butoxycarbonylamino]propanamido-*N*-hexylbenzamide (**11**)

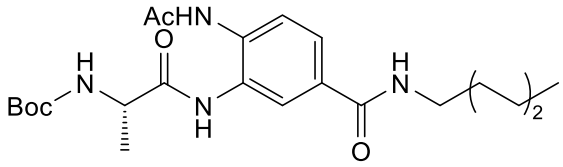

To a solution of compound **14** (300 mg, crude) and hexylamine (1.60 ml, 2.1416 mmol) in DMF (10 ml), HBTU (620 mg, 1.634 mmol) and DIPEA (0.57 ml, 4.410 mmol) were added. After starring at rt for 16 h, the solvent was removed in *vacuo.* The residue was diluted in dichloromethane (100 ml) and washed with $NaHCO_3$ (20 ml x 3) and then with H_2O (25 ml x 1). The organic layer was dried over anhydrous Na_2SO_4 and concentrated under *vacuum*. The residue was subjected to flash column chromatography ($CHCl_3$/MeOH, 5:0.5) and then further purified with second flash column chromatography (ethyl acetate/ hexane/ MeOH, 2:2:1.5) to give compound **11** (300 mg, 83%) as beige solid. R_f 0.43 (ethyl acetate/ hexane/ MeOH, 2:2:1.5), $[\alpha]_D^{22}$ - 24.9 (C 1.0, $CHCl_3$). ^{1}H NMR (500 MHz, chloroform-*d*): δ 9.03 (s, 1H), 8.89 (s, 1H), 7.61 (s, 1H), 7.49 (d, *J* = 8.2 Hz, 1H), 7.31 (s, 1H), 7.06 (s, 1H), 5.77 (s, 1H), 4.17 (m, 1H), 3.34 (t, *J* = 6.6 Hz, 2H), 2.15 (s, 3H), 1.57 (q, *J* = 7.0 Hz, 3H), 1.42 (s, 9H), 1.36 – 1.08 (m, 8H), 0.90 (m, 3H).^{13}C NMR (126 MHz, chloroform-*d*): δ 173.08, 170.09, 167.06, 155.93, 134.77, 131.37, 128.32, , 124.96, 123.42, 80.08, 51.04, 40.28, 39.45, 31.55, 31.45, 29.66, 28.38, 28.32, 26.51, 23.89, 22.53, 17.78, 14.00. MS m/z calcd for $C_{23}H_{36}N_4O_5$: 448.268; and found: 471.25 [M+Na].

6.13 4-Acetamido-3-[2-(*S*)-*tert*-butoxycarbonylamino]propanamido-*N*-decylbenzamide (**12**)

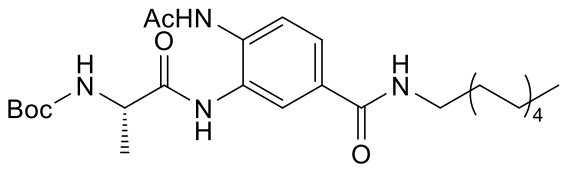

In a similar way as described for the preparation of **11**, to a solution of compound **14** (270 mg, crude) and decylamine (0.68 ml, 4.348 mmol) in DMF (5 ml), HBTU (1.73 g, 4.5595 mmol) and DIPEA (1.59 ml, 12.3017 mmol) were added to give **12** (220 mg, 59%) as beige product. R_f 0.28 ($CHCl_3$/ MeOH, 5.5:0.5), $[\alpha]_D^{22}$ - 8.6 (C 1.0, $CHCl_3$/ MeOH 1:1). ^{1}H NMR (500 MHz, chloroform-*d*): δ 9.04 (s, 1H), 8.82 (s, 1H), 7.58 (d, *J* = 8.4 Hz, 1H), 7.37 (d, *J* = 8.4 Hz, 1H), 6.58 (s, 1H), 5.61 (s, 1H), 4.21 (m, 1H), 3.36 (m, 2H), 2.18 (s, 3H), 1.60 (m, 2H), 1.45 (s, 9H), 1.35 (d, J = 7.0 Hz, 3H), 1.33 – 1.19 (m, 14H), 0.88 (t, *J* = 6.8 Hz, 3H). ^{13}C NMR (126 MHz, chloroform-*d*): δ 173.04, 172.08, 170.07, 167.10, 155.94, 134.79, 131.66, 128.70, 125.08. 123.65, 80.20, 51.30, 40.08, 31.92, 29.57, 29.43, 28.44, 28.42, 27.06, 23.96, 23.24, 22.67, 17.99, 14.06. MS m/z calcd for $C_{27}H_{44}N_4O_5$: 504.33; found: 527.32 [M+Na]

6.14 4-Acetamido-3-[2-(*S*)-*tert*-butoxycarbonylamino]propanamido-*N*-hexadecylbenzamide (**13**)

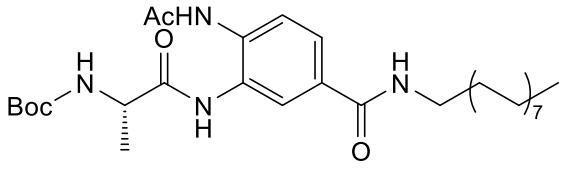

In a similar way as described for the preparation of **11**, to a solution of compound **14** (200 mg, crude) and hexadecyl amine (123 mg, 0.5466 mmol) in DMF (5 ml), HBTU (414 mg, 1.0911 mmol) and DIPEA (0.38 ml, 2.9400 mmol) were added to give **13** (275 mg, 85%) as beige product. R_f 0.85 (ethyl acetate/hexane/MeOH, 2:2:1.5), $[\alpha]_D^{22}$ + 8.2 (C 1.0, $CHCl_3$/MeOH 1:1) ^{1}H NMR (500 MHz, chloroform-*d*): δ 8.91 (s, 1H), 8.81 (s, 1H), 7.60 (d, *J* = 8.3 Hz, 1H), 7.45 (s, 1H), 7.34 (dd, *J* = 8.3, 2.0 Hz, 1H), 6.79 (t, *J* = 5.8 Hz, 1H), 5.63 – 5.59 (m, 1H), 4.19 (m, 1H), 3.37 (m, 2H), 2.19 (s, 3H), 1.60 (m, 2H), 1.46 (s, 9H), 1.37 (d, *J* = 6.8 Hz, 3H), 1.26 (br s, 26H), 0.88 (t, *J* = 6.8 Hz, 3H).^{13}C NMR (126 MHz, chloroform-*d*): δ 173.09, 170.22, 167.17, 156.07, 143.93, 131.53, 128,47, 125.30, 124.99, 123.58, 51.18, 40.42, 32.03, 29.83, 29.80, 29.78, 29.76, 29.68, 29.66, 29.53, 29.48, 29.42, 28.46, 27.23, 22.80, 14.24. MS m/z calcd for $C_{33}H_{56}N_4O_5$: 588.425; found: 611.39 [M+Na].

6.15 4-Acetamido-3-[(*S*)-2-aminopropanamido]-*N*-hexylbenzamide (**32**)

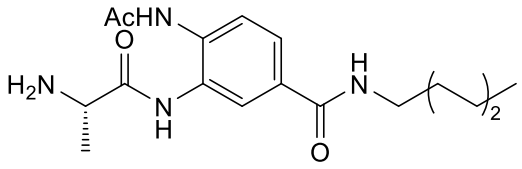

A solution of **11** (300 mg, 0.6688 mmol) in mixture of TFA/Dichloromethane (1:1) was stirred at 0 - 21 °C for 16 h. The solvent was removed in *vacuo*, and the residue was dissolved with CH_2Cl_2 (70 ml) and washed with $NaHCO_3$ (10 ml x 3), then with H_2O (15 ml x1). The organic layer was dried over anhydrous Na_2SO_4 and concentrated under *vacuum* to give the free amine product **32** (213 mg, 91%) as white solid. Compound **32** was used directly in the next coupling reaction.

6.16 4-Acetamido-3-[(*S*)-2-aminopropanamido]-*N*-decylbenzamide (**33**)

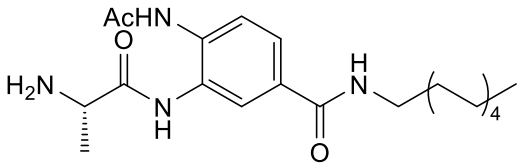

In a similar way as described for the preparation of **32**, a solution of **12** (230 mg, 0.4557mmol) in mixture of TFA/dichloromethane (1:1) was stirred at 0 - 21 °C for 16 h. Then, the solvent was removed in *vacuo,* and the residue was dissolved with CH_2Cl_2 (70 ml) and washed with $NaHCO_3$ (10 ml x 3), then with H_2O (15 ml x1). The organic layer was dried over anhydrous Na_2SO_4 and concentrated under *vacuum* to give the amine **33** (220 mg, quant) as white solid. Compound **33** was used directly in the next coupling reaction.

6.17 4-Acetamido-3-[(S)-2-aminopropanamido]-*N*-hexadecylbenzamide (**34**)

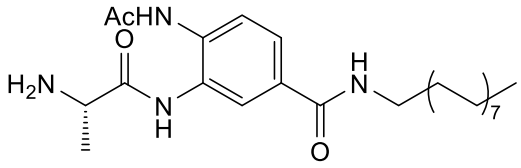

In a similar way as described for the preparation of **32**, a solution of **13** (100 mg, 0.170mmol) in mixture of TFA/dichloromethane (1:1) was stirred at 0 - 21 °C for 16 h. Then, the solvent was removed in *vacuo*, and the residue was dissolved with CH_2Cl_2 (70 ml) and washed with $NaHCO_3$ (10 ml x 3), then with H_2O (15 ml x1). The organic layer was dried over anhydrous Na_2SO_4 and concentrated under *vacuum* to give the intermediate **34** (140 mg, quant) as white solid. Compound **34** was used directly in the next coupling reaction.

6.18 4-Acetamido-3-[(*S*)-2-aminopropanamido]benzoic acid (**35**)

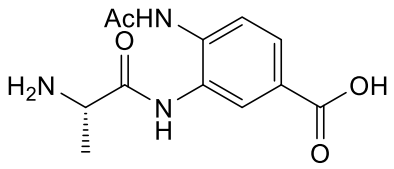

In a similar way as described for the preparation of **32**, a solution of **14** (120 mg, 0.328 mmol) in mixture of TFA/dichloromethane (1:1) was stirred at 0 - 21 °C for 16 h. Then, the solvents were removed in *vacuo* to give the intermediate **35** (140 mg, crude) as white solid. Compound **35** was used directly in the next coupling reaction.

6.19 2,5-Dioxo-pyrrolidin-*N*-yl 2-(*R*)-(2-acetamido-2-deoxy-1-*O*-benzyl-4,6-di-*O*-benzylidene-α-D-glucopyranos-3-*O*-yl)-propanoate (**36**)

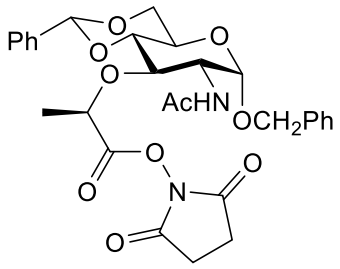

A mixture of **10**[53,54,55](1.13 g, 2.397mmol), *N*-hydroxy succinimide (NHS) (303 mg, 2.637 mmol), and *N,N'*-dicyclohexylcarbodiimide (DCC) (521 mg, 2.517 mmol) in dry THF (30 ml) was stirred at 0-21 °C for 16 h. The solid was filtered and washed with 2 ml of dry dichloromethane. The filtrate was concentrated in *vacuo* to afford **36** as white solid (1.13

g, 86%). Compound **36** was used directly in the next coupling reaction without further purification.

6.20 4-Acetamido-3-{(*S*)-2-[(*R*)-2-(2-acetamido-1-benzyl-4,6-*O*-benzylidene-1-*O*-benzyl-α-D-glucopyranos-3-*O*-yl)-propanamido]-propanamido}-*N*-hexylbenzamide (**37**)

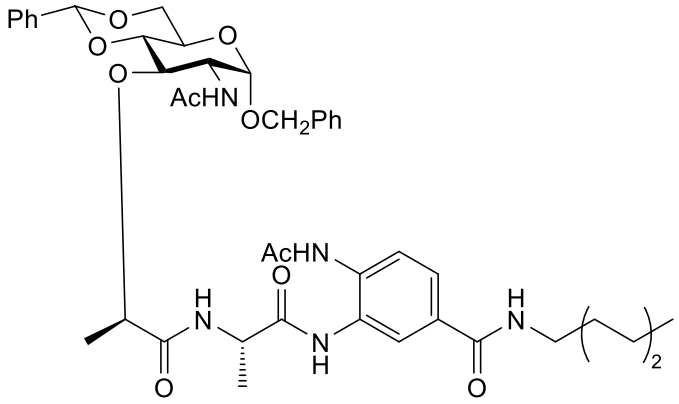

To a solution of **32** (213 mg, 0.611 mmol) in dry dichloromethane (5 ml), **36** (347 mg, 0.611 mmol) was added. The mixture was stirred under argon gas at rt for 24 hs. The solvent was then removed in *vacuo.* The residue was purified by flash column chromatography ($CHCl_3$/MeOH, 3:0.25) to afford **37** (260 mg, 53%) as white solid. R_f 0.49 ($CHCl_3$/MeOH, 3:0.25); $[\alpha]_D^{22}$ + 42.7 (C 1.0, $CHCl_3$/MeOH, 1:1). ^{1}H NMR (500 MHz, DMSO-d_6): δ 9.63 (s, 1H), 9.29 (s, 1H), 8.41 (t, *J* = 5.7 Hz, 1H), 8.20 (d, *J* = 8.3 Hz, 1H), 7.91 (s, 1H), 7.78 (d, *J* = 8.3 Hz, 1H), 7.72 (d, *J* = 2.1Hz, 1H), 7.65 (dd, *J* = 8.3, 2.1 Hz, 1H), 7.48 – 7.24 (m, 10H), 5.70 (s, 1H), 4.89 (s, 1H), 4.71 (d, *J* = 12.4 Hz, 1H), 4.51 (d, *J* = 12.4 Hz, 1H), 4.40 (q, *J* = 6.6 Hz, 1H), 4.32 – 4.21 (m, 1H), 4.21 – 4.13 (m, 1H), 4.05 (td, *J* = 9.0, 8.6, 3.6 Hz, 1H), 3.83 – 3.70 (m, 4H), 3.21 (m, 2H), 2.07 (s, 3H), 1.81 (s, 3H), 1.49 (m, 2H), 1.37 (d, *J* = 7.0 Hz, 3H), 1.27 (br s, 9H), 0.91 – 0.81 (m, 3H).

^{13}C NMR (126 MHz, DMSO-d_6): δ 173.10, 171.79, 170.22 169.42, 165.62, 138.05, 137.99, 134.92, 131.00, 129.27, 129.00, 128.74, 128.61, 128.23, 128.11, 126.37, 125.47, 124.92, 123.12, 100.79, 97.47, 81.25, 77.32, 76.64, 69.27, 68.37, 63.36, 53.64, 49.52, 46.68, 45.12, 31.52, 29.58, 26.65, 24.19, 23.06, 22.56, 19.25, 18.16, 14.43. MS m/z calcd for $C_{43}H_{55}N_5O_{10}$: 801.39; found: 824.40 [M+Na].

6.21 4-Acetamido-3-{(*S*)-2-[(*R*)-2-(2-acetamido-1-benzyl-4,6-*O*-benzylidene-1-*O*-benzyl-α-D-glucopyranos-3-*O*-yl)-propanamido]-propanamido}-*N*-decylbenzamide (**38**)

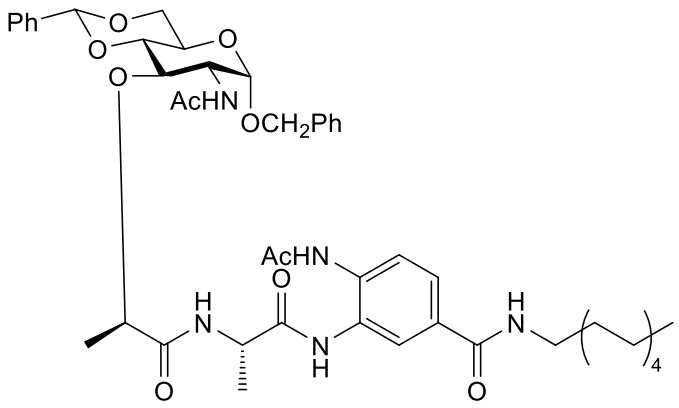

In a similar way as described for the preparation of **37**, to a solution of **33** (200 mg, 0.495 mmol) in dry dichloromethane (5 ml), **36** (281 mg, 0. 495 mmol) was added. The residue was purified by flash column chromatography ($CHCl_3$/MeOH, 5:1) to afford **38** (290 mg, 69%) as white solid. R_f 0.53 ($CHCl_3$/MeOH, 5:1); $[\alpha]_D^{22}$ + 82.6 (C 1.0, $CHCl_3$/MeOH, 1:1), ^{1}H NMR (500 MHz, DMSO-d_6): δ 9.60 (s, 1H), 9.26 (s, 1H), 8.39 (t, *J* = 5.7 Hz, 1H), 8.18 (d, *J* = 8.4 Hz, 1H), 7.90 (s, 1H), 7.77 (d, *J* = 8.4 Hz, 1H), 7.71 (d, *J* = 5.7 Hz, 1H), 7.64 (dd, *J* = 8.4, 2.1 Hz, 1H), 7.46 – 7.21 (m, 10H), 5.69 (s, 1H), 4.88 (s, 1H), 4.70 (d, *J* = 12.4 Hz, 1H), 4.51 (d, *J* = 12.4 Hz, 1H), 4.38 (m, 1H), 4.25 (q, *J* =

7.1 Hz, 1H), 4.17 (dd, *J* = 9.4, 3.4 Hz, 1H), 4.07 – 3.99 (m, 1H), 3.80 – 3.69 (m, 4H), 3.21 (q, *J* = 6.8 Hz, 2H), 2.06 (s, 3H), 1.78 (s, 3H), 1.45 (m, 2H), 1.36 (d, *J* = 7.1 Hz, 3H), 1.30 – 1.19 (m, 17H), 0.84 (m, 3H). ^{13}C NMR (126 MHz, DMSO-d_6) δ 173.18, 171.83, 170.36, 169.57, 165.70, 138.01, 137.95, 131.02, 129.29, 129.04, 128.74, 128.61, 128.22, 128.12, 126.87, 126.36, 100.80, 97.42, 81.21, 77.31, 76.65, 69.27, 68.42, 63.36, 53.61, 49.54, 31.76, 29.55, 29.46, 29.43, 29.25, 29.17, 26.93, 26.90, 24.14, 23.02, 22.57, 19.22, 18.06, 14.44. MS m/z calcd for $C_{47}H_{63}N_5O_{10}$: 857.457; found: 880.47 [M+Na].

6.22 4-Acetamido-3-{(*S*)-2-[(*R*)-2-(2-acetamido-1-benzyl-4,6-*O*-benzylidene-1-*O*-benzyl-α-D-glucopyranos-3-*O*-yl)-propanamido]-propanamido}-*N*-hexadecylbenzamide (**39**)

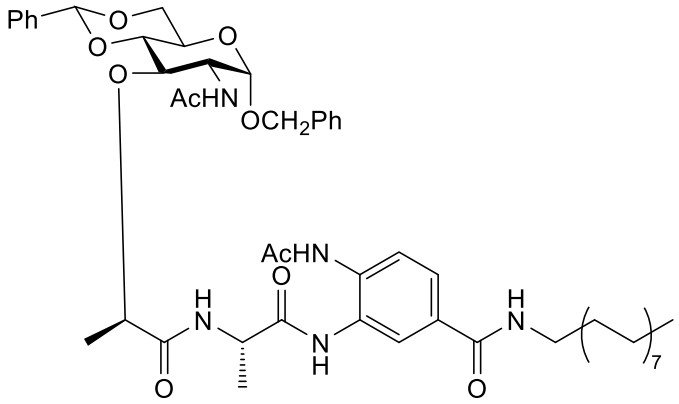

In a similar way as described for the preparation of **37**, to a solution of **34** (86 mg, 0.205 mmol) in dry dichloromethane (5 ml), compound **36** (97 mg, 0. 205 mmol) was added. The residue was purified by flash column chromatography ($CHCl_3$/MeOH/AcOH, 5:1:0.2) to afford **39** (120 mg, 71%) as white solid. R_f 0.34 ($CHCl_3$/MeOH/AcOH, 5:1:0.2); $[\alpha]_D^{22}$ + 23.6 (C 1.0, $CHCl_3$/MeOH,1:1) ^{1}H NMR (500 MHz, DMSO-d_6): δ 7.81

(d, *J* = 8.5 Hz, 1H), 7.70 (s, 1H), 7.57 (d, *J* = 8.5 Hz, 1H), 7.49 (m, 2H), 7.38 – 7.31 (m, 8H), 5.56 (s, 1H), 4.91 (d, *J* = 3.6 Hz, 1H), 4.72 (d, *J* = 11.7 Hz, 1H), 4.49 (d, *J* = 11.7 Hz, 1H), 4.31 (m, 1H), 4.25 (dd, *J* = 10.3, 4.8 Hz, 1H), 4.09 (q, *J* = 6.8 Hz, 1H), 3.88 (m, 1H), 3.81 – 3.72 (m, 2H), 3.66 (t, *J* = 9.2 Hz, 2H), 3.37 (t, *J* = 7.2 Hz, 2H), 2.04 (s, 3H), 1.87 (s, 3H), 1.59 (m, 2H), 1.52 (d, *J* = 7.1 Hz, 3H), 1.39 (d, *J* = 6.8 Hz, 3H), 1.26 (br s, 26H), 0.85 (m, 3H). ^{13}C NMR (126 MHz, DMSO-*d*$_6$) δ 173.10, 171.79, 170.22, 169.42, 165.62, 138.05, 137.99, 134.92, 131.00, 129.27, 129.00, 128.74, 128.61, 128.23, 128.11, 126.37, 125.47, 124.92, 123.12, 100.79, 97.47, 81.25, 77.32, 76.64, 69.27, 68.37, 63.36, 53.64, 49.52, 46.68, 45.12, 45.01, 45.00, 31.52, 29.58, 26.65, 24.19, 23.06, 22.56, 19.25, 18.16, 14.43. MS m/z calcd for $C_{53}H_{75}N_5O_{10}$: 942.55; found: 964.54 [M+Na].

6.23 4-Acetamido-3-{(*S*)-2-[(*R*)-2-(2-acetamido-1-benzyl-4,6-benzylidene-1-*O*-benzyl-α-D-glucopyranos-3-*O*-yl)-propanamido]-propanamido}-benzoic acid (**40**)

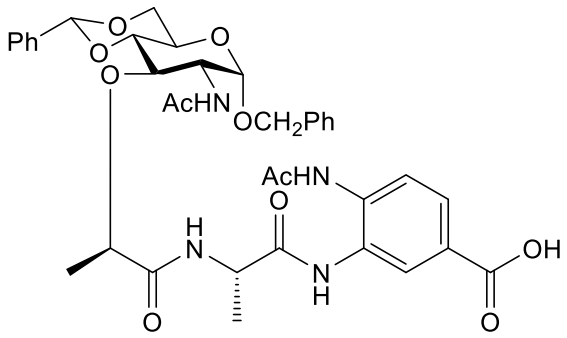

To a solution of **35** (69 mg, 0.261mmol) and **36** (114mg, 0.201 mmol) in DMF (5 ml), DIPEA (0.36ml, 2.785 mmol) was added, and the mixture was stirred at rt for 3 days. The solvent was removed in *vacuo*. The residue was subjected to dry loading flash

column chromatography ($CHCl_3$/MeOH/AcOH, 5:0.5:0.1) to give product **40** (100 mg) which was slightly impure. For structure characterization, impure product **40** was converted to its benzyl ester in the following reaction.

6.24 Benzyl 4-Acetamido-3-{(*S*)-2-[(*R*)-2-(2-acetamido-1-benzyl-4,6-*O*-benzylidene-1-*O*-benzyl-α-D-glucopyranos-3-*O*-yl)-propanamido]-propanamido}-benzoate (**41**)

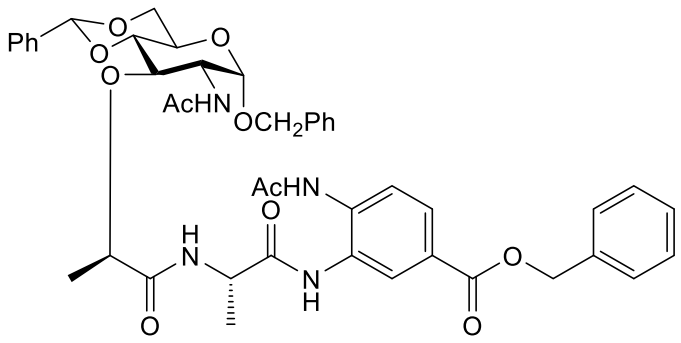

A solution of the impure product **40** (100 mg, crude), benzyl bromide (78 mg, 0.456 mmol), and DIPEA (0.23 ml, 1.779 mmol) in acetonitrile (3 ml) was stirred at rt for 16 h. The solvent was removed in *vacuo*. The residue was subjected to flash column chromatography ($CHCl_3$/MeOH, 5:0.2, then 5:0.7) to give product **41** (90 mg, 89% over two steps). R_f 0.22 ($CHCl_3$/MeOH, 5:0.2); $[\alpha]_D^{22}$ + 24 (C 1.0, MeOH); ^{1}H NMR (500 MHz, chloroform-*d*): δ 8.02 (s, 1H), 7.99 (d, *J* = 8.6 Hz, 1H), 7.94 (dd, *J* = 8.6, 2.0 Hz, 1H), 7.49 – 7.31 (m, 15H), 5.58 (s, 1H), 5.33 (s, 2H), 4.91 (d, *J* = 3.7 Hz, 1H), 4.72 (d, *J* = 11.7 Hz, 1H), 4.50 (d, *J* = 11.7 Hz, 1H), 4.35 – 4.20 (m, 4H), 4.11 (m, 1H), 3.95 – 3.88 (m, 1H), 3.80 (dt, *J* = 10.4, 5.3 Hz, 1H), 3.68 (t, *J* = 10.4 Hz, 1H), 2.19 (s, 3H), 1.87 (s, 3H), 1.26 (d, *J* = 7.0 Hz), 1.38 (d, *J* = 6.8 Hz, 3H). ^{13}C NMR (126 MHz, chloroform-d/methanol-d_4, 2:1): δ 179.08, 174.60, 172.26, 172.09, 170.92, 166.08, 137.24, 137.07,

136.97,136.02, 129.34, 128.78, 128.61, 128.50, 128.39, 128.01, 127.85 126.58, 126.51, 126.14, 123.34, 101.73, 97.58, 81.58, 70.25, 69.04, 67.13, 63.36, 62.64, 59.82, 53.47, 46.73, 45.80, 45.28, 37.28, 23.96, 22.90, 22.71, 19.08, 17.18, 14.20. MS m/z calcd for $C_{44}H_{48}N_4O_{11}$: 808.33; found: 831.33 [M+Na].

6.25 Benzyl 4-Acetamido-3-{(*S*)-2-[(*R*)-2-(2-acetamido-1-*O*-benzyl-α-D-glucopyranos-3-*O*-yl)-propanamido]-propanamido}-benzoate (**42**)

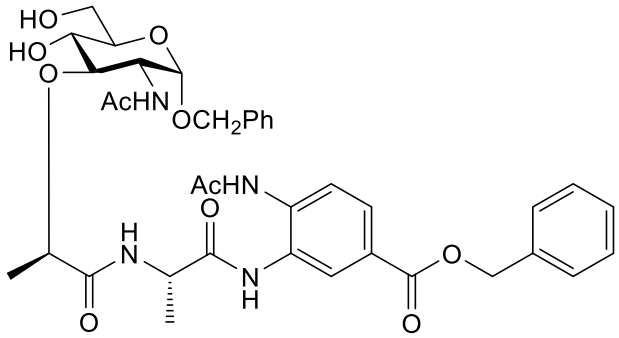

A solution of **41** (24 mg, 0.0297 mmol) in a mixture of dichloromethane (3 mL), TFA (2.75), and H_2O (0.25 ml) was stirred at 0 °C for 1 h. The solvents were then removed in *vacuo.* The residue was subjected to flash column chromatography (CH_2Cl_2/MeOH/H_2O, 5:0.5:0.1, then 5:2:0.1) to afford **42** (20 mg, 94%) as white solid. R_f 0.07 (CH_2Cl_2/MeOH, 5:0.5:); $[\alpha]_D^{22}$ + 15.00 (C 0.5, $CHCl_3$/MeOH, 1:1). ^{1}H NMR (500 MHz, methanol-d_4): δ 8.07 (s, 1H), 7.93 (s, 1H), 7.66 (t, *J* = 3.1 Hz, 1H), 7.45 (s, 8H), 7.36 – 7.21 (m, 2H), 5.33 (s, 2H), 4.85 (d, *J* = 3.5 Hz, 1H), 4.68 (d, *J* = 11.8 Hz, 1H), 4.46 (d, *J* = 11.8 Hz, 1H), 4.24 (q, *J* = 6.7 Hz, 1H), 4.07 (dd, *J* = 10.5, 3.6 Hz, 1H), 3.79 (m, 2H), 3.77 – 3.69 (m, 3H), 3.68 – 3.54 (m, 3H), 2.23 (s, 3H), 1.87 (s, 3H), 1.52 (d, *J* = 7.1 Hz, 3H), 1.39 (d, *J* = 6.7 Hz, 3H). ^{13}C NMR (126 MHz, chloroform- *methanol-d_4*) δ

175.02, 172.76, 171.93, 171.02, 166.09, 137.22, 136.16, 128.83, 128.73, 128.62, 128.54, 128.42,128.39, 128.33, 128.00,126.86, 123.44, 97.14, 79.85, 72.58, 70.01, 69.94, 67.15, 62.64, 61.93, 59.94, 53.33, 46.84, 45.88, 41.41, 32.14, 29.71, 23.88, 22.80 18.76, 17.14, 14.10. MS m/z calcd for $C_{37}H_{44}N_4O_{11}$: 720.30; found: 721.33 [M+H], and 743.32 [M+Na].

6.26 4-Acetamido-3-{(*S*)-2-[(*R*)-2-(2-acetamido-α/β-D-glucopyranos-3-*O*-yl)-propanamido]-propanamido}-benzoic acid (**2**)

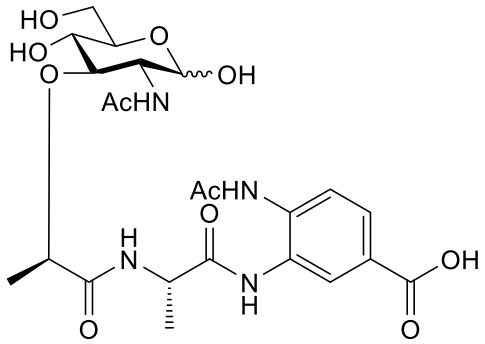

To a solution of **41** (20 mg, 0.0247mmol) in a mixture of THF/ AcOH 1:1, Pd-C (10%, 20 mg) was added. The mixture was stirred under hydrogen gas with bubbling technique for a week. The mixture was filtrated, and the solid washed with acetic acid (5 ml x 2). The filtrate was concentrated by *vacuum*. The residue was subjected to purification by flash column chromatography ($CHCl_3$/MeOH/H_2O, 5:1:0.1) to afford **2** (5mg, 38%) as white solid. Rf 0.1 (chloroform/methanol, 5:1). Compound **2** was not pure and therefore not structurally characterized.

6.27 4-Acetamido-3-{(*S*)-2-[(*R*)-2-(2-acetamido-1-*O*-benzyl-α-D-glucopyranos-3-*O*-yl)-propanamido]-propanamido}benzoic acid (**3**)

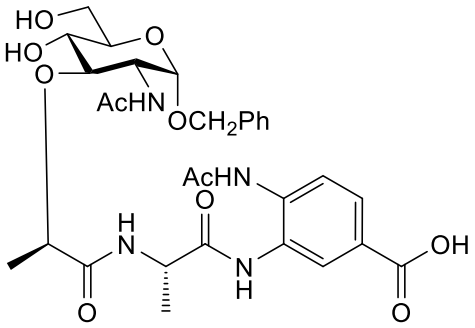

A solution of **41** (10 mg, 0.013 mmol) was dissolved in THF (2 ml) and aqueous 1 M LiOH solution (1 ml) was added. The mixture was stirred at rt for 16 h. The mixture was neutralized by adding strong acidic ion-exchange resin (Amberlite IR-120H, H^+ form). The resin was filtrated and the filtrate concentrated in vacuo. The residue was then subjected to purification through reversed-phase cartridge filtration to yield **3** (5 mg, 63%) as light beige product. R_f 0.1(dichloromethane/methanol, 4:1) Compound **3** was not pure and therefore not structurally characterized.

6.28 4-Acetamido-3-{(*S*)-2-[(*R*)-2-(2-acetamido-α/β-D-glucopyranos-3-*O*-yl)-propanamido]-propanamido}-*N*-hexylbenzamide (**4**)

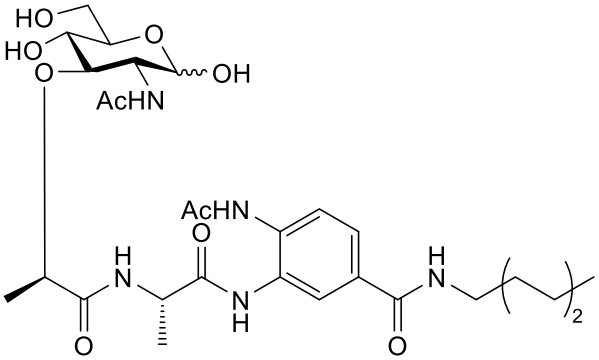

To a solution of **37** (35 mg, 0.044 mmol) in a mixture of THF-AcOH (1:1, 40 ml), Pd-C (10%, 70 mg) was added. The mixture was stirred under hydrogen gas for a week. The mixture was filtrated, and the solid washed with acetic acid (5 ml, x 2) The solvents were removed under vacuum. The residue was purified by flash column chromatography ($CHCl_3$/MeOH/H_2O, 5:1:0.1) to afford **4** (27 mg, 69%) as white solid. Compound **4** was obtained as an anomeric mixture with α/β ratio of approximately 10:1. R_f 0.12 ($CHCl_3$/MeOH 5:1), $[\alpha]_D^{22}$ + 10.2 (C 1.0, $CHCl_3$/MeOH, 1:1). ^{1}H NMR (500 MHz, methanol-d_4) for the α-isomer: δ 7.91 (s, 1H), 7.86 (dd, *J* = 8.6, 2.1 Hz, 1H), 7.71 (dd, *J* = 8.6, 2.1 Hz, 1H), 5.11 (d, *J* = 3.5 Hz, 1H), 4.43 (q, *J* = 7.1 Hz, 1H), 4.38 – 4.35 (m, 1H), 3.99 (dd, *J* = 10.5, 3.5 Hz, 1H), 3.83 – 3.80 (m, 1H), 3.74 – 3.71 (m, 1H), 3.55 – 3.47 (m, 1H), 3.40 – 3.36 (m, 4H), 2.26 (s, 3H), 1.94 (s, 3H), 1.68 – 1.61 (m, 2H), 1.55 (d, *J* = 7.1 Hz, 3H), 1.43 (d, *J* = 7.0 Hz, 3H), 1.41 – 1.32 (m, 6H), 1.00 – 0.91 (m, 3H). ^{13}C NMR (126 MHz, methanol-d_4) for the α-isomer: δ 176.62, 174.33, 173.59, 172.59, 169.10, 132.94, 130.25, 162.71, 126.62, 124.88, 92.83, 81.18, 78.60, 73.40, 71.48, 63.93, 62.89, 60.50, 58.29, 55.47, 41.28, 32.85, 30.61, 27.93, 23.78, 23.03, 19.60, 17.72, 14.51.MS m/z calcd for $C_{29}H_{45}N_5O_{10}$: 623.32; found: 646.33 [M+Na].

6.29 4-Acetamido-3-{(*S*)-2-[(*R*)-2-(2-acetamido-α/β-D-glucopyranos-3-*O*-yl)-propanamido]-propanamido}-*N*-decylbenzamide (**5**)

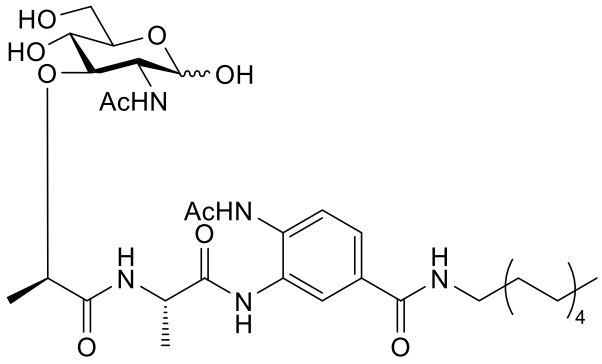

In a similar way as described for the preparation of **4**, to a solution of **38** (90 mg, 0.105 mmol) in a mixture of THF/AcOH (1:1, 60 ml), Pd-C (10%, 80 mg) was added. The mixture was stirred under hydrogen gas at 35°C for eight days. The solvents were removed in vacuum. The residue was purified by flash column chromatography ($CHCl_3$/MeOH/H_2O, 5:1:0.2) to afford **5** (22 mg, 31%) as white solid. Compound **5** was obtained as an anomeric mixture with α/β ratio of approximately 3:1. R_f 0.12 ($CHCl_3$/MeOH, 5:1). $[\alpha]_D^{22}$ +12 (C 0.25, $CHCl_3$/MeOH, 1:1). ^{1}H NMR (500 MHz, methanol-d_4): δ 8.05 – 7.50 (m, 3H), 5.14 (d, 3.6 Hz, 1H, H-1 for the α-isomer), 4.00 (dd, *J* = 10.4, 3.6 Hz, 1H), 3.87 (m, 1H), 3.82 (m, 1H), 3.78 – 3.66 (m, 4H), 3.56 – 3.46 (m, 1H), 3.37 (m, 2H), 2.24 (s, 3H), 1.98 (s, 3/4 H), 1.96 (s, 9/4H), 1.63 (m, 2H), 1.53 (d, *J* = 7.0 Hz, 3H), 1.43 (d, *J* = 6.7 Hz, 3H), 1.35 – 1.21 (m, 14H), 0.89 (m, 3H). ^{13}C NMR (126 MHz, methanol-d_4): δ 174.94, 172.61, 171.90, 167.63, 167.17, 132.88, 128.44, 125.60, 124.86,122.30, 91.40, 71.65, 70.18, 62.37, 59.46, 55.87, 53.70, 46.43, 45.00, 40.12, 31.73, 26.92, 22.55, 22.40,18.41, 16.76, 13.64. MS m/z calcd for $C_{33}H_{53}N_5O_{10}$: 679.38; found: 702.39 [M+Na].

6.30 4-Acetamido-3-{(*S*)-2-[(*R*)-2-(2-acetamido-α/β-D-glucopyranos-3-*O*-yl)-propanamido]-propanamido}-*N*-hexadecylbenzamide (**6**)

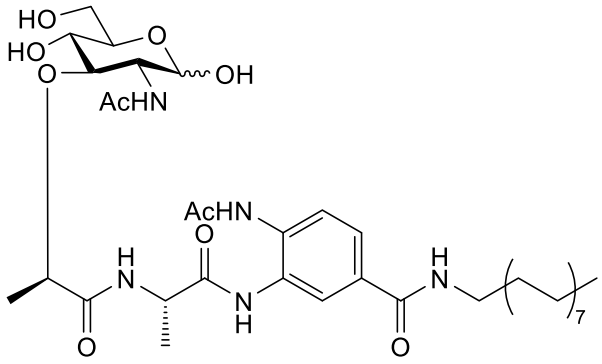

In a similar way as described for the preparation of **4**, to a solution of **39** (50 mg, 0.0546 mmol) in a mixture of THF/AcOH (1:1, 40 ml), Pd-C (10%, 45 mg) was added. The mixture was stirred under hydrogen gas for eight days. The solvents were removed by vacuum. The residue was purified by flash column chromatography ($CHCl_3$/MeOH/H_2O, 5:1:0.1) to afford **6** (26 mg, 63%) as an anomeric mixture (α/β = ~ 6:1) as white solid. R_f 0.18 ($CHCl_3$/MeOH 5:1). $[\alpha]_D^{22}$ + 15.7 (C 1.0, $CHCl_3$/MeOH, 1:1). ^{1}H NMR (500 MHz, methanol-d_4) for the α-isomer): δ 7.86 (s, 1H), 7.81 (d, *J* = 8.5 Hz, 1H), 7.72 (d, *J* = 8.5 Hz, 1H), 5.12 (s, 1H), 4.45 – 4.27 (m, 3H), 3.99 (dd, *J* = 10.4, 2.1 Hz, 1H), 3.82 (m, 2H), 3.75 – 3.72 (m, 4H), 3.68 (m, 1H), 3.55 – 3.44 (m, 1H), 3.41 – 3.33 (m, 2H), 2.25 (s, 3H), 1.94 (s, 3H), 1.62 (m, 2H), 1.53 (d, *J* = 7.2 Hz, 3H), 1.43 (d, *J* = 6.8 Hz, 3H), 1.27 (s, 26H), 0.89 (t, *J* = 6.8 Hz, 3H). ^{13}C NMR (126 MHz, methanol-d_4): δ 174.99 172.74, 172.05, 171.12, 167.65, 164.76, 159.86, 134.73, 131.46, 128.40, 125.52, 125.07, 123.42, 91.31, 71.72, 69.84, 62.42, 61.49, 58.06, 56.40, 53.80, 52.49, 51.08, 46.30, 45.43 40.01, 31.77, 29.51, 29.48, 29.44, 29.23, 28.8926.90, 23.01, 22.48, 22.01 18.30, 16.54,13.52. MS m/z calcd for $C_{39}H_{65}N_5O_{10}$: 763.47; found: 646.33 [M+Na].

6.31 4-Acetamido-3-{(*S*)-2-[(*R*)-2-(2-acetamido-1-*O*-benzyl-α-D-glucopyranos-3-*O*-yl)-propanamido]-propanamido}-*N*-hexylbenzamide (**7**)

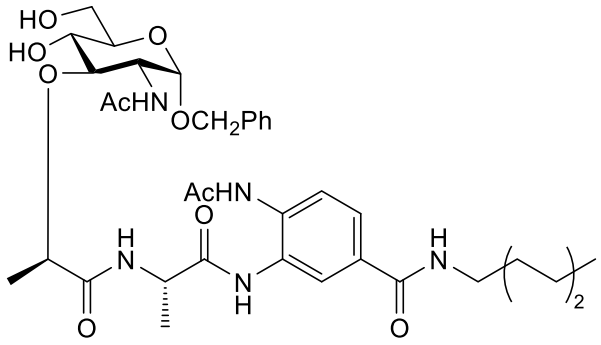

A solution of **37**(27 mg, 0.03366 mmol) in a mixture of dichloromethane (3 ml), TFA (2.75 ml) and H_2O (0.25 ml) was stirred at 0 °C for 1 h. The solvents were then removed in *vacuo.* The residue was subjected to flash column chromatography (CH_2Cl_2/MeOH/H_2O, 5:0.5:0.1) to afford **7** (24 mg, quant) as white solid. R_f 0.15 (CH_2Cl_2/MeOH/H_2O, 5:0.5:0.1); $[\alpha]_D^{22}$ + 48.8 (C 1.0, MeOH). ^{1}H NMR (500 MHz, methanol-d_4): δ 8.10 (d, *J* = 2.1 Hz, 1H), 7.96 (d, *J* = 8.5 Hz, 1H), 7.86 (dd, *J* = 8.5, 2.1 Hz, 1H), 7.56 – 7.40 (m, 5H), 5.01 (d, *J* = 3.6 Hz, 1H), 4.67 (d, *J* = 10.6 Hz, 1H), 4.59 (t, *J* = 10.6 Hz, 1H), 4.55 – 4.49 (m, 2H), 4.19 (dd, *J* = 10.6, 3.6 Hz, 1H), 4.05 – 3.96 (m, 1H), 3.72 – 3.62 (m, 1H), 3.55 – 3.47 (m, 4H), 2.38 (s, 3H), 2.04 (s, 3H), 1.84 – 1.73 (m, 2H), 1.68 (d, *J* = 7.1 Hz, 3H), 1.59 (d, *J* = 6.7 Hz, 2H), 1.54 – 1.44 (m, 6H), 1.12 – 1.03 (m, 3H). ^{13}C NMR (126 MHz, methanol-d_4): δ 174.98, 172.73, 171.97, 171.06, 167.50, 137.45, 134.75, 131.52, 128.00, 127.96, 127.49, 125.11, 125.03, 123.42, 96.18, 79.68, 77.08, 72.84, 70.04, 68.86, 62.38, 61.22, 58.11, 56.47, 53.33, 49.93, 39.74, 31.28,

29.05, 26.36, 22.46, 22.20, 21.42, 18.10, 16.20, 12.93. MS m/z calcd for $C_{36}H_{51}N_5O_{10}$: 713.36; found: 736.35 [M+Na].

6.32 4-Acetamido-3-{(*S*)-2-[(*R*)-2-(2-acetamido-1-*O*-benzyl-α-D-glucopyranos-3-*O*-yl)-propanamido]-propanamido}-*N*-decylbenzamide (**8**)

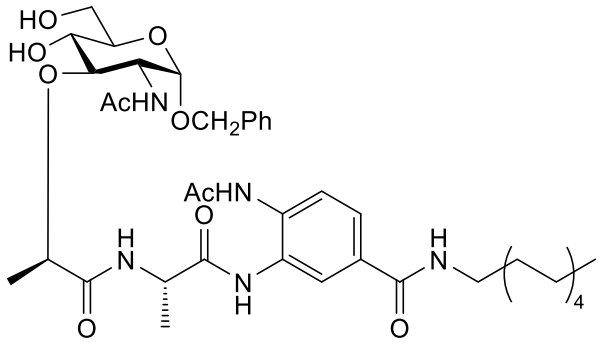

In a similar way as described for the preparation of **7**, a solution of **38** (98 mg, 0.1143 mmol) in a mixture of dichloromethane (3 ml), TFA (2.75 ml) and H_2O (0.25 ml) was stirred at 0 °C for 1 h. The solvents were then removed in *vacuo.* The residue was subjected to flash column chromatography (CH_2Cl_2/MeOH/H_2O, 5:1:0.1) to afford **8** (45 mg, 51%) as white solid. R_f 0.47 (CH_2Cl_2/MeOH/H_2O, 5:1); $[\alpha]_D^{22}$ + 26.2 (C 1.0, $CHCl_3$MeOH,1:1). ^{1}H NMR (500 MHz, Methanol-d_4): δ 7.95 (d, *J* = 2.1 Hz, 1H), 7.83 (d, *J* = 8.5 Hz, 1H), 7.71 (dd, *J* = 8.5, 2.1 Hz, 1H), 7.40 – 7.23 (m, 5H), 4.84 (d, *J* = 3.6 Hz, 1H), 4.71 (d, *J* = 11.7 Hz, 1H), 4.52 (d, *J* = 11.7 Hz, 1H), 4.44 – 4.33 (m, 3H), 4.02 (dd, *J* = 10.6, 3.6 Hz, 1H), 3.84 (dd, *J* = 10.6, 2.0 Hz, 1H), 3.57 – 3.48 (m, 1H), 3.41 – 3.29 (m, 4H), 2.23 (s, 3H), 1.87 (s, 3H), 1.61 (m, 2H), 1.53 (d, *J* = 7.1 Hz, 3H), 1.42 (d, *J* = 6.8 Hz, 3H), 1.36 – 1.24 (m, 14H), 0.92 (t, *J* = 6.8 Hz, 3H).^{13}C NMR (126 MHz, methanol-d_4): δ 174.97, 172.71, 171.95, 171.05, 167.46, 137.41, 137.39, 134.76,

128.05, 128.00, 127.98,127.97,127.54, 127.52, 125.22, , 96.18, 79.67, 72.80, 69.98, 68.88, 62.39, 61.25, 59.06, 57.96, 56.42, 53.31, 39.82, 31.67, 29.30, 29.13,29.05 26.75, 22.64, 22.49, 21.56, 18.20, 16.31, 13.17.MS m/z calcd for $C_{40}H_{59}N_5O_{10}$: 769.43; found: 792.44 [M+Na].

6.33 4-Acetamido-3-{(*S*)-2-[(*R*)-2-(2-acetamido-1-*O*-benzyl-α-D-glucopyranos-3-*O*-yl)-propanamido]-propanamido}-*N*-hexadecylbenzamide (**9**)

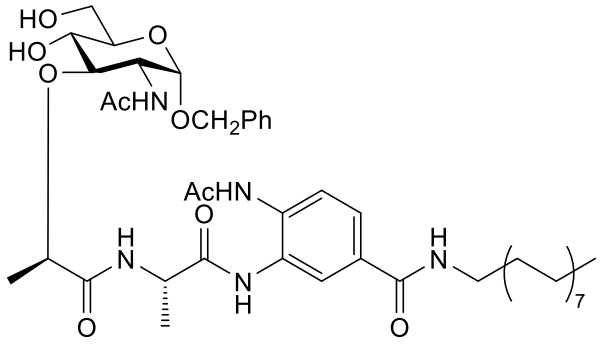

In a similar way as described for the preparation of **7**, a solution of **39** (20 mg, 0.0218 mmol) in a mixture of dichloromethane (3 ml), TFA (2.75 ml) and H_2O (0.25 ml) was stirred at 0 °C for 1 h. The solvents were then removed in *vacuo.* The residue was subjected to flash column chromatography (CH_2Cl_2/MeOH/H_2O, 5:1) to afford **9** (10 mg, 72%) as white solid. R_f 0.47 (CH_2Cl_2/MeOH/H_2O, 5:1); $[\alpha]_D^{22}$ + 30.2 (C 1.0, $CHCl_3$/MeOH, 1:1). ^{1}H NMR (500 MHz, methanol-d_4): δ 7.95 (d, *J* = 2.1 Hz, 1H), 7.83 (d, *J* = 8.5 Hz, 1H), 7.71 (dd, *J* = 8.5, 2.1 Hz, 1H), 7.42 – 7.23 (m, 5H), 4.84 (d, *J* = 3.6 Hz, 1H), 4.71 (d, *J* = 12.0 Hz, 1H), 4.51 (d, *J* = 12.0 Hz, 1H), 4.36 (m, 3H), 4.02 (dd, *J* = 10.6, 3.6 Hz, 1H), 3.91 – 3.81 (m, 1H), 3.58 – 3.48 (m, 1H), 3.37 (m, 4H), 2.23 (s, 3H), 1.87 (s, 3H), 1.61 (m, 3H), 1.53 (d, *J* = 7.1 Hz, 3H), 1.43 (d, *J* = 6.7 Hz, 3H), 1.31 (br s,

26H), 0.92 (t, *J* = 6.7 Hz, 3H).^{13}C NMR (126 MHz, methanol-d_4): δ 174.99, 172.76, 171.97, , 167.43, 159.93, 137.43, 134.77, 131.33, 128.73, 127.99 , 127.97, 127.49, 125.10, 125.08, 123.33, 95.99, 85.93, 79.67, 77.16, 72.82, 69.91, 68.68, 64.78, 62.38, 61.15, 58.92, 58.16, 56.43, 55.40, 53.29, 49.90, 46.16, 45.11, 39.71, 31.70, 29.42, 29.39 ,29.35, 29.32,29.09, 26.72, 22.36, 21.36, 18.09, 16.16, 13.08. MS m/z calcd for $C_{46}H_{71}N_5O_{10}$: 854.099; found: 876.52 [M+Na].

7. REFERENCES

1. Saxena, M., & Yeretssian, G. (2014). NOD-like receptors: master regulators of inflammation and cancer. *Frontiers in Immunology*, *5*, 327.
2. Behr, M. A., & Divangahi, M. (2015). Freund's adjuvant, NOD2 and mycobacteria. *Current Opinion in Microbiology*, *23*, 126-132.
3. Janeway Jr, C. A., & Medzhitov, R. (2002). Innate immune recognition. *Annual Review of Immunology*, *20*(1), 197-216.
4. Chaplin, D. D. (2010). Overview of the immune response. *Journal of Allergy and Clinical Immunology*, *125*(2), S3-S23.
5. Diacovich, L., & Gorvel, J. P. (2010). Bacterial manipulation of innate immunity to promote infection. *Nature Reviews Microbiology*, *8*(2), 117.
6. Kusumoto, S., Fukase, K., & Shiba, T. (2010). Key structures of bacterial peptidoglycan and lipopolysaccharide triggering the innate immune system of higher animals: chemical synthesis and functional studies. *Proceedings of the Japan Academy, Series B*, *86*(4), 322-337.
7. Kim, Y. K., Shin, J. S., & Nahm, M. H. (2016). NOD-like receptors in infection, immunity, and diseases. *Yonsei Medical Journal*, *57*(1), 5-14.
8. Cui, J., Chen, Y., Wang, H. Y., & Wang, R. F. (2014). Mechanisms and pathways of innate immune activation and regulation in health and cancer. *Human Vaccines & Immunotherapeutics*, *10*(11), 3270-3285.
9. Jin, H. S., Park, J. K., & Jo, E. K. (2014). Toll-like receptors and NOD-like receptors in innate immune defense during pathogenic infection. *Journal of Bacteriology and Virology*, *44*(3), 215-225.

10. Latz, E., Xiao, T. S., & Stutz, A. (2013). Activation and regulation of the inflammasomes. *Nature Reviews Immunology*, *13*(6), 397.
11. Jakopin, Z., Gobec, M., Mlinarič-Raščan, I., & Sollner Dolenc, M. (2012). Immunomodulatory properties of novel nucleotide oligomerization domain 2 (nod2) agonistic desmuramyldipeptides. *Journal of Medicinal Chemistry*, *55*(14), 6478-6488.
12. Strober, W., Murray, P. J., Kitani, A., & Watanabe, T. (2006). Signalling pathways and molecular interactions of NOD1 and NOD2. *Nature Reviews Immunology*, *6*(1), 9.
13. Boyle, J. P., Parkhouse, R., & Monie, T. P. (2014). Insights into the molecular basis of the NOD2 signalling pathway. *Open biology*, *4*(12), 140178.
14. Ogawa, C., Liu, Y. J., & S Kobayashi, K. (2011). Muramyl dipeptide and its derivatives: peptide adjuvant in immunological disorders and cancer therapy. *Current Bioactive Compounds*, *7*(3), 180-197.
15. Laman, A. G., Lathe, R., Shepelyakovskaya, A. O., Gartseva, A., Brovko, F. A., Guryanova, S., ... & Ivanov, V. T. (2016). Muramyl peptides activate innate immunity conjointly via YB1 and NOD2. *Innate Immunity*, *22*(8), 666-673.
16. Glucosaminylmuramyl dipeptide. (n.d.). Retrieved from https://pubchem.ncbi.nlm.nih.gov/compound/3035438
17. Rubino, S. J., Magalhaes, J. G., Philpott, D., Bahr, G. M., Blanot, D., & Girardin, S. E. (2013). Identification of a synthetic muramyl peptide derivative with enhanced Nod2 stimulatory capacity. *Innate Immunity*, *19*(5), 493-503.
18. Cario, E. (2005). Bacterial interactions with cells of the intestinal mucosa: Toll-

like receptors and NOD2. *Gut*, *54*(8), 1182-1193.

19. Barnich, N., Aguirre, J. E., Reinecker, H. C., Xavier, R., & Podolsky, D. K. (2005). Membrane recruitment of NOD2 in intestinal epithelial cells is essential for nuclear factor–κB activation in muramyl dipeptide recognition. *J Cell Biol*, *170*(1), 21-26.
20. Mo, J., Boyle, J. P., Howard, C. B., Monie, T. P., Davis, B. K., & Duncan, J. A. (2012). Pathogen sensing by nucleotide-binding oligomerization domain-containing protein 2 (NOD2) is mediated by direct binding to muramyl dipeptide and ATP. *Journal of Biological Chemistry*, *287*(27), 23057-23067.
21. Chen, K. T., Huang, D. Y., Chiu, C. H., Lin, W. W., Liang, P. H., & Cheng, W. C. (2015). Synthesis of Diverse N-Substituted Muramyl Dipeptide Derivatives and Their Use in a Study of Human NOD2 Stimulation Activity. *Chemistry-A European Journal*, *21*(34), 11984-11988.
22. Jakopin, Z. (2013). Murabutide revisited: a review of its pleiotropic biological effects. *Current Medicinal Chemistry*, *20*(16), 2068-2079.
23. Meyers, P. A. (2009). Muramyl tripeptide (mifamurtide) for the treatment of osteosarcoma. *Expert Review of Anticancer Therapy*, *9*(8), 1035-1049.
24. Gobec, M., Mlinarič-Raščan, I., Dolenc, M. S., & Jakopin, Ž. (2016). Structural requirements of acylated Gly-l-Ala-d-Glu analogs for activation of the innate immune receptor NOD2. *European Journal of Medicinal Chemistry*, *116*, 1-12.
25. Yang, H. Z., Xu, S., Liao, X. Y., Zhang, S. D., Liang, Z. L., Liu, B. H., & Liu, G. (2005). A novel immunostimulator, N 2-[α-O-Benzyl-N-(acetylmuramyl)-L-alanyl-D-isoglutaminyl]-N 6-trans-(m-nitrocinnamoyl)-L-lysine, and its adjuvancy on the

hepatitis B surface antigen. *Journal of medicinal chemistry*, *48*(16), 5112-5122.

26. Khan, F. A., Ulanova, M., Bai, B., Yalamati, D., & Jiang, Z. H. (2017). Design, synthesis and immunological evaluation of novel amphiphilic desmuramyl peptides. *European Journal of Medicinal Chemistry*, *141*, 26-36.
27. Darcissac, E. C., Truong, M. J., Dewulf, J., Mouton, Y., Capron, A., & Bahr, G. M. (2000). The synthetic immunomodulator murabutide controls human immunodeficiency virus type 1 replication at multiple levels in macrophages and dendritic cells. *Journal of Virology*, *74*(17), 7794-7802.
28. Darcissac, E. C., Bahr, G. M., Pouillart, P. R., Riveau, G. J., & Parant, M. A. (1996). Selective potentiation of cytokine expression in human whole blood by murabutide, a muramyl dipeptide analogue. *Cytokine*, *8*(8), 658-666.
29. Samsel, M., Dzierzbicka, K., & Trzonkowski, P. (2014). Synthesis and antiproliferative activity of conjugates of adenosine with muramyl dipeptide and nor-muramyl dipeptide derivatives. *Bioorganic & Medicinal Chemistry Letters*, *24*(15), 3587-3591.
30. Chedid, L. A., Parant, M. A., Audibert, F. M., Riveau, G. J., Parant, F. J., Lederer, E., & Lefrancier, P. L. (1982). Biological activity of a new synthetic muramyl peptide adjuvant devoid of pyrogenicity. *Infection and Immunity*, *35*(2), 417-424
31. Knotigová, P. T., Zyka, D., Masˇ k, J., Kovalová, A., Křupka, M., Bartheldyová, E., & Vacek, A. (2015). Molecular adjuvants based on nonpyrogenic lipophilic derivatives of norAbuMDP/GMDP formulated in nanoliposomes: stimulation of innate and adaptive immunity. *Pharmaceutical Research*, *32*(4), 1186-1199.

32. Yoo, Y. C., Saiki, I., Sato, K., & Azuma, I. (1992). B30-MDP, a synthetic muramyl dipeptide derivative for tumour vaccination to enhance antitumour immunity and antimetastatic effect in mice. *Vaccine*, *10*(11), 792-797
33. Pabst, M. J., Cummings, N. P., Shiba, T., Kusumoto, S., & Kotani, S. (1980). Lipophilic derivative of muramyl dipeptide is more active than muramyl dipeptide in priming macrophages to release superoxide anion. *Infection and Immunity*, *29*(2), 617-622.
34. Kager, L., Pötschger, U., & Bielack, S. (2010). Review of mifamurtide in the treatment of patients with osteosarcoma. *Therapeutics and Clinical Risk Management*, *6*, 279.
35. Knotigová, P. T., Zyka, D., Masˇ k, J., Kovalová, A., Křupka, M., Bartheldyová, E., & Vacek, A. (2015). Molecular adjuvants based on nonpyrogenic lipophilic derivatives of norAbuMDP/GMDP formulated in nanoliposomes: stimulation of innate and adaptive immunity. *Pharmaceutical Research*, *32*(4), 1186-1199.
36. Strober, W., & Watanabe, T. (2011). NOD2, an intracellular innate immune sensor involved in host defense and Crohn's disease. *Mucosal Immunology*, *4*(5), 484.
37. Caruso, R., Warner, N., Inohara, N., & Núñez, G. (2014). NOD1 and NOD2: signaling, host defense, and inflammatory disease. *Immunity*, *41*(6), 898-908.
38. Chamaillard, M., Girardin, S. E., Viala, J., & Philpott, D. J. (2003). Nods, Nalps and Naip: Intracellular regulators of bacterial-induced inflammation. *Cellular Microbiology*, *5*(9), 581-592.
39. Delany, I., Rappuoli, R., & De Gregorio, E. (2014). Vaccines for the 21st

century. *EMBO Molecular Medicine*, *6*(6), 708-720.

40. Hackett, C. J., & Harn Jr, D. A. (Eds.). (2007). *Vaccine Adjuvants*. Springer Science & Business Media

41.. Maisonneuve, C., Bertholet, S., Philpott, D. J., & De Gregorio, E. (2014). Unleashing the potential of NOD-and Toll-like agonists as vaccine adjuvants. *Proceedings of the National Academy of Sciences*, *111*(34), 12294-12299.

42. Coulombe, F., Divangahi, M., Veyrier, F., de Léséleuc, L., Gleason, J. L., Yang, Y., & Behr, M. A. (2009). Increased NOD2-mediated recognition of N-glycolyl muramyl dipeptide. *Journal of Experimental Medicine*, *206*(8), 1709-1716

43. Maisonneuve, C., Bertholet, S., Philpott, D. J., & De Gregorio, E. (2014). Unleashing the potential of NOD- and Toll-like agonists as vaccine adjuvants. *Proceedings of the National Academy of Sciences of the United States of America*, *111*(34), 12294–12299.

44. Strober, W., Kitani, A., Fuss, I., Asano, N., & Watanabe, T. (2008). The molecular basis of NOD2 susceptibility mutations in Crohn's disease. *Mucosal Immunology*, *1*(1s), S5.

45. Goasduff, T., Darcissac, E. C. A., Vidal, V., Capron, A., & Bahr, G. M. (2002). The transcriptional response of human macrophages to murabutide reflects a spectrum of biological effects for the synthetic immunomodulator. *Clinical & Experimental Immunology*, *128*(3), 474-482.

46. Thundimadathil, J. (2012). Cancer treatment using peptides: current therapies and future prospects. *Journal of Amino Acids*, *2012*,1–13.

47. Yamamoto, S., & Ma, X. (2009). Role of Nod2 in the development of Crohn's disease. *Microbes and Infection*, *11*(12), 912-918.
48. Akira, S., Uematsu, S., & Takeuchi, O. (2006). Pathogen recognition and innate immunity. *Cell*, *124*(4), 783-801.
49. Correa, R. G., Milutinovic, S., & Reed, J. C. (2012). Roles of NOD1 (NLRC1) and NOD2 (NLRC2) in innate immunity and inflammatory diseases. *Bioscience Reports*, *32*(6), 597-608.
50. Ma, Y., Zhao, N., & Liu, G. (2011). Conjugate (MTC-220) of muramyl dipeptide analogue and paclitaxel prevents both tumor growth and metastasis in mice. *Journal of Medicinal Chemistry*, *54*(8), 2767-2777.
51. Bahr, G. M., Darcissac, E., Bevec, D., Dukor, P., & Chedid, L. (1995). Immunopharmacological activities and clinical development of muramyl peptides with particular emphasis on murabutide. *International Journal of Immunopharmacology*, *17*(2), 117-131.
52. Dong, Y., Wang, S., Wang, C., Li, Z., Ma, Y., & Liu, G. (2017). Antagonizing NOD2 signaling with conjugates of paclitaxel and muramyl dipeptide derivatives sensitizes paclitaxel therapy and significantly prevents tumor metastasis. *Journal of Medicinal Chemistry*, *60*(3), 1219-1224.
53. Vlahovič k-Kahlina, K., & Jakas, A. (2015). Synthesis of orthogonally protected muramic acid building blocks for solid phase peptide synthesis. *Croatica Chemica Acta*, *88*(2), 151-157.
54. Lefrancier, P., Choay, J., Derrien, M., & Lederman, I. (1977). Synthesis of N-acetyl-muramyl-L-alanyl-D-isoglutamine, an adjuvant of the immune response,

and of some N-acetyl-muramyl-peptide analogs. *Chemical Biology & Drug Design*, *9*(4), 249-257.

55. Osawa, T., & Jeanloz, R. W. (1965). An improved, stereoselective synthesis of 2-amino-3-O-(D-1-carboxyethyl)-2-deoxy-D-glucose (muramic acid). *The Journal of Organic Chemistry*, *30*(2), 448-450.

8. APPENDIX

^{1}H NMR, ^{13}C NMR and MALDI-MS spectra of synthesized compounds

^{1}H NMR spectrum of compound **18** (500 MHz, chloroform-*d*)

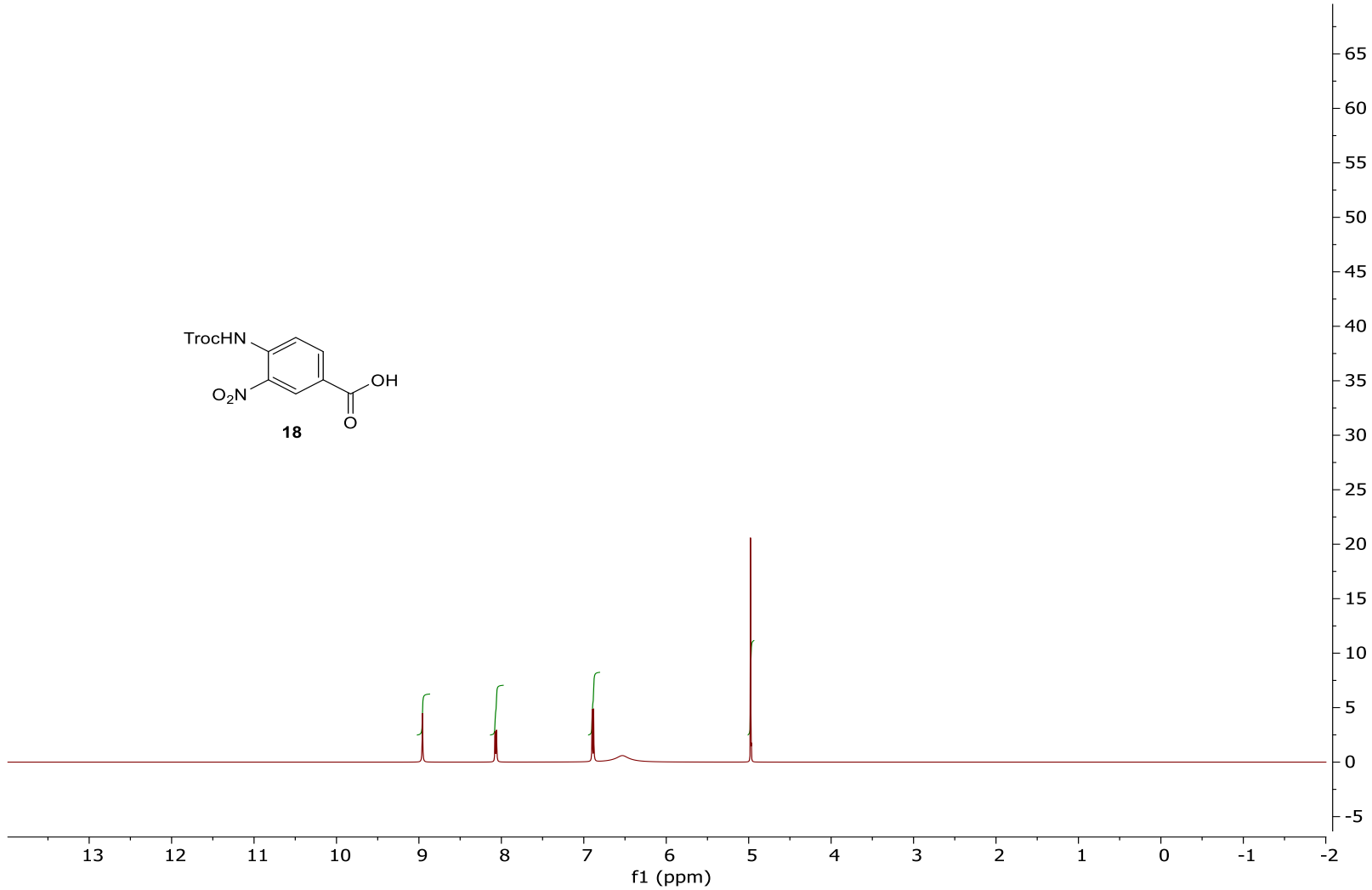

^{1}H NMR spectrum of compound **20**. (500 MHz, chloroform-*d*)

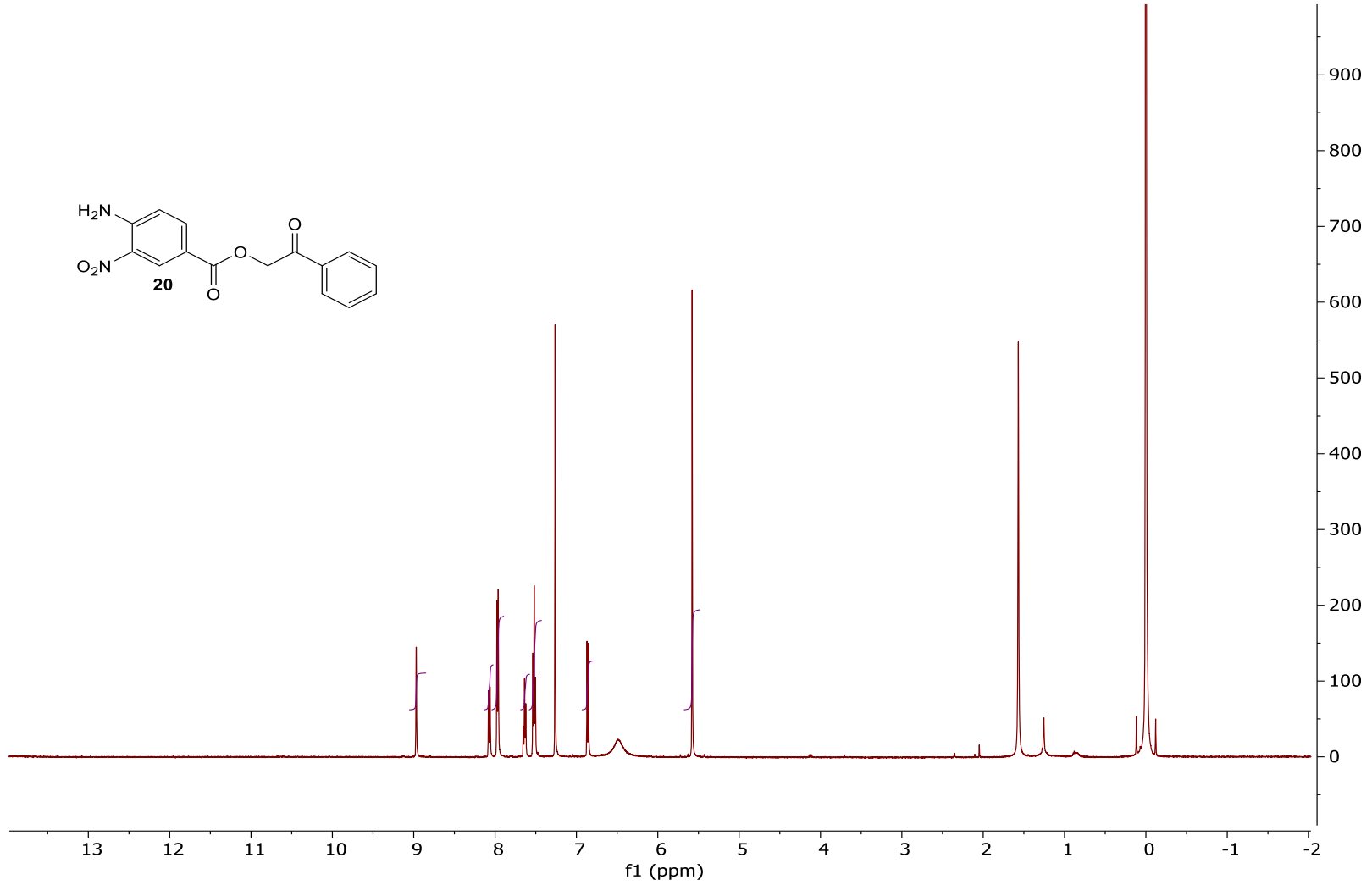

^{13}C NMR spectrum for compound **20**. (126 MHz, chloroform-*d*)

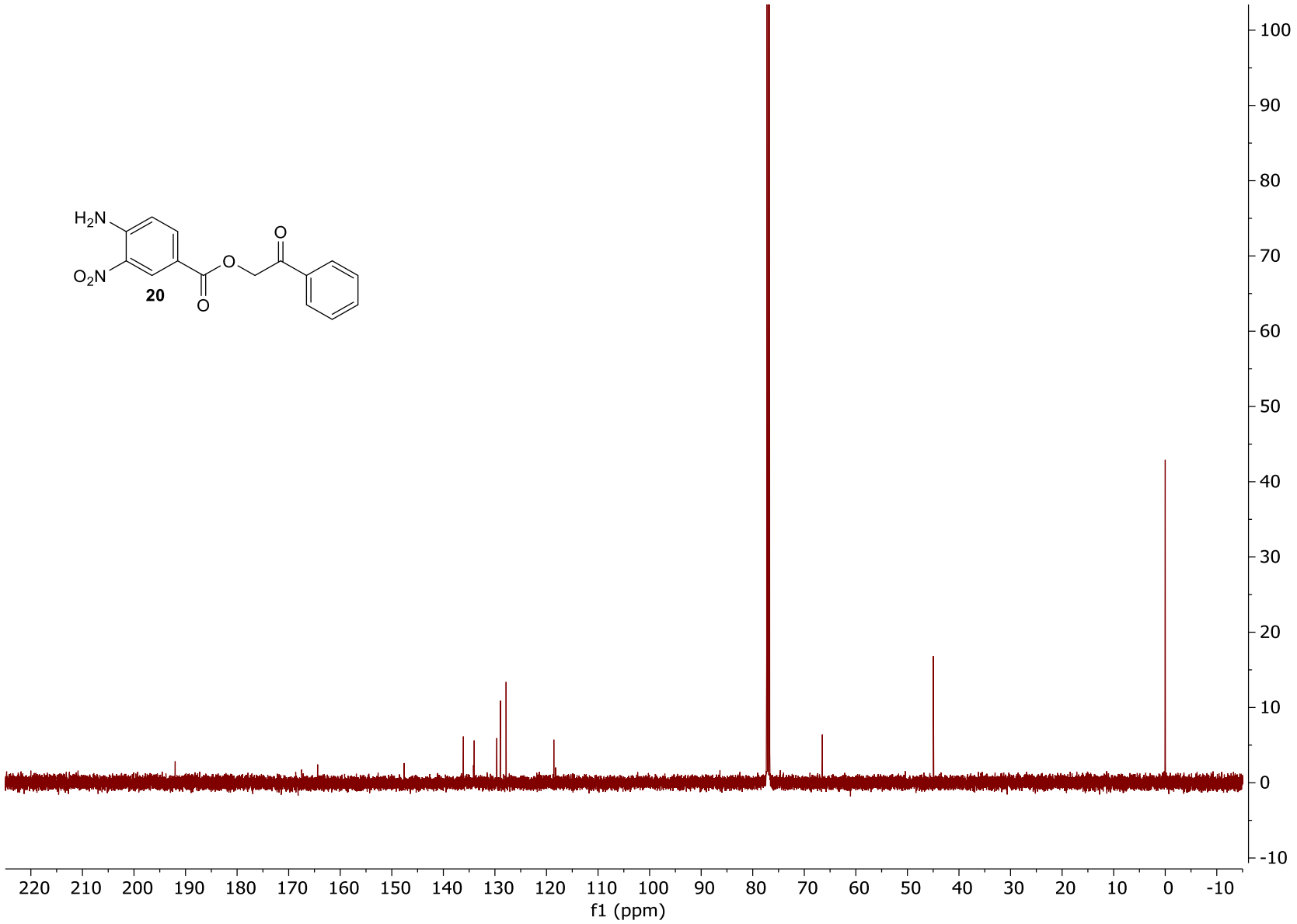

^{1}H NMR spectrum of compound **21**. (500 MHz, chloroform-*d*)

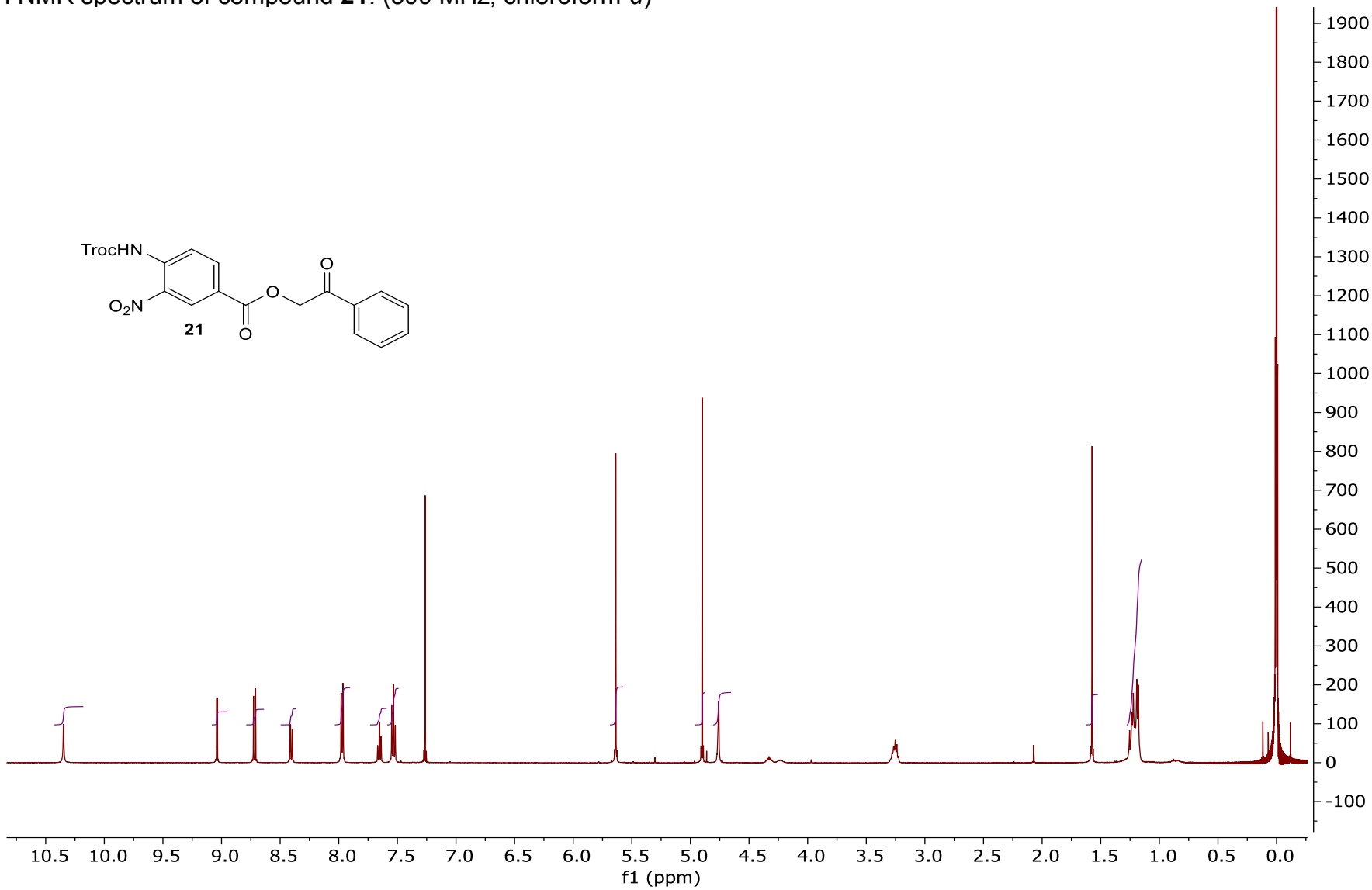

^{13}C NMR spectrum for compound **21**. (126 MHz, chloroform-*d*)

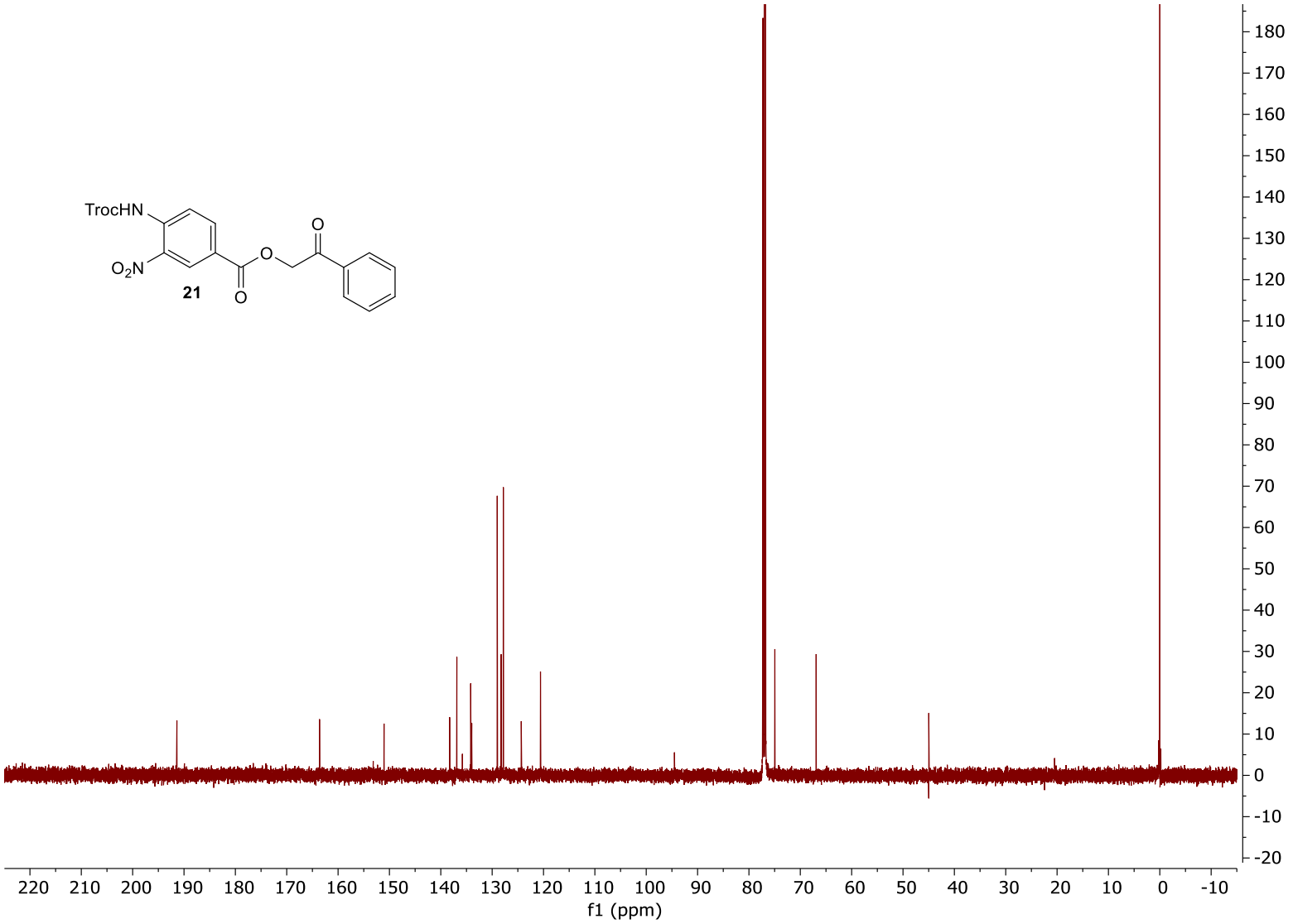

^{1}H NMR spectrum of compound **24**. (500 MHz, chloroform-*d*))

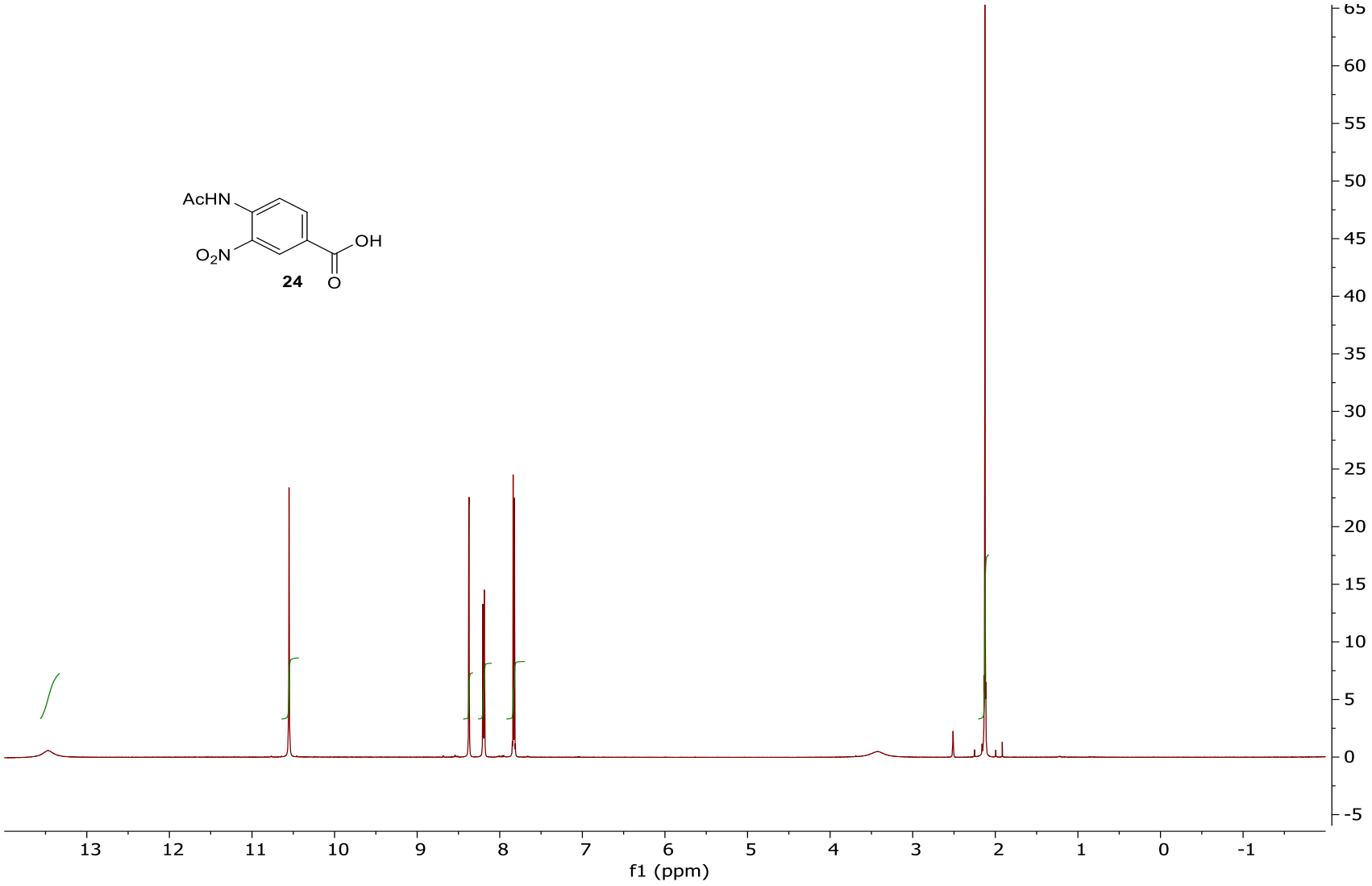

^{13}C NMR spectrum of compound **24**. (126 MHz, chloroform-*d*))

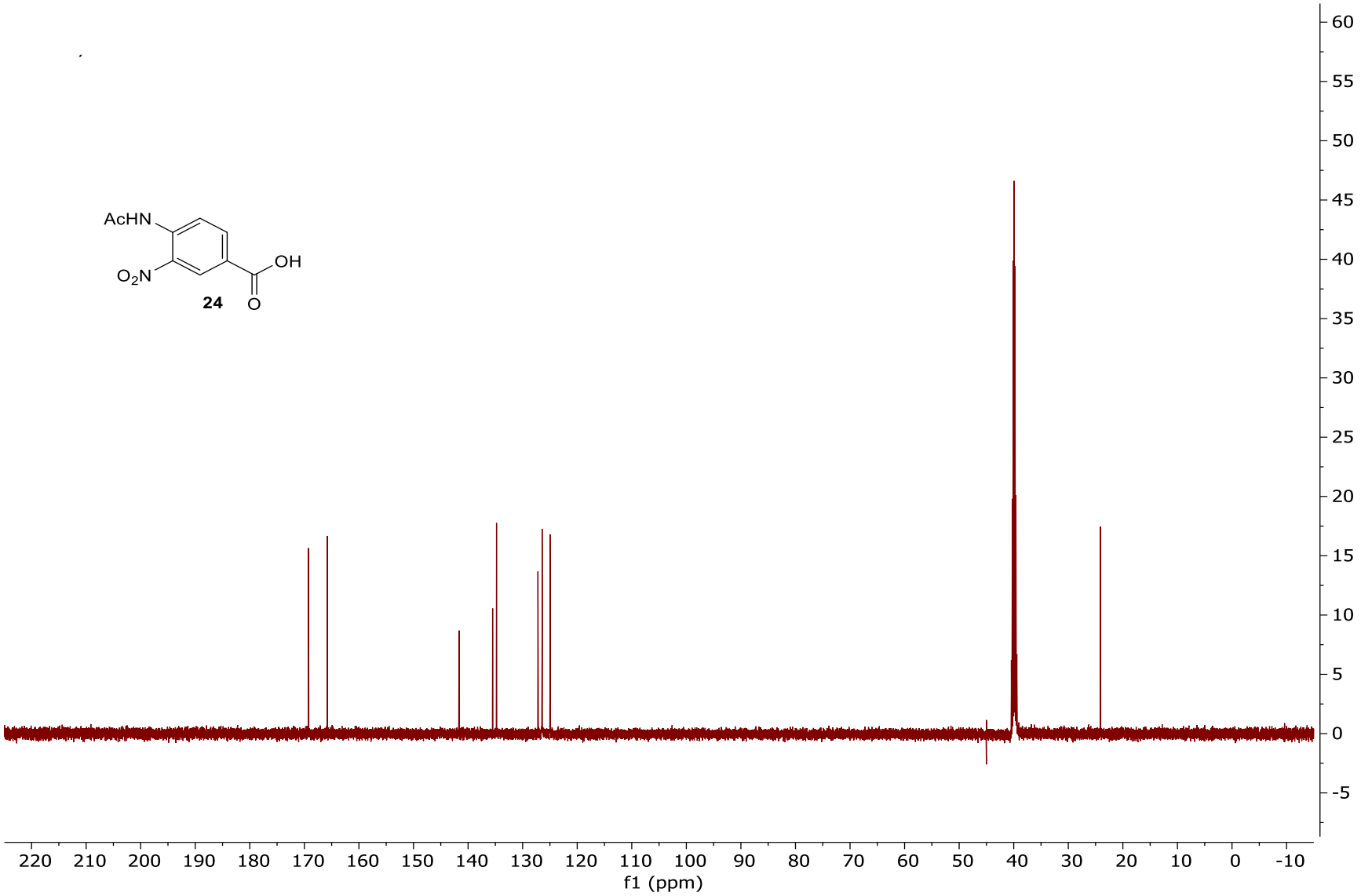

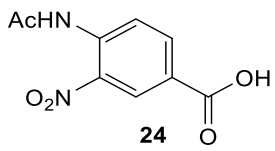

24

MALDI-MS m/z calcd for $C_9H_8N_2O_5$: 224.043; found: 225.048 [M+H], 247.030 [M+Na] and 263.002 [M+K].

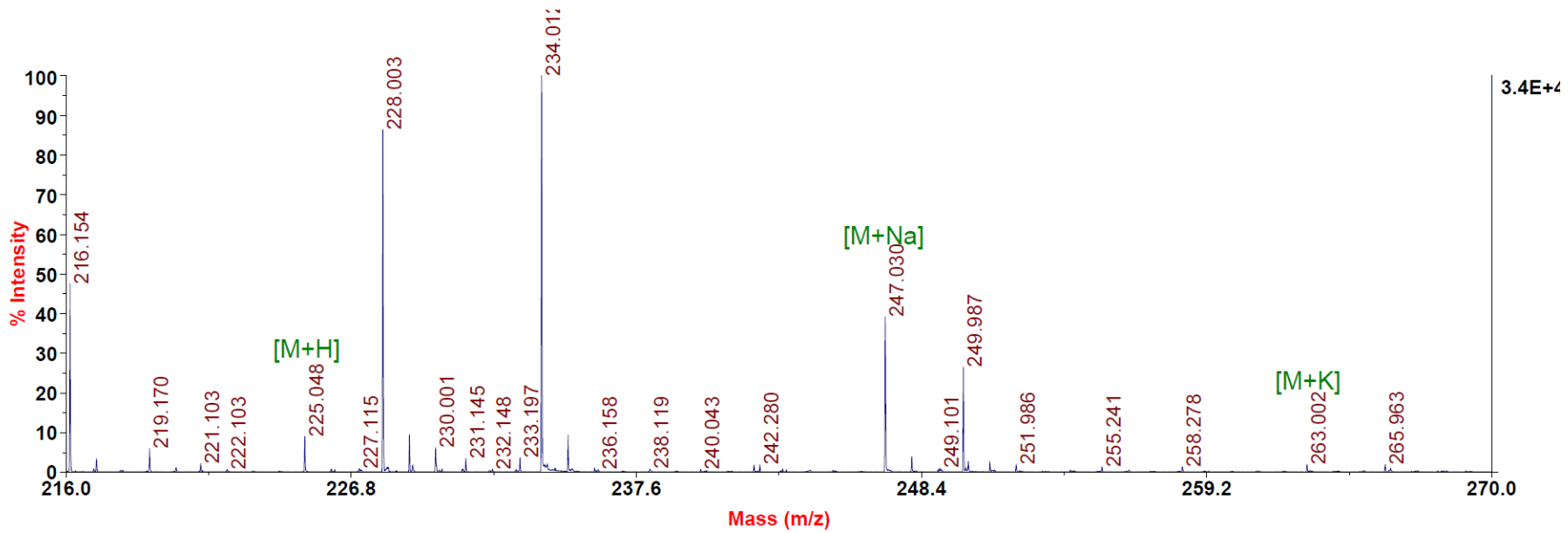

^{1}H NMR spectrum of compound **25**. (500 MHz, chloroform-*d*))

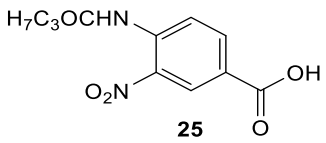

25

^{13}C NMR spectrum of compound **25**. (126 MHz, chloroform-*d*)

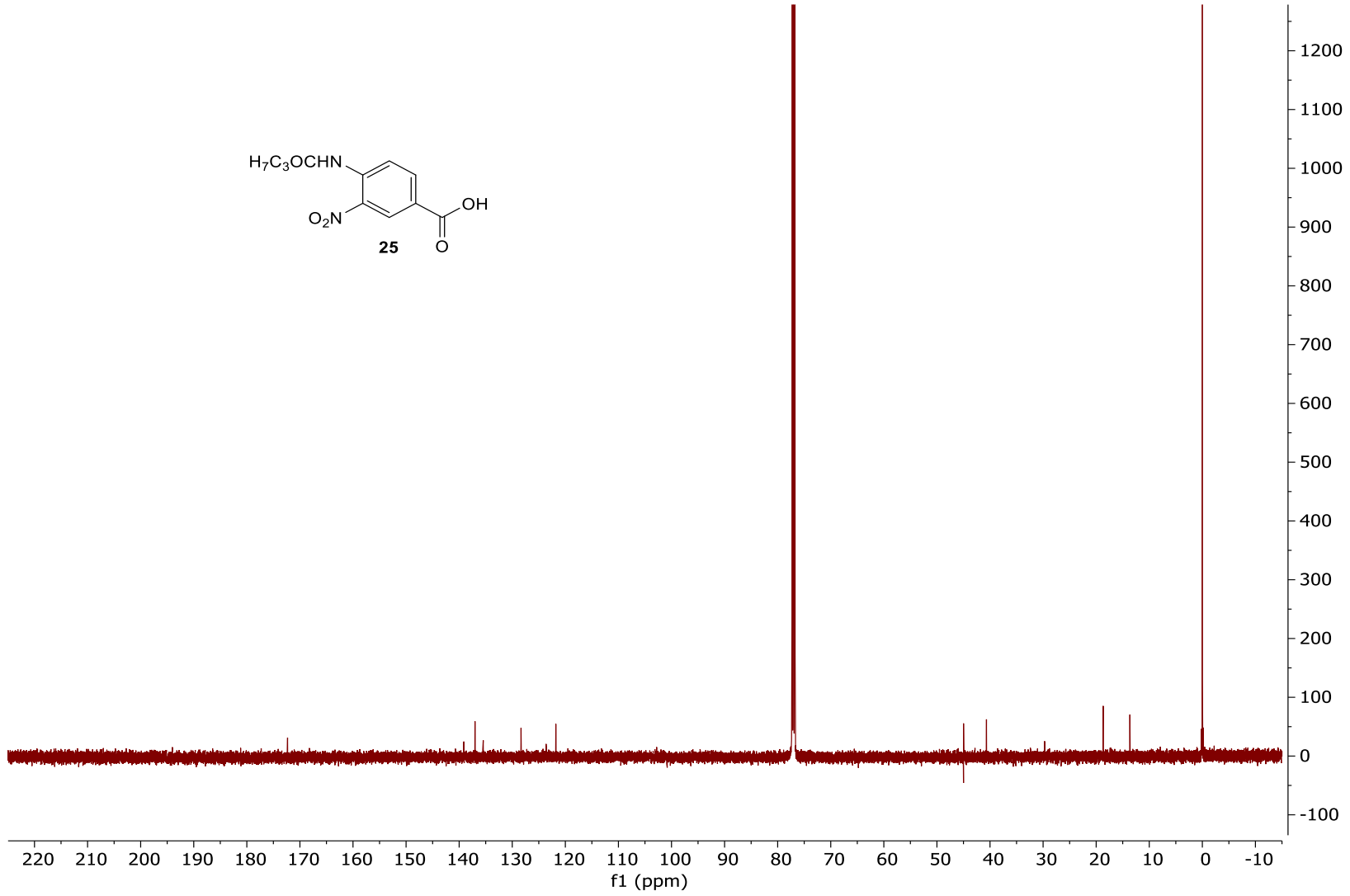

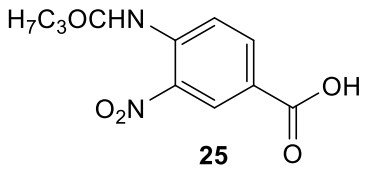

25

MALDI MS m/z calcd for $C_{11}H_{12}N_2O_5$: 252.23; found: 253.065 [M+H], 275.055 [M+Na] and 291.030 [M+K].

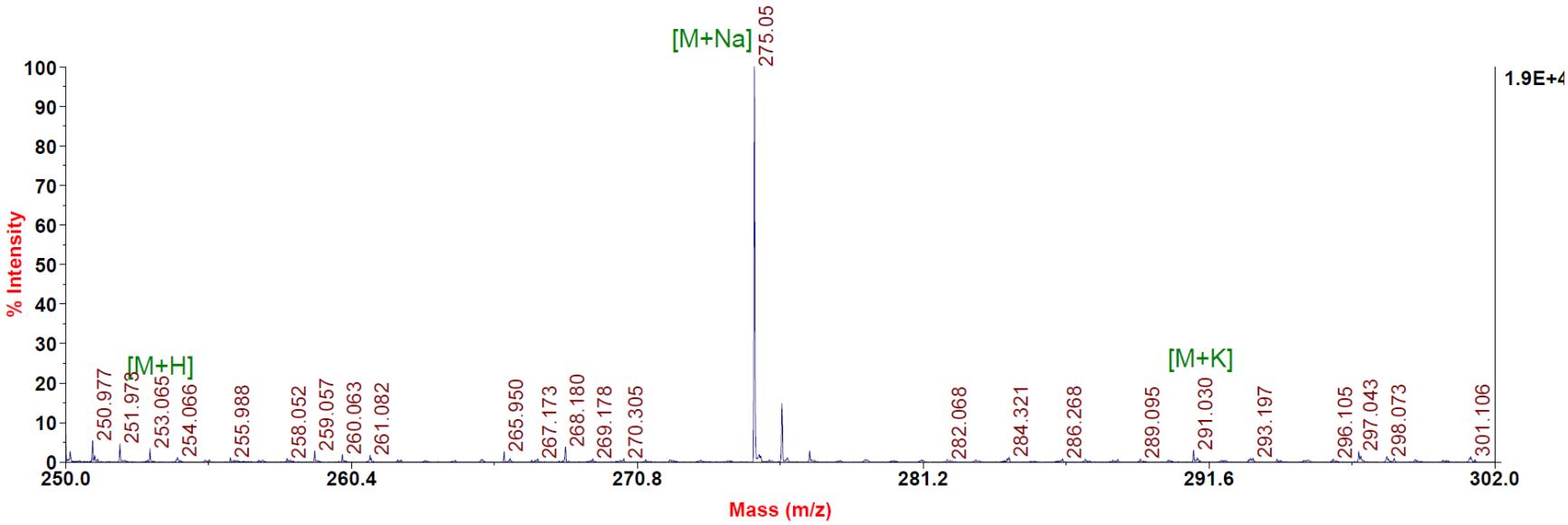

^{1}H NMR spectrum of compound **26**. (500 MHz, chloroform-*d*))

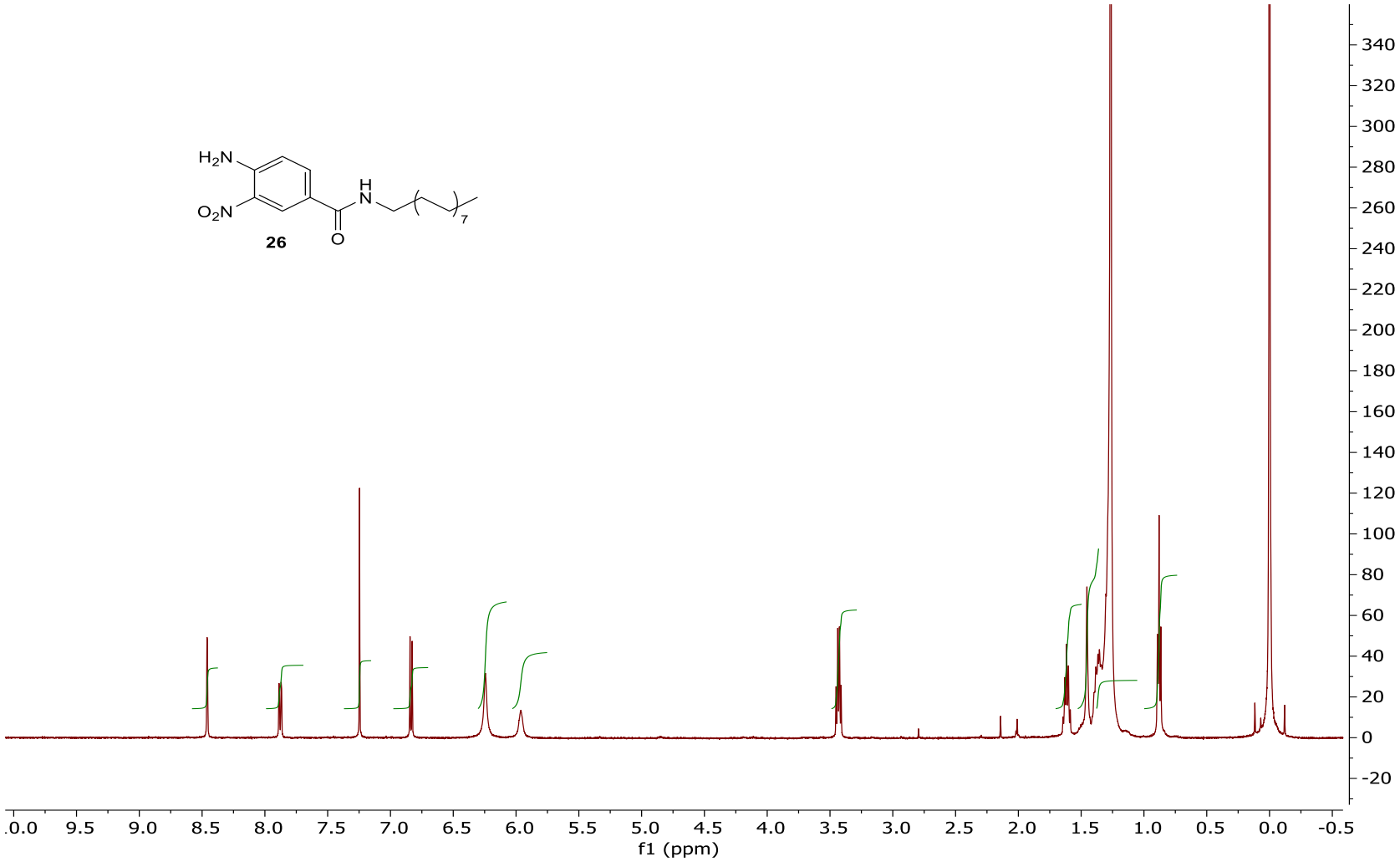

^{13}C NMR spectrum of compound **26**. (126 MHz, chloroform-*d*))

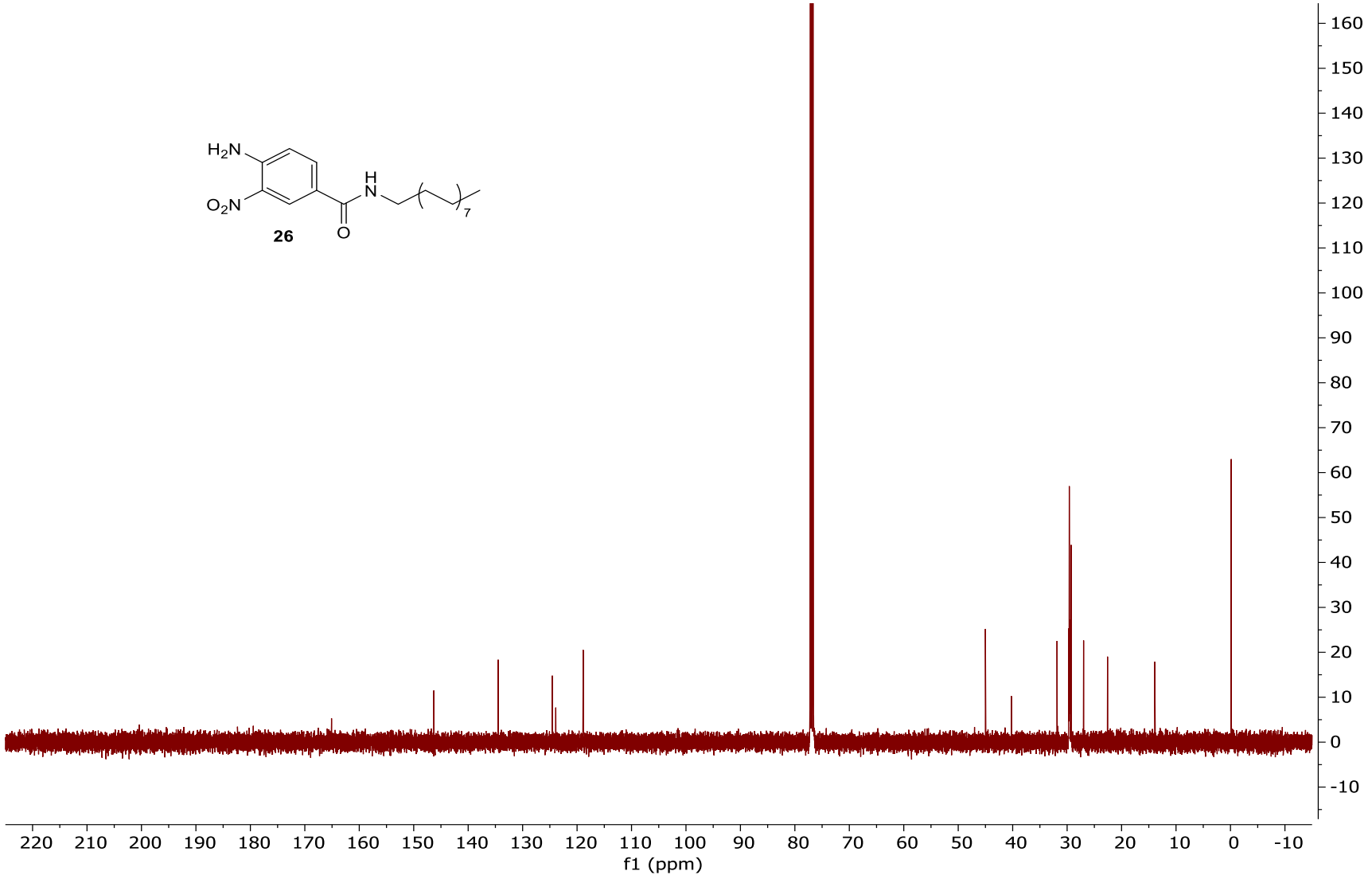

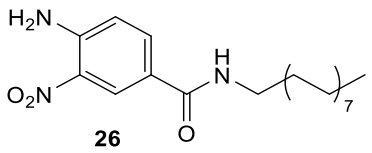

26

MALDI-MS m/z calcd for $C_{23}H_{39}N_3O_3$: 405.29; found: 406.298 [M+H], 428.27 [M+Na] and 444.247 [M+K].

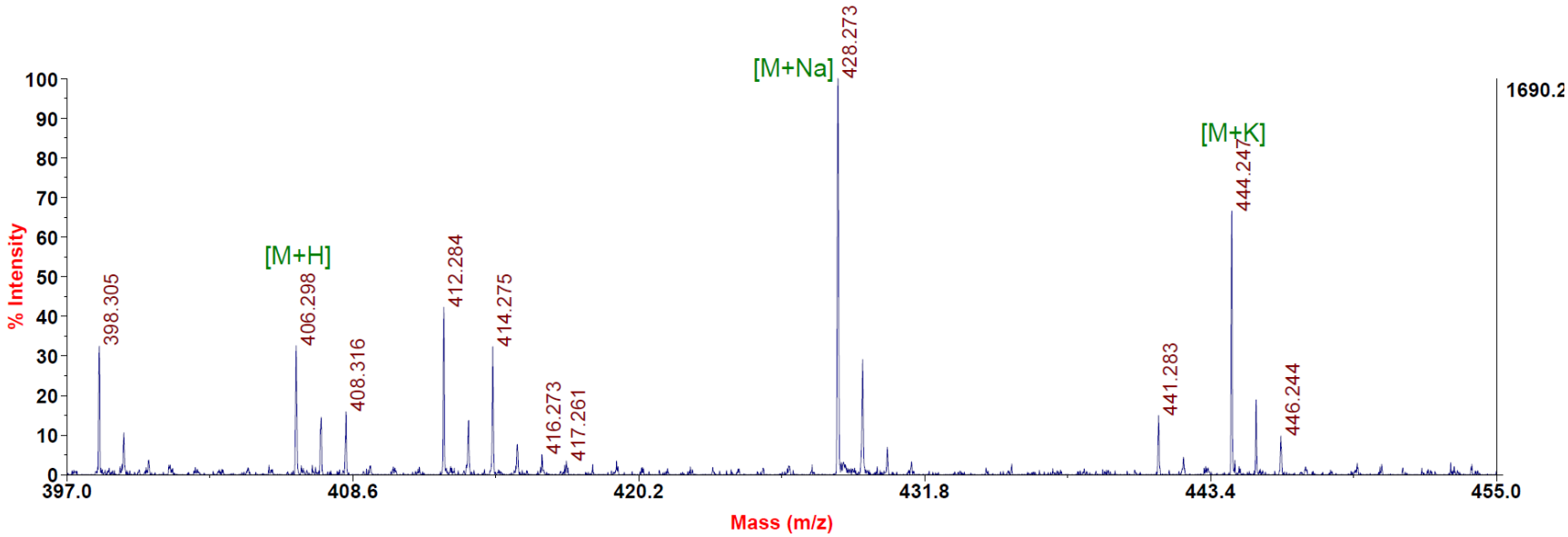

^{1}H NMR spectrum of compound **27**. (500 MHz, chloroform-*d*))

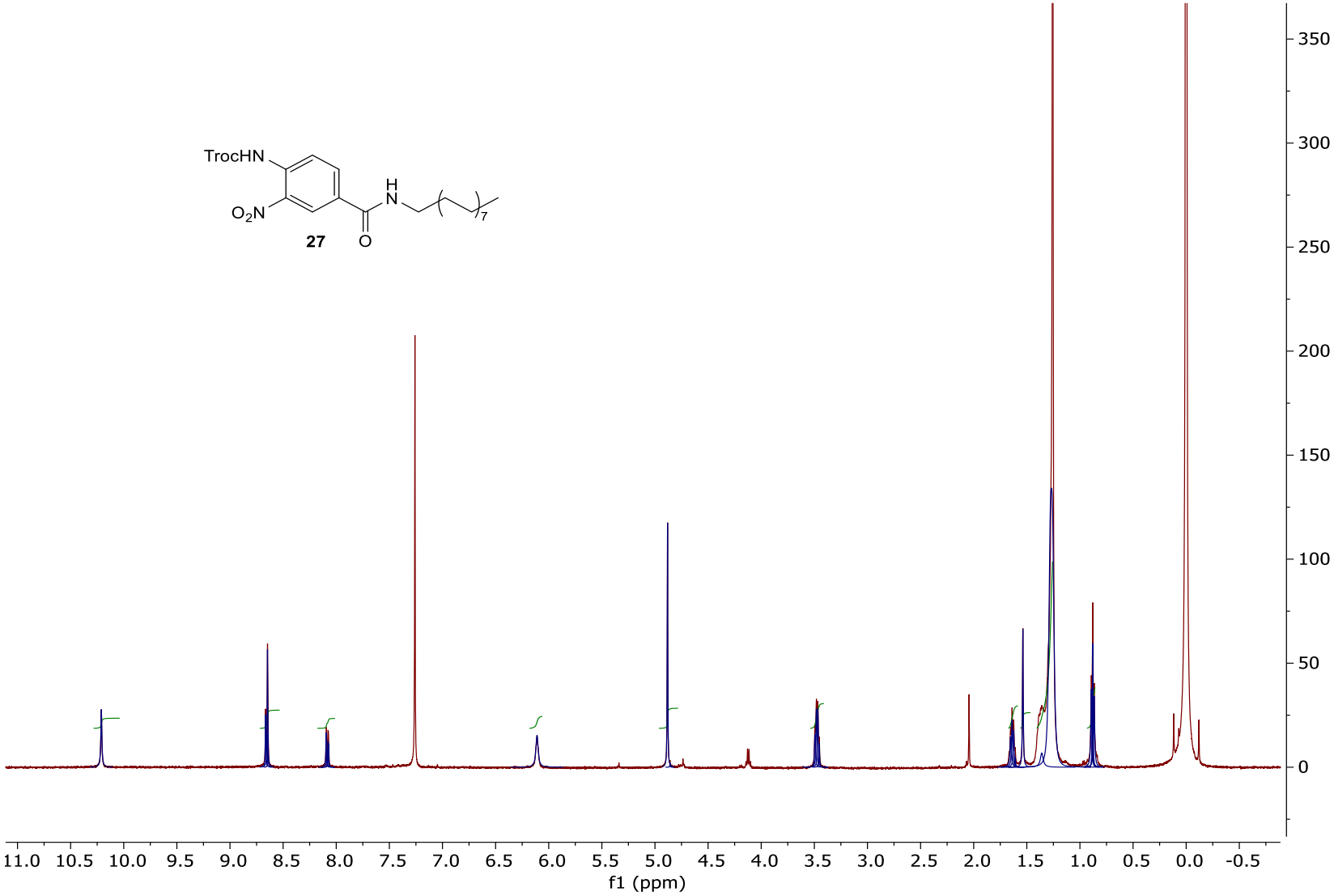

^{13}C NMR spectrum of compound **27**. (126 MHz, chloroform-*d*))

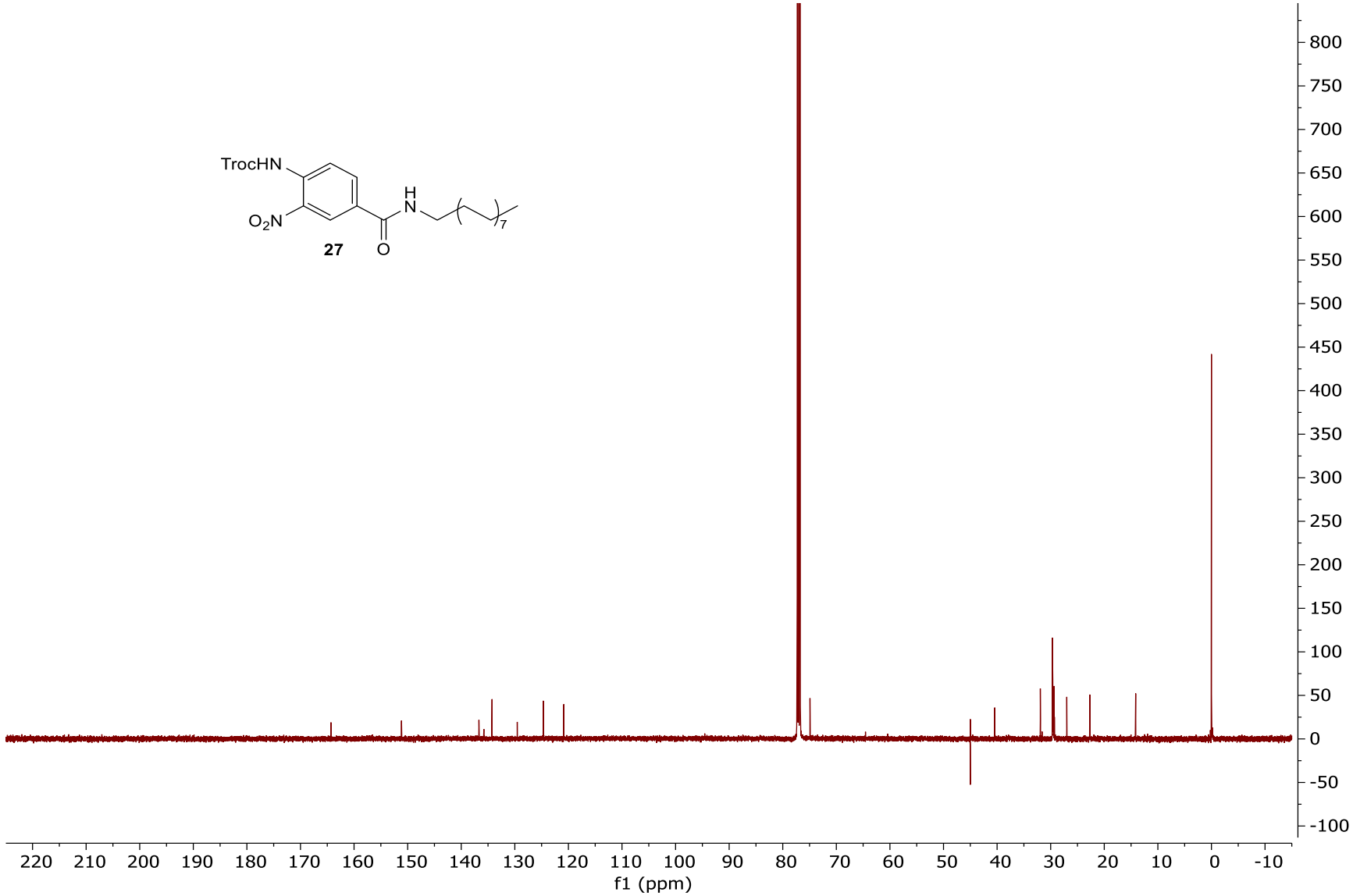

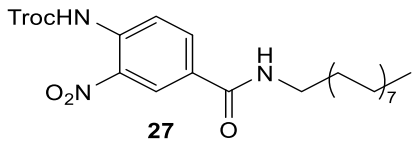

27

MALDI-MS m/z calcd for $C_{26}H_{40}Cl_3N_3O_5$: 579.97; found: 580.232 [M+H], and 602.204 [M+Na].

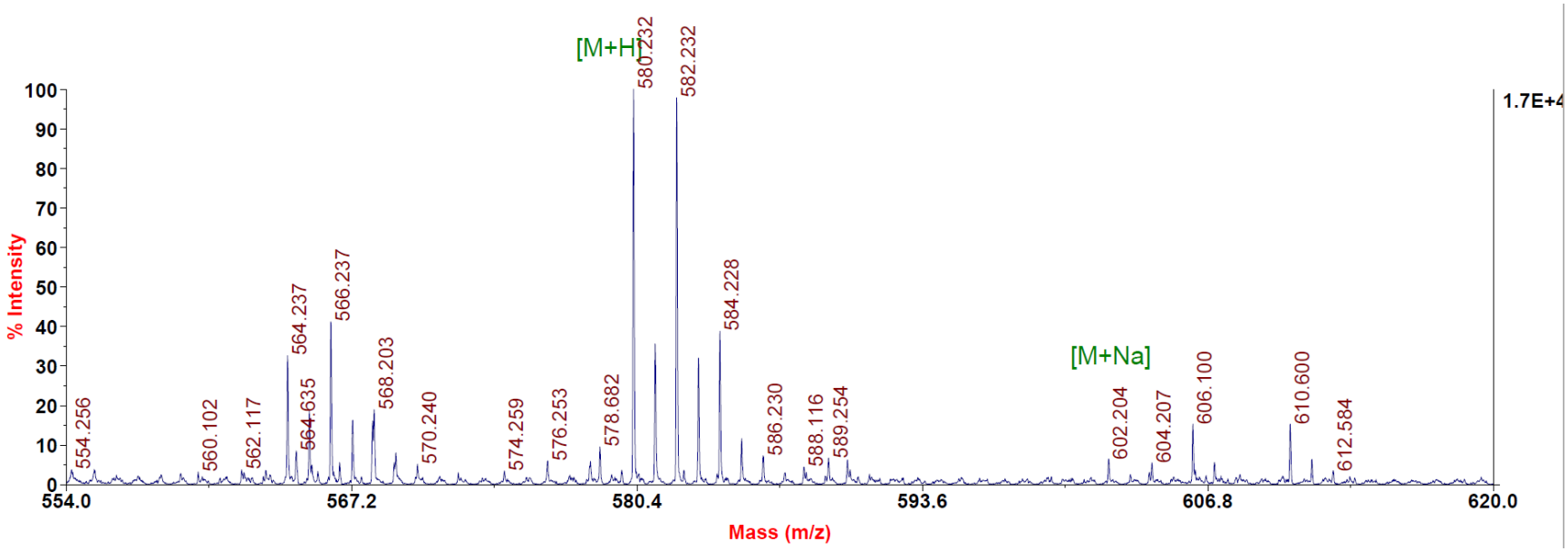

^{1}H NMR spectrum of compound **28**. (500 MHz, chloroform-*d*))

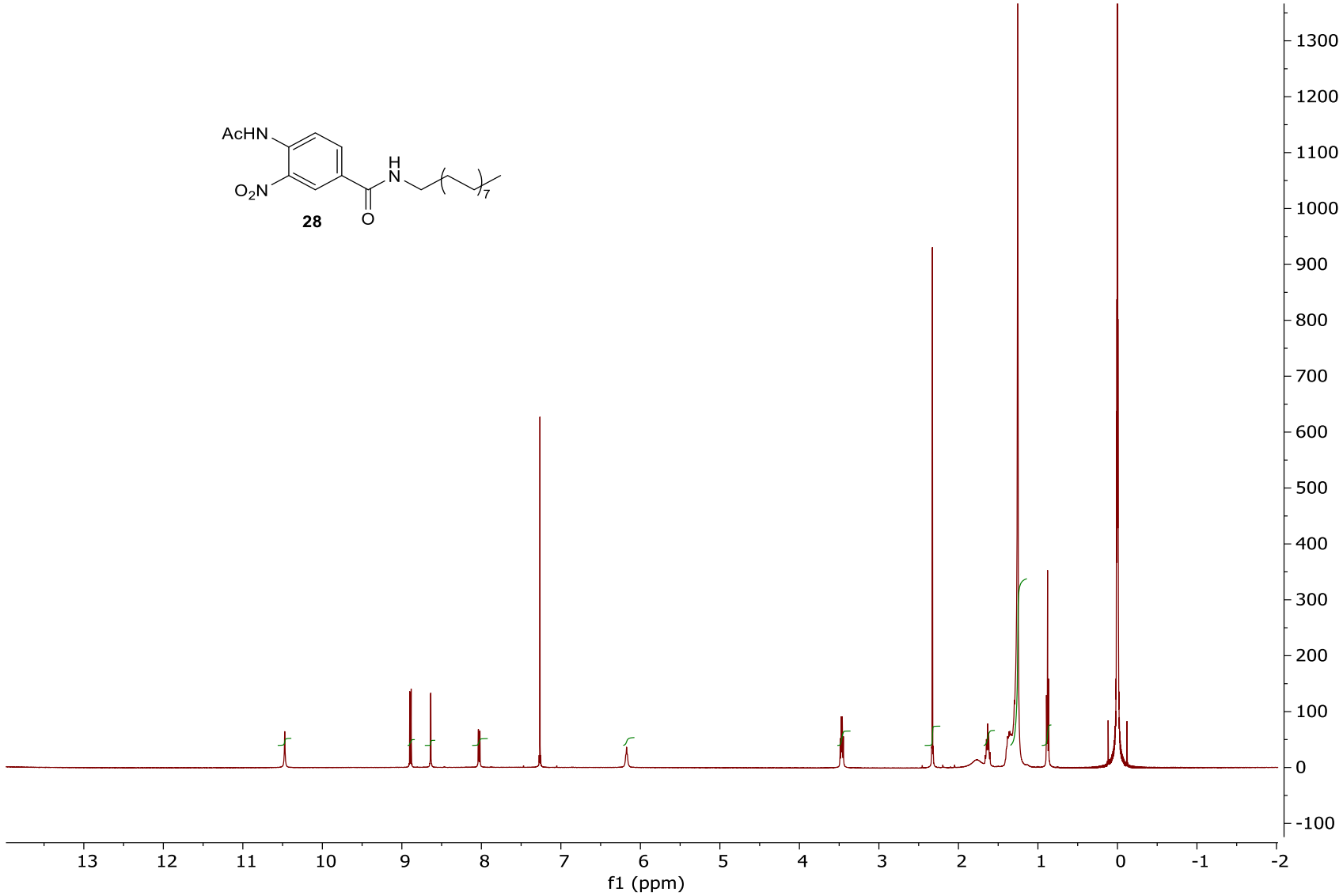

^{13}C NMR spectrum of compound **28**. (126 MHz, chloroform-*d*)

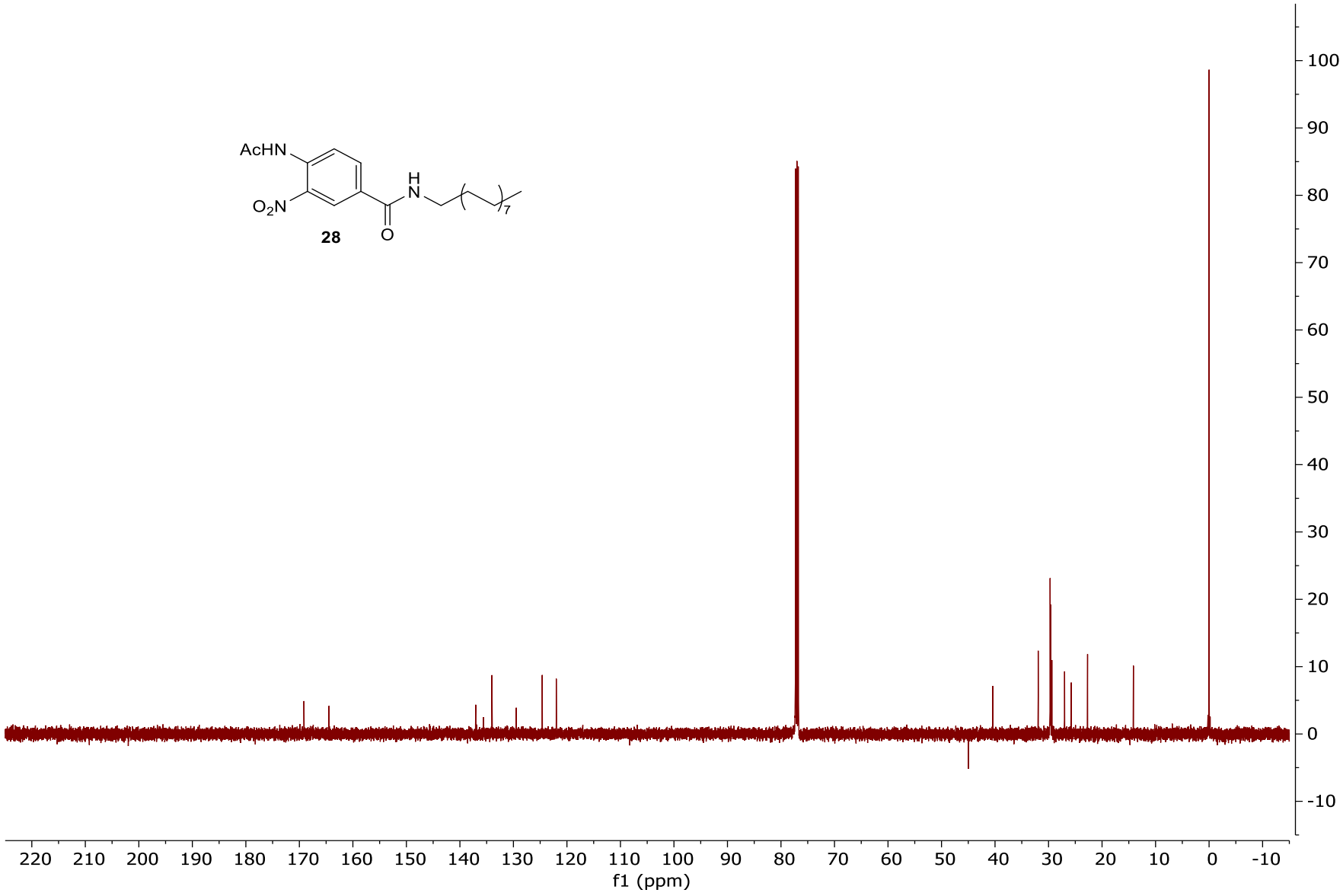

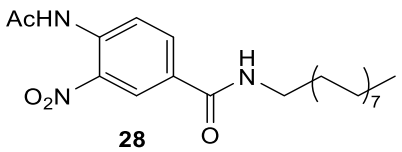

28

MALDI-MS m/z calcd for $C_{25}H_{41}N_3O_4$: 447.309; found: 448.317 [M+H], 470.288 [M+Na] and 486.262 [M+K].

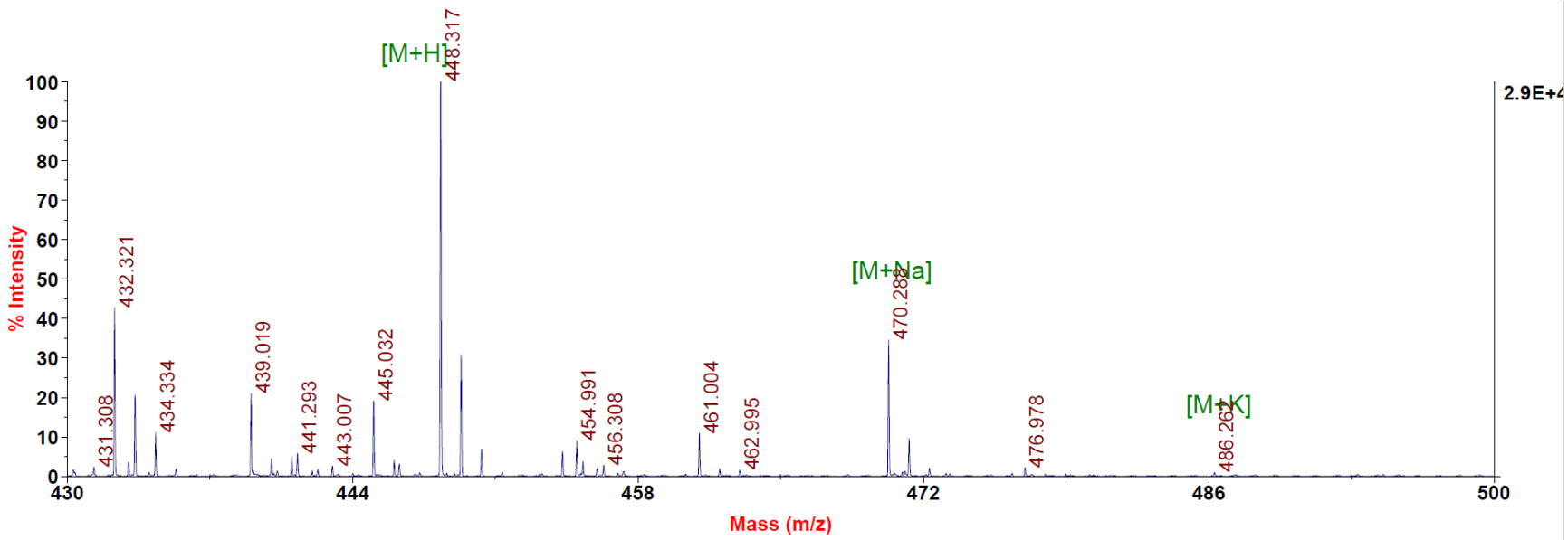

^{1}H NMR spectrum of compound **31**. (500 MHz, CD_3OD)

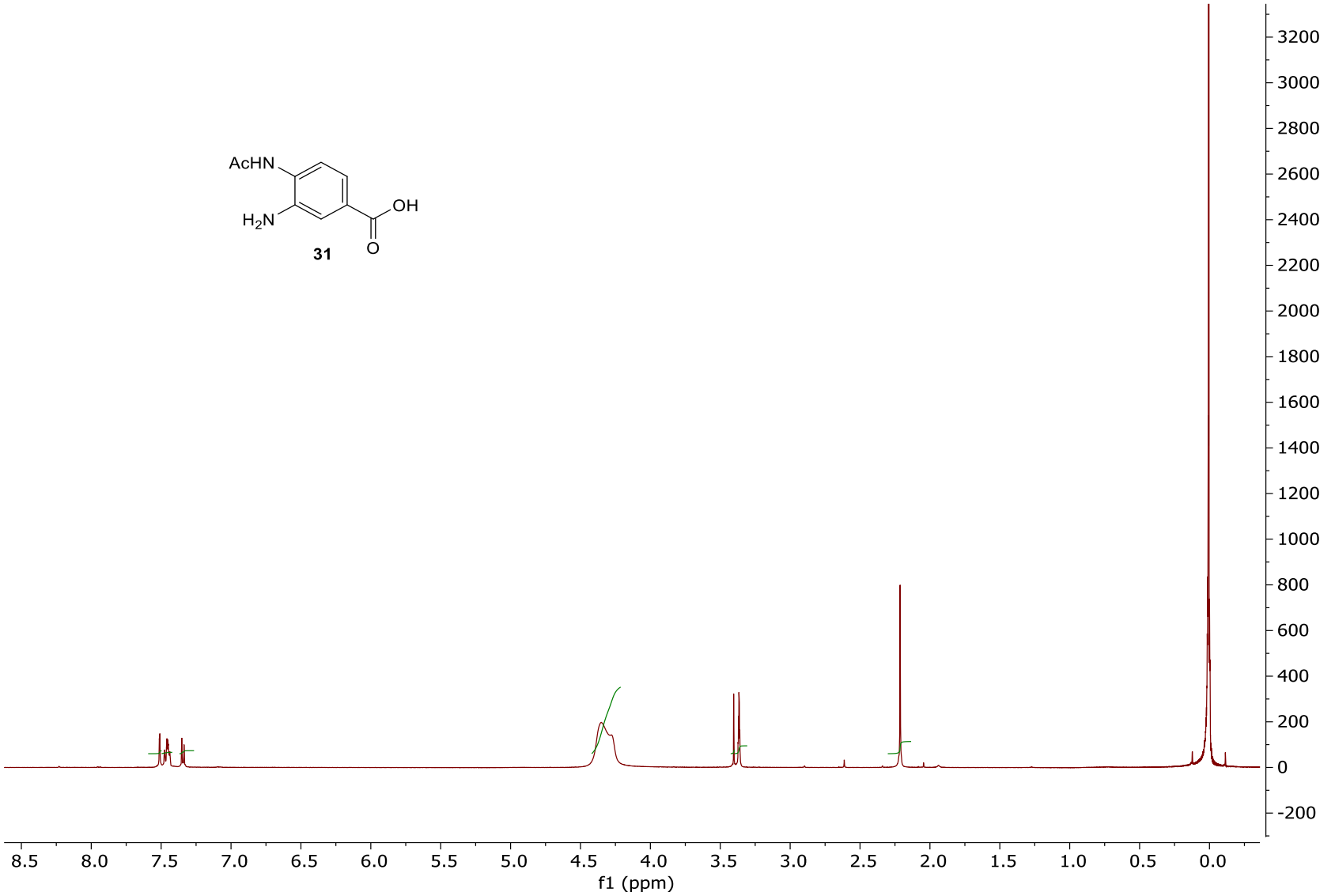

^{13}C NMR spectrum of compound **31**. (126 MHz, CD3OD)

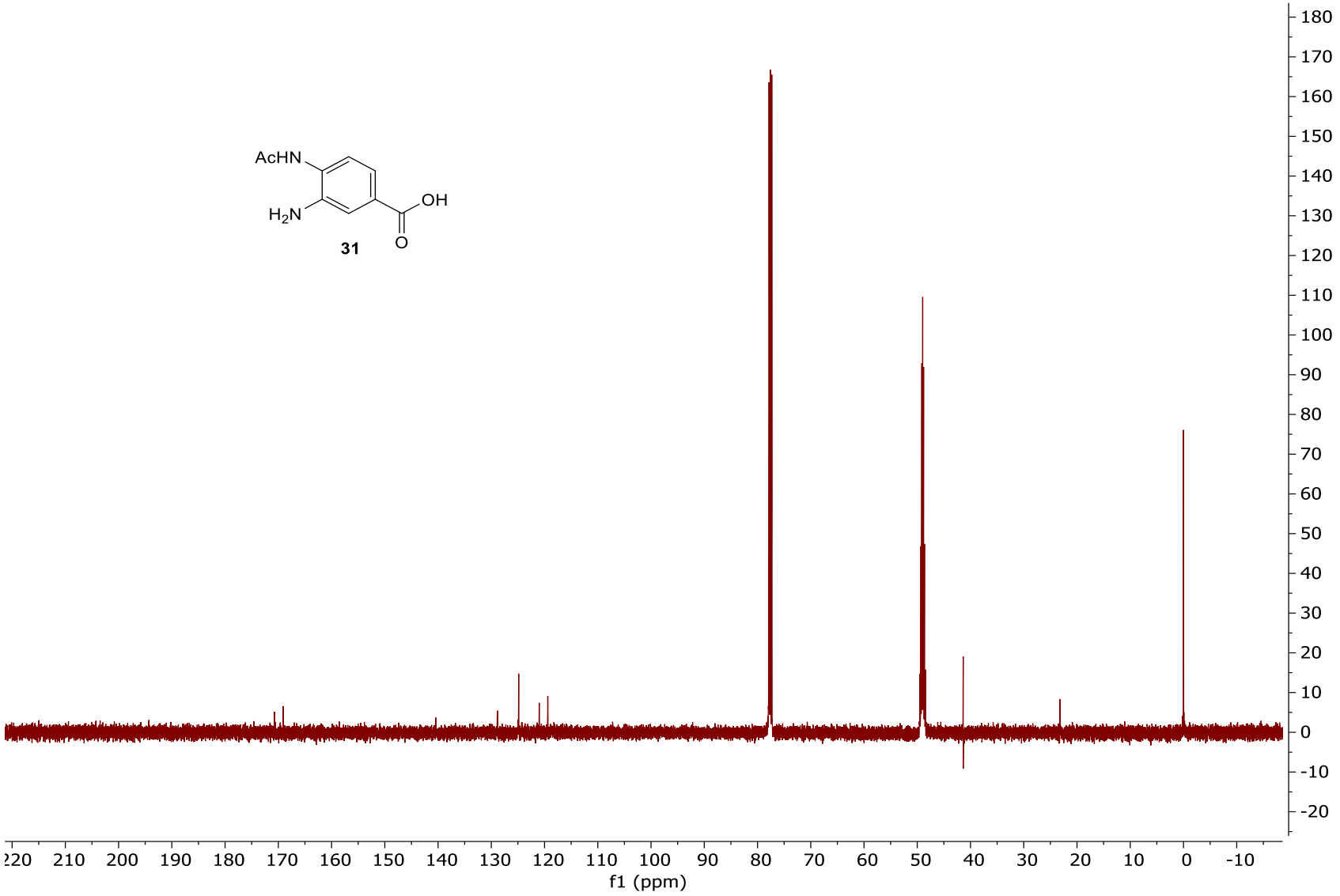

^{1}H NMR spectrum of compound **14**. (500 MHz, DMSO-d_6)

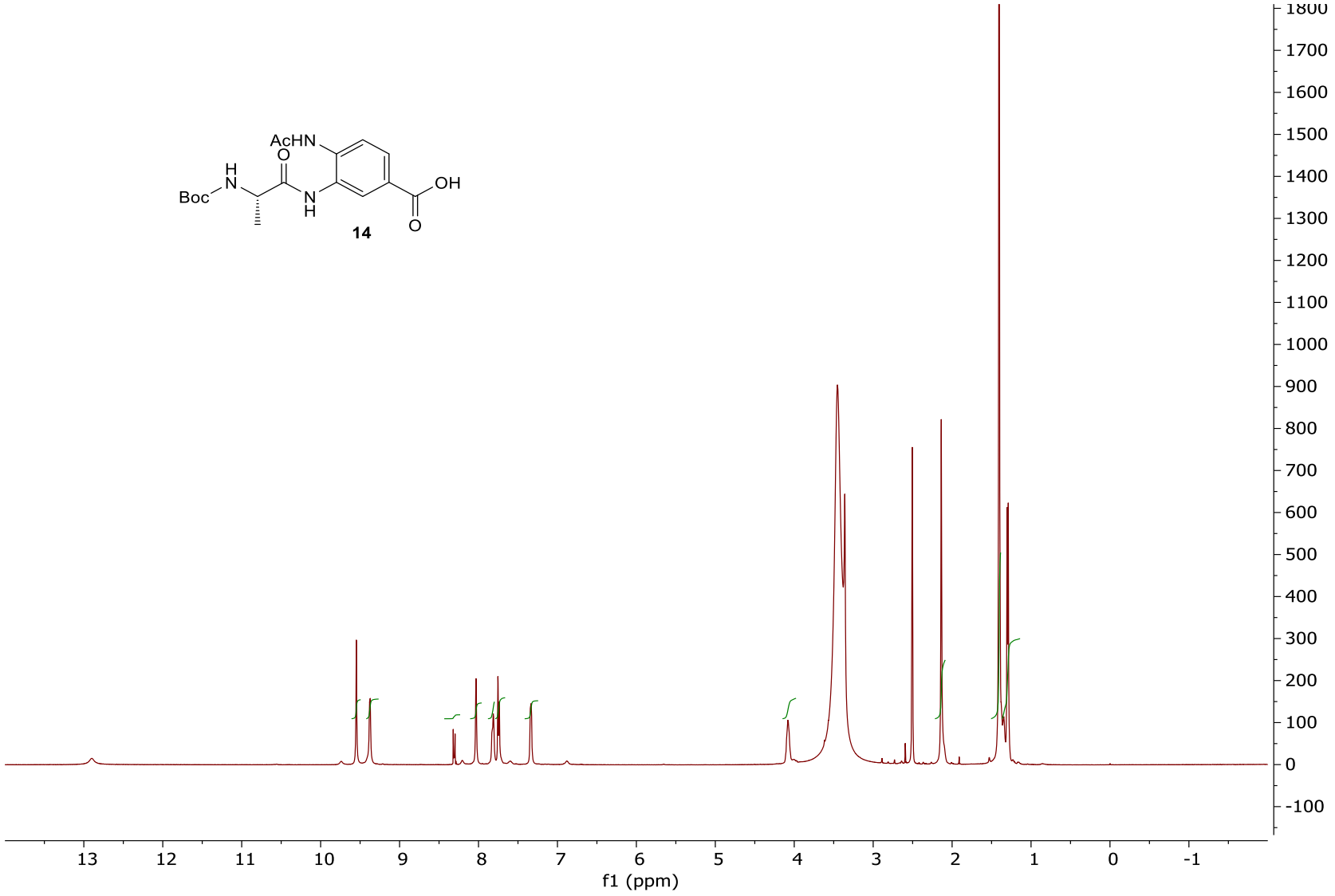

^{13}C NMR spectrum of compound **14**. (126 MHz, DMSO-d_6)

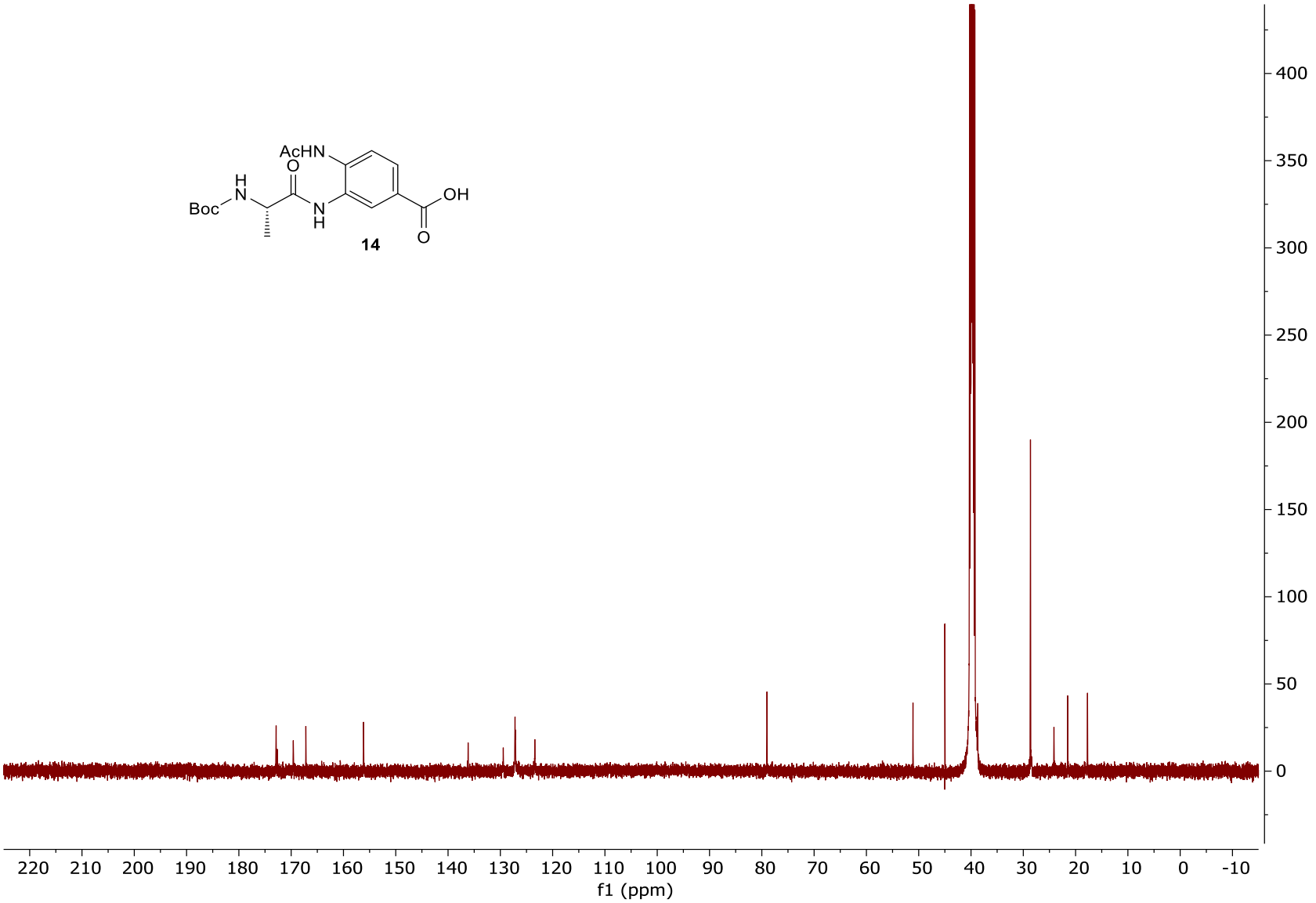

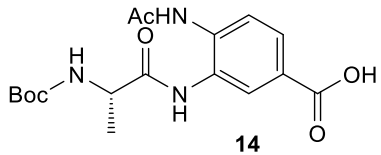

14

MALDI-MS m/z calcd for $C_{17}H_{23}N_3O_6$: 365.158; found: 366.158 [M+H], 388.150 [M+Na] and 404.129 [M+K].

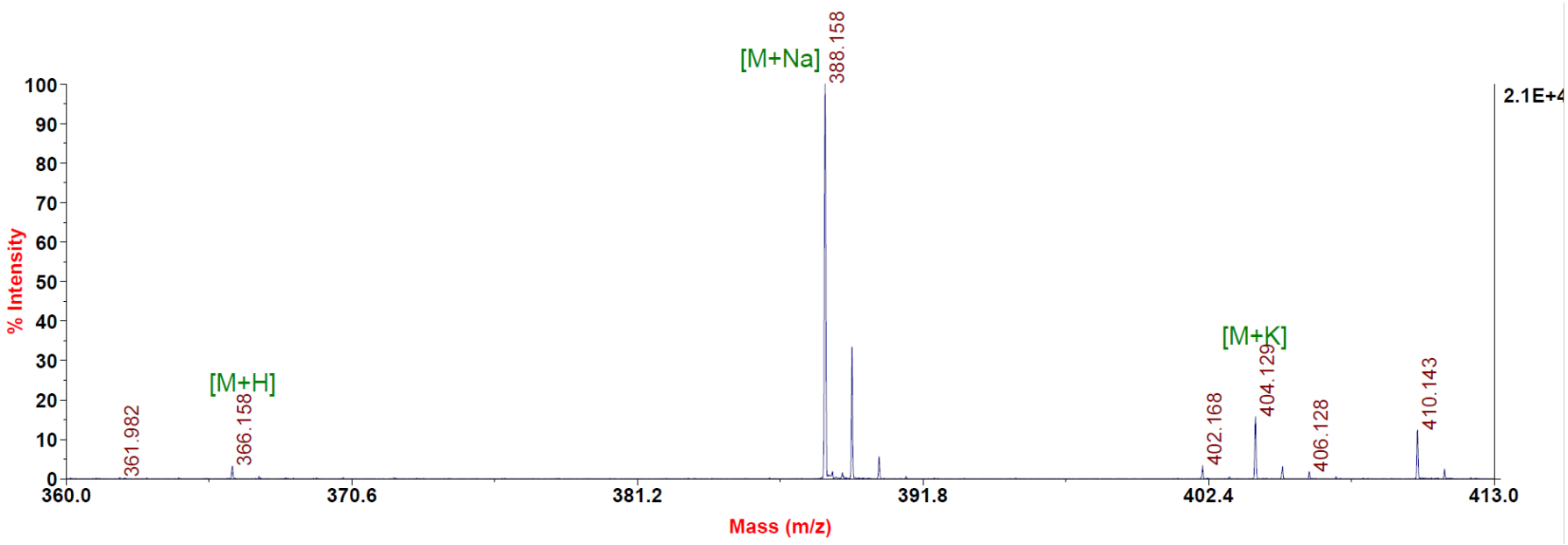

^{1}H NMR spectrum of compound **11**. (500 MHz, chloroform-*d*))

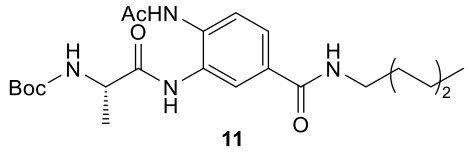

11

^{13}C NMR spectrum of compound **11**. (126 MHz, chloroform-*d*)

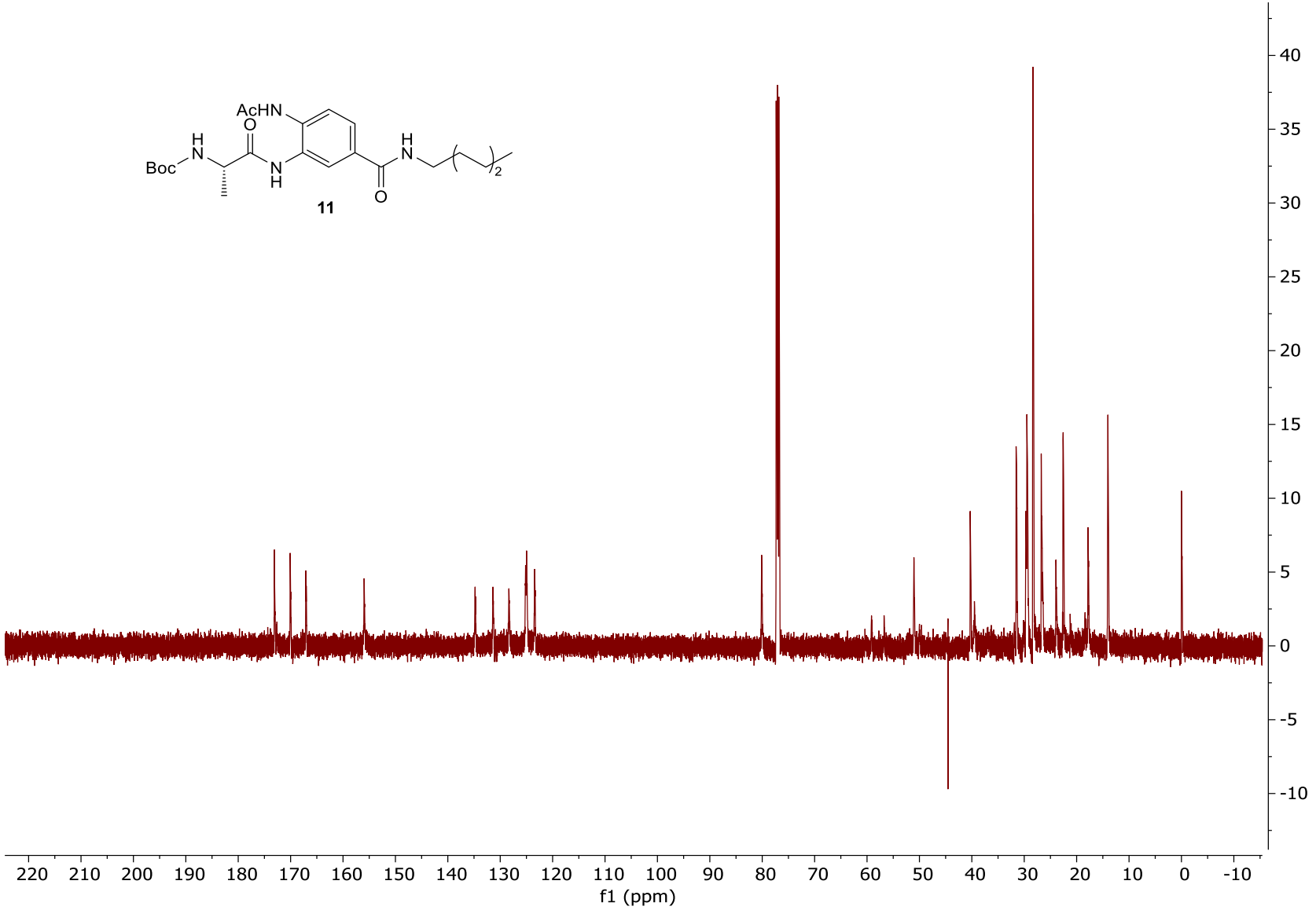

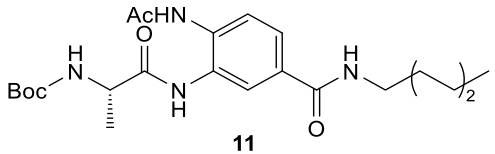

11

MALDI-MS m/z calcd for $C_{23}H_{36}N_4O_5$: 448.268; and found: 471.25 [M+Na].

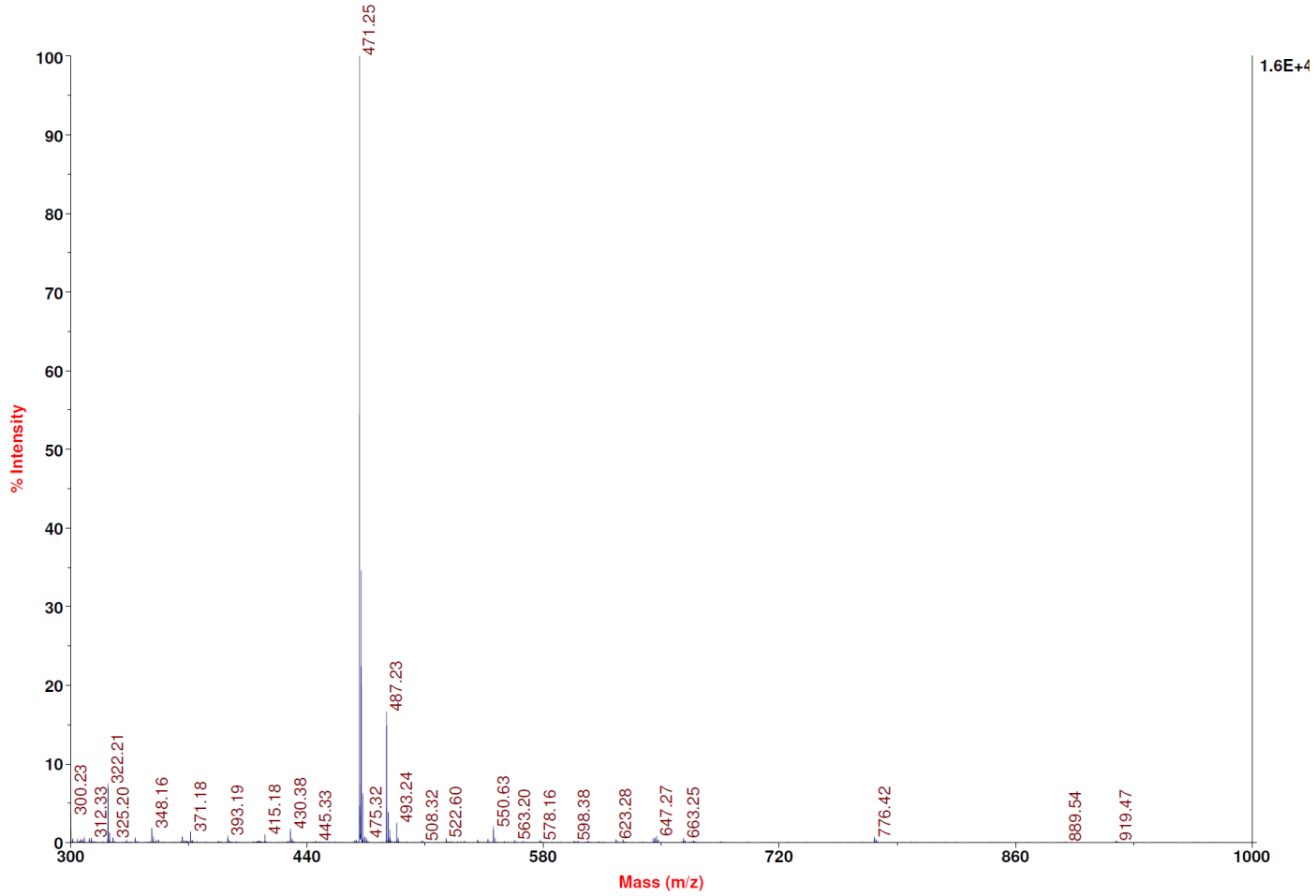

^{1}H NMR spectrum for compound **12.** (500 MHz, chloroform-*d*)

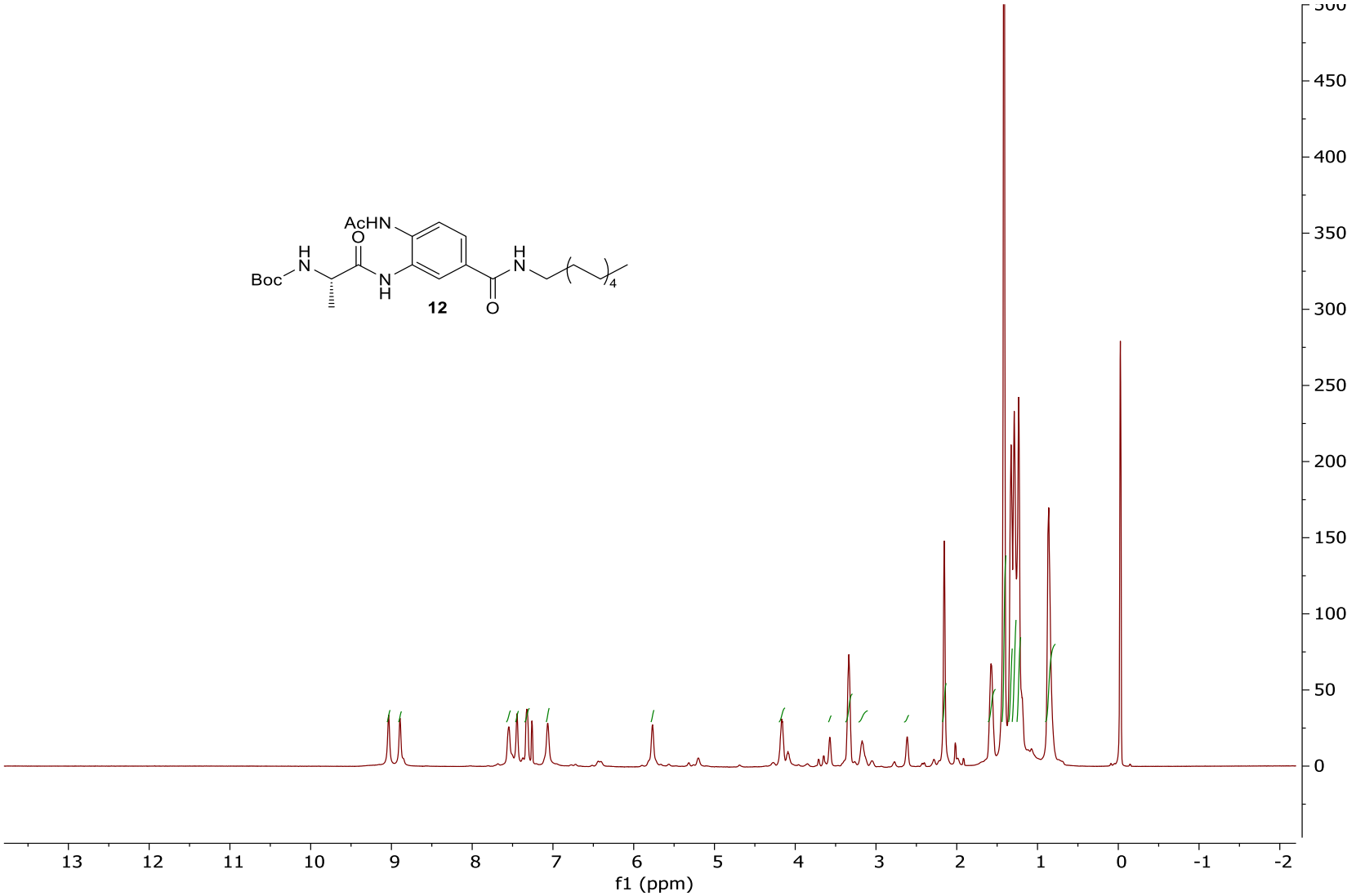

^{13}C NMR spectrum for compound **12.** (126 MHz, chloroform-*d*)

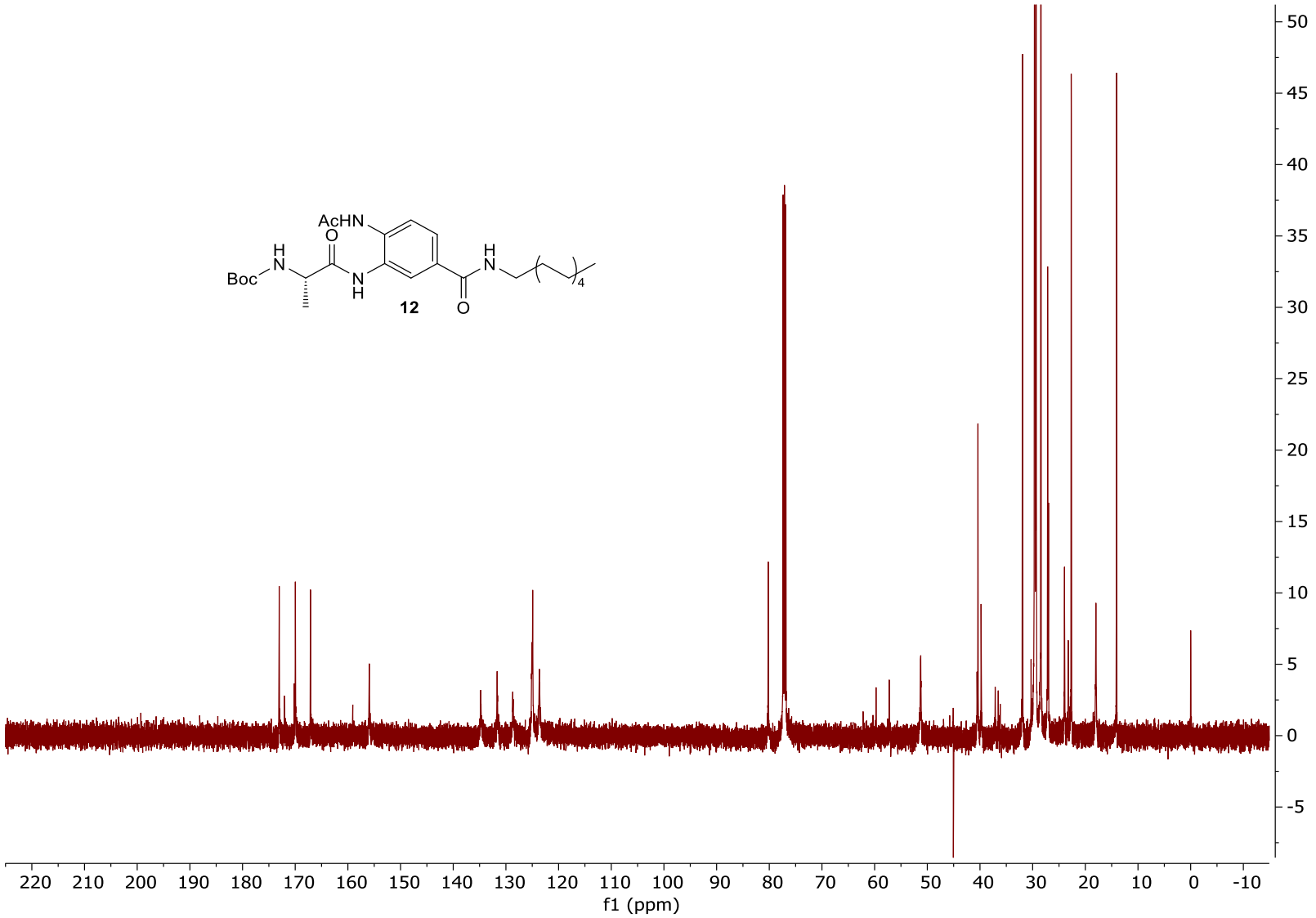

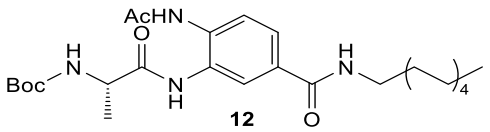

12

MALDI- MS m/z calcd for $C_{27}H_{44}N_4O_5$: 504.33; found: 527.32 [M+Na]

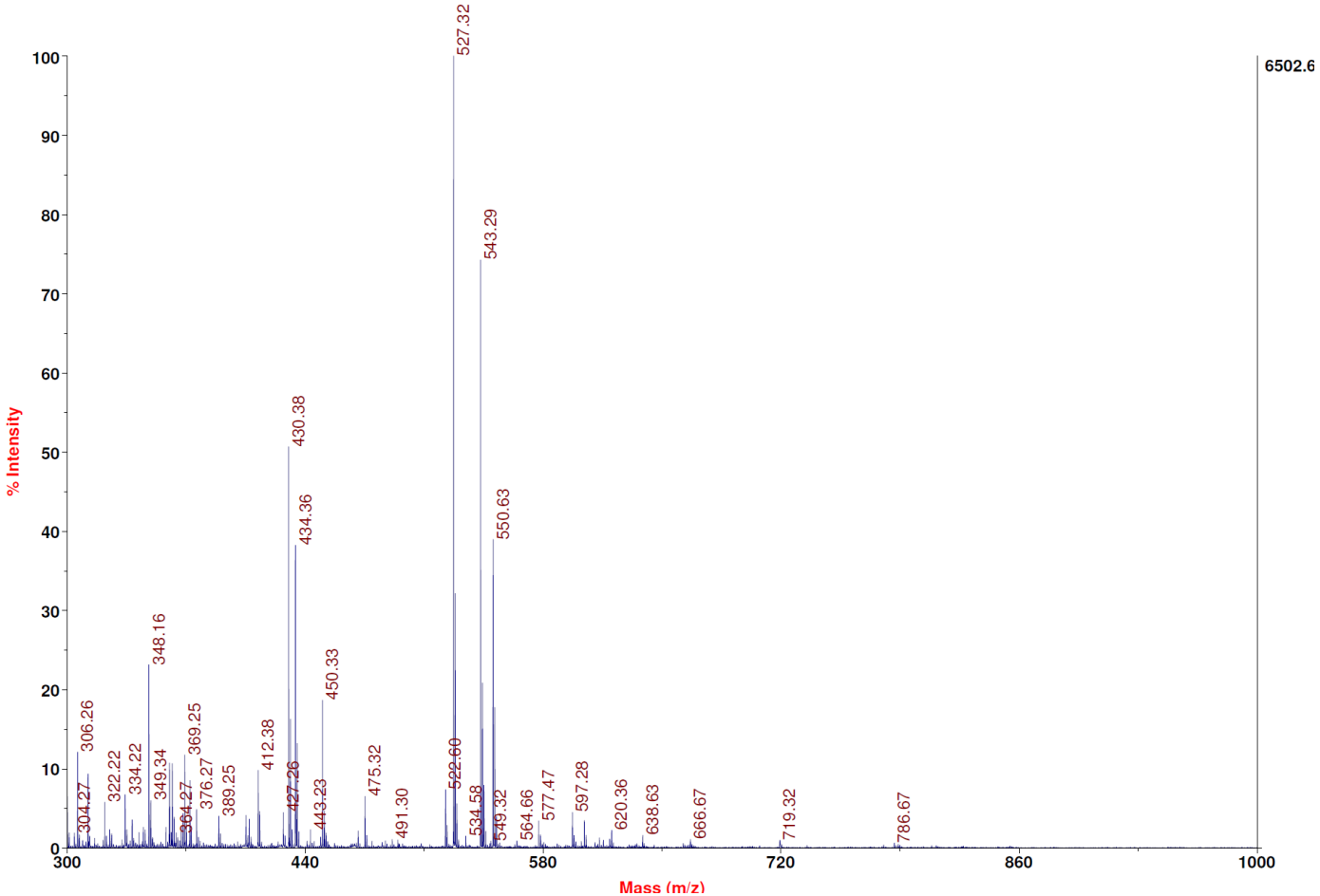

^{1}H NMR spectrum for compound **13.** (500 MHz, chloroform-*d*)

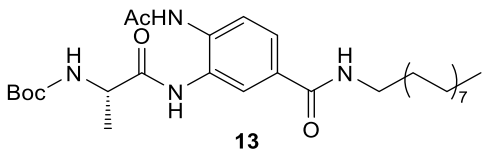

13

^{13}C NMR spectrum for compound **13.** (126 MHz, chloroform-*d*)

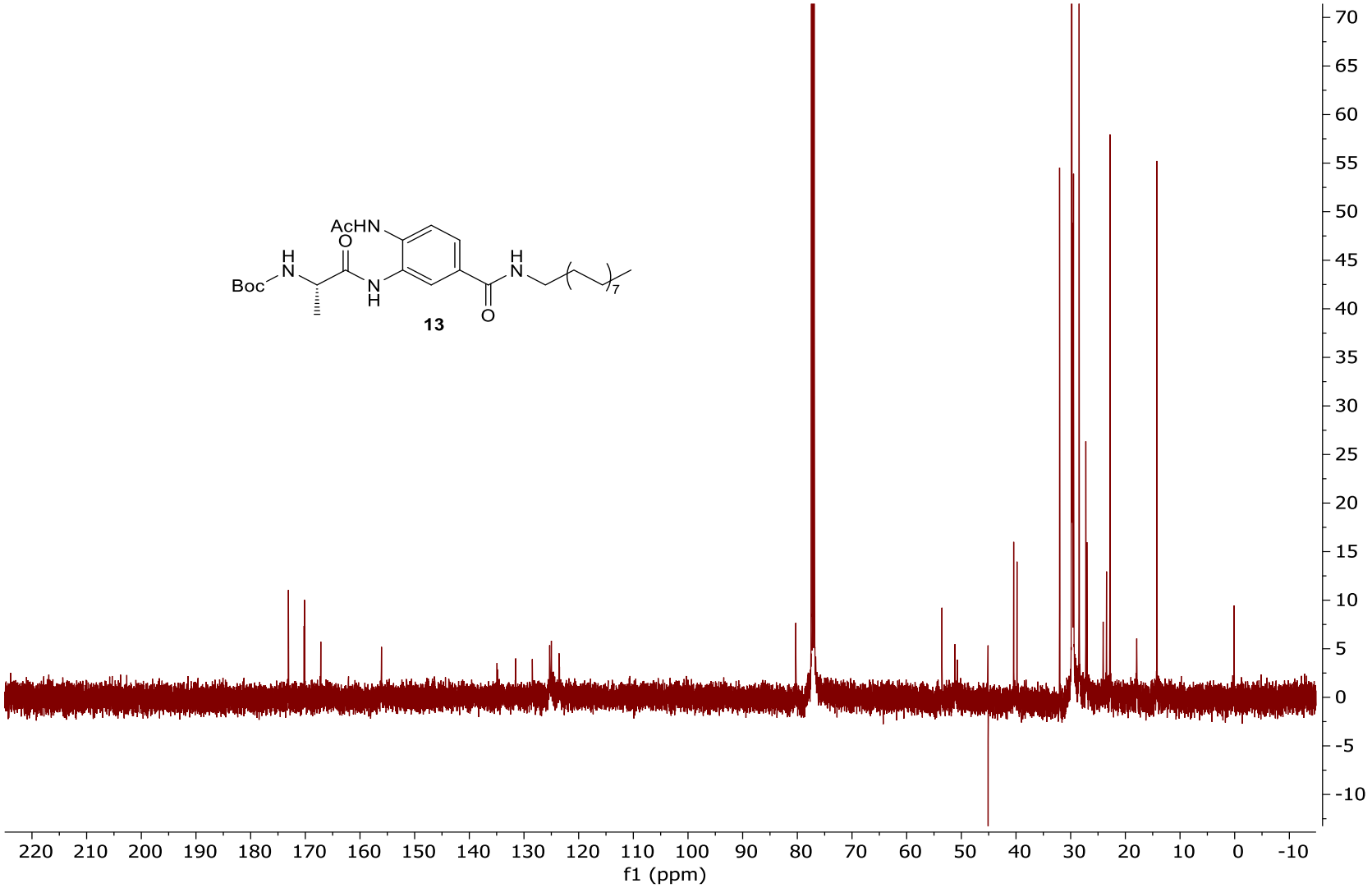

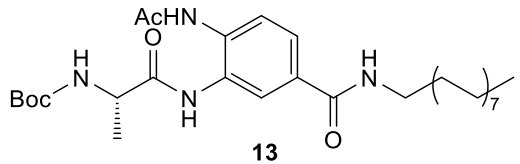

13

MALDI-MS m/z calcd for $C_{33}H_{56}N_4O_5$: 588.425; found: 611.39 [M+Na].

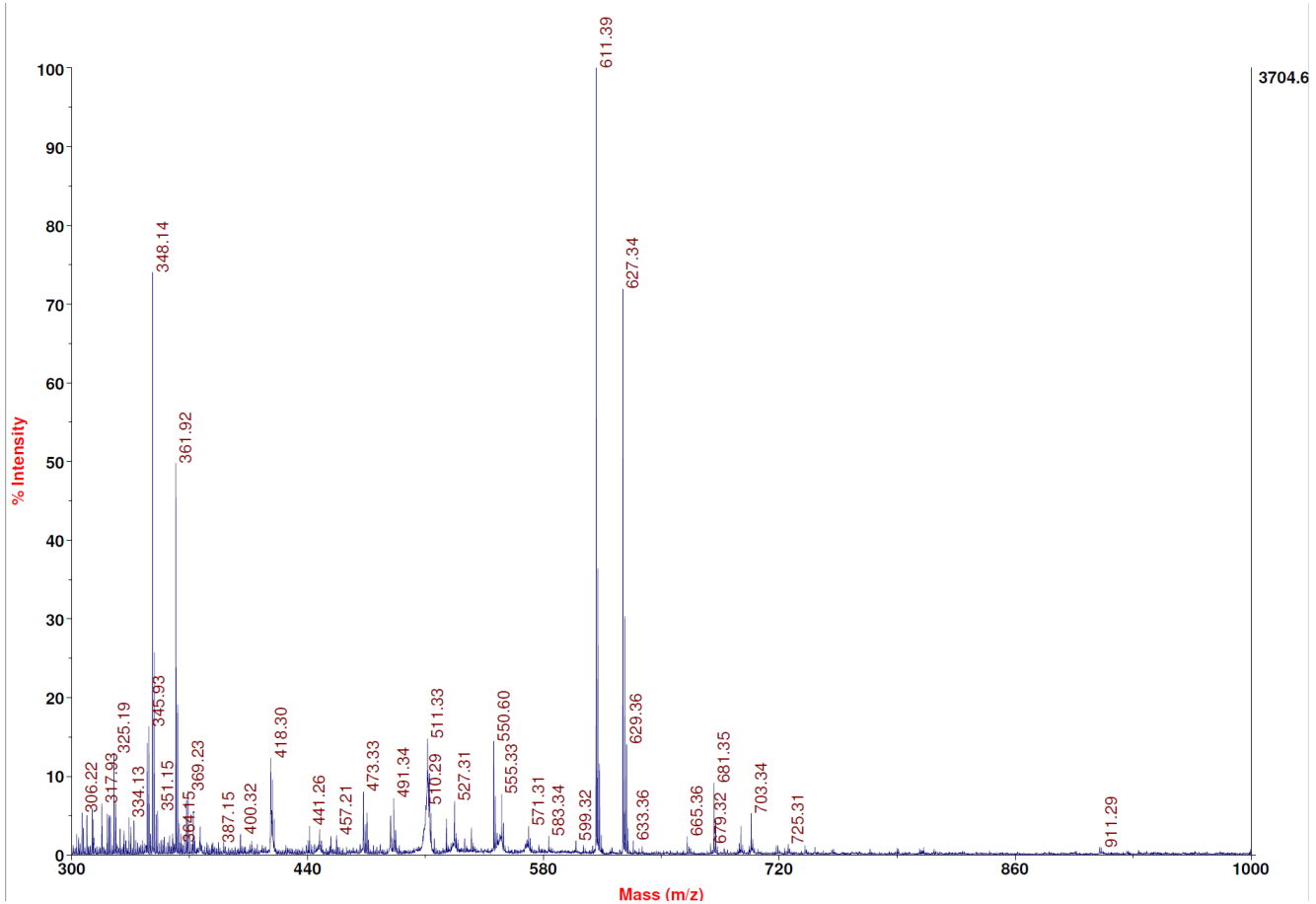

^{1}H NMR spectrum for compound **37** (500 MHz, DMSO-d_6)

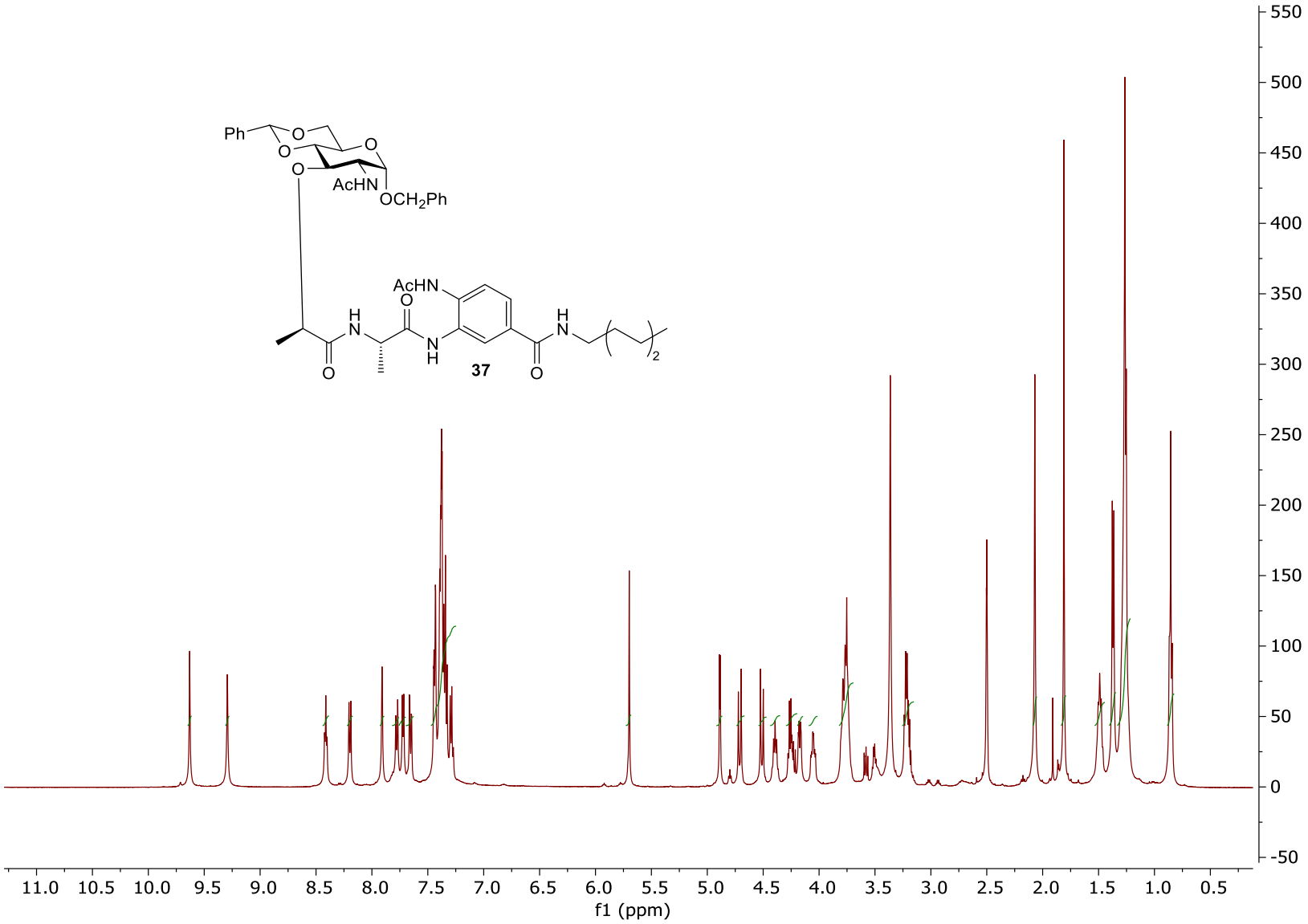

^{13}C NMR spectrum for compound **37** (126 MHz, DMSO-d_6)

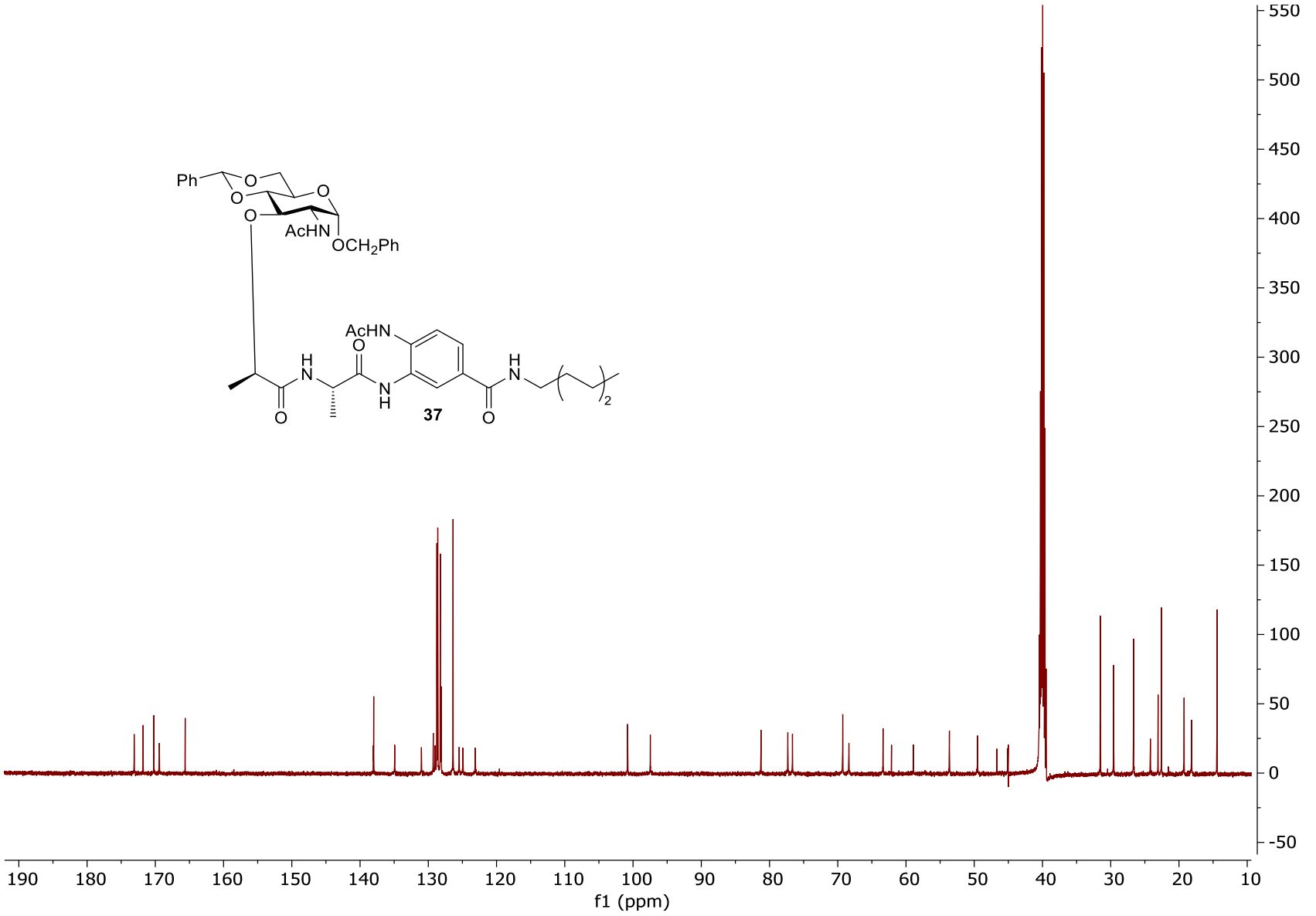

MALDI-MS m/z calcd for $C_{43}H_{55}N_5O_{10}$: 801.39; found: 824.40 [M+Na].

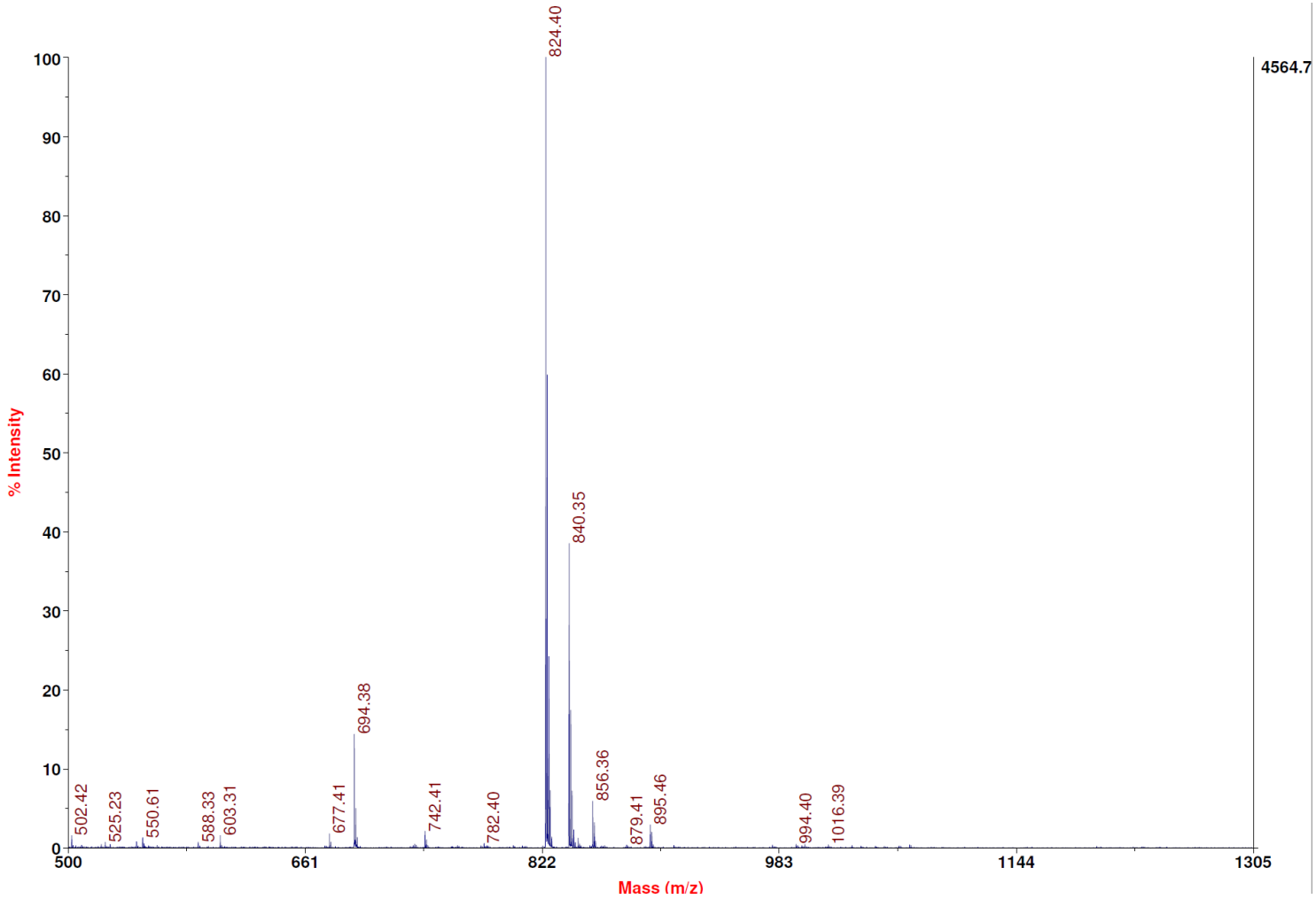

^{1}H NMR spectrum for compound **38** (500 MHz, DMSO-d_6)

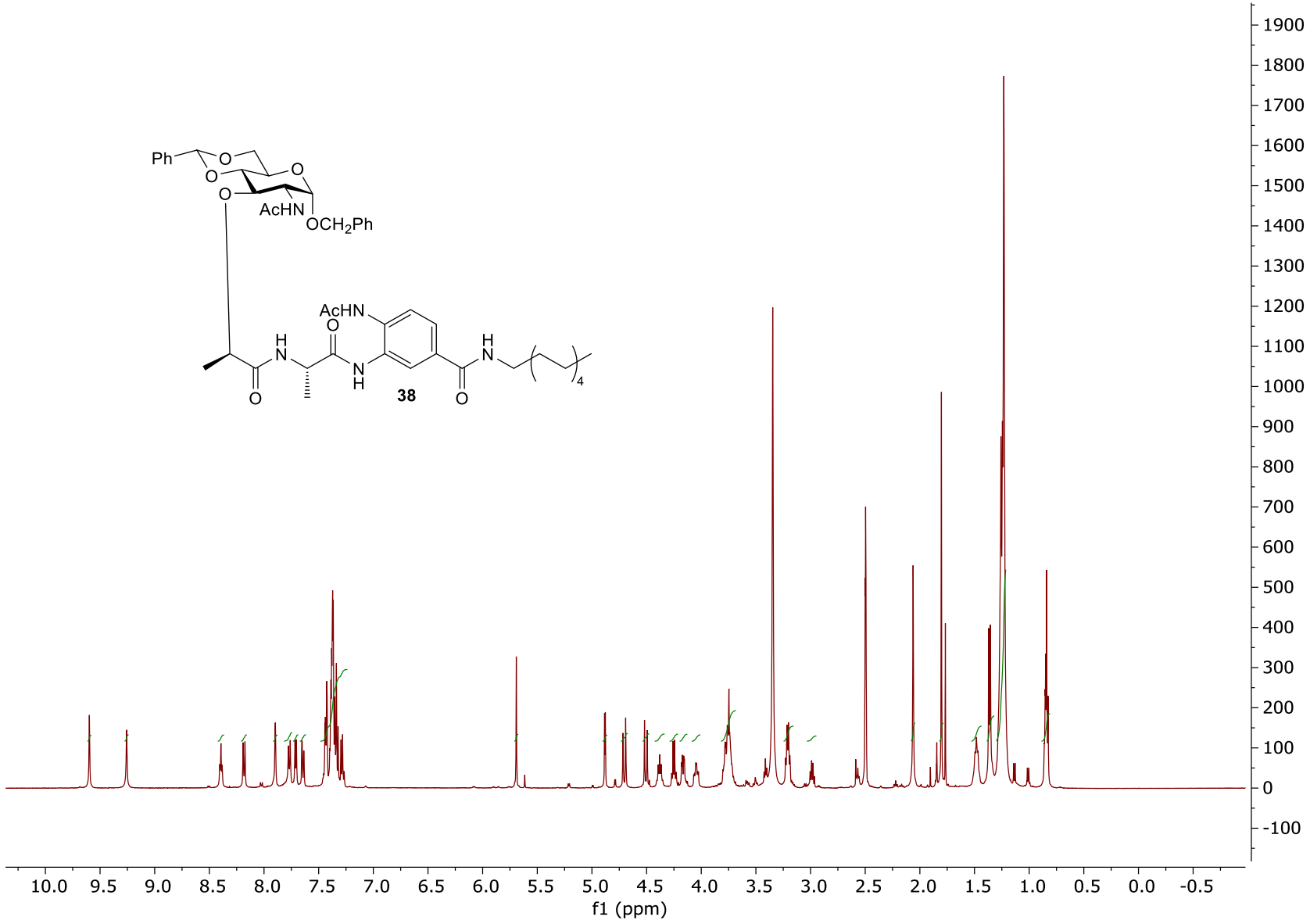

^{13}C NMR spectrum for compound **38** (126 MHz, DMSO-d_6)

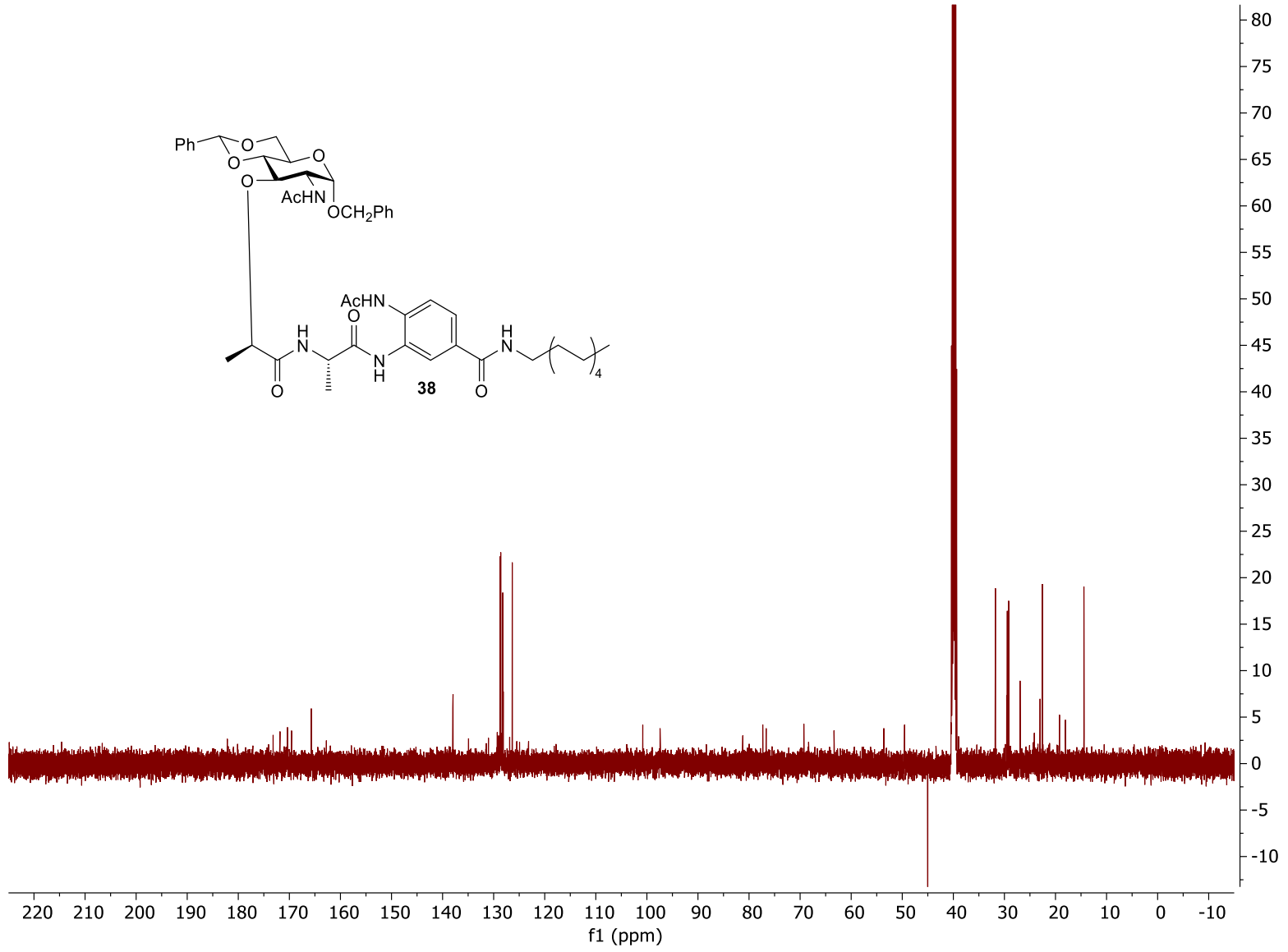

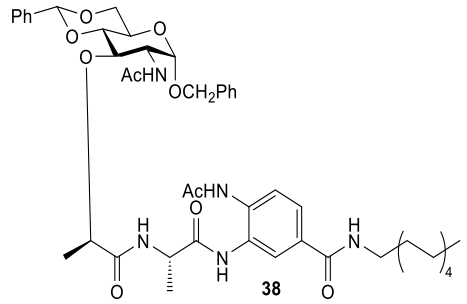

38

MALDI-MS m/z calcd for $C_{47}H_{63}N_5O_{10}$: 857.457; found: 880.47 [M+Na].

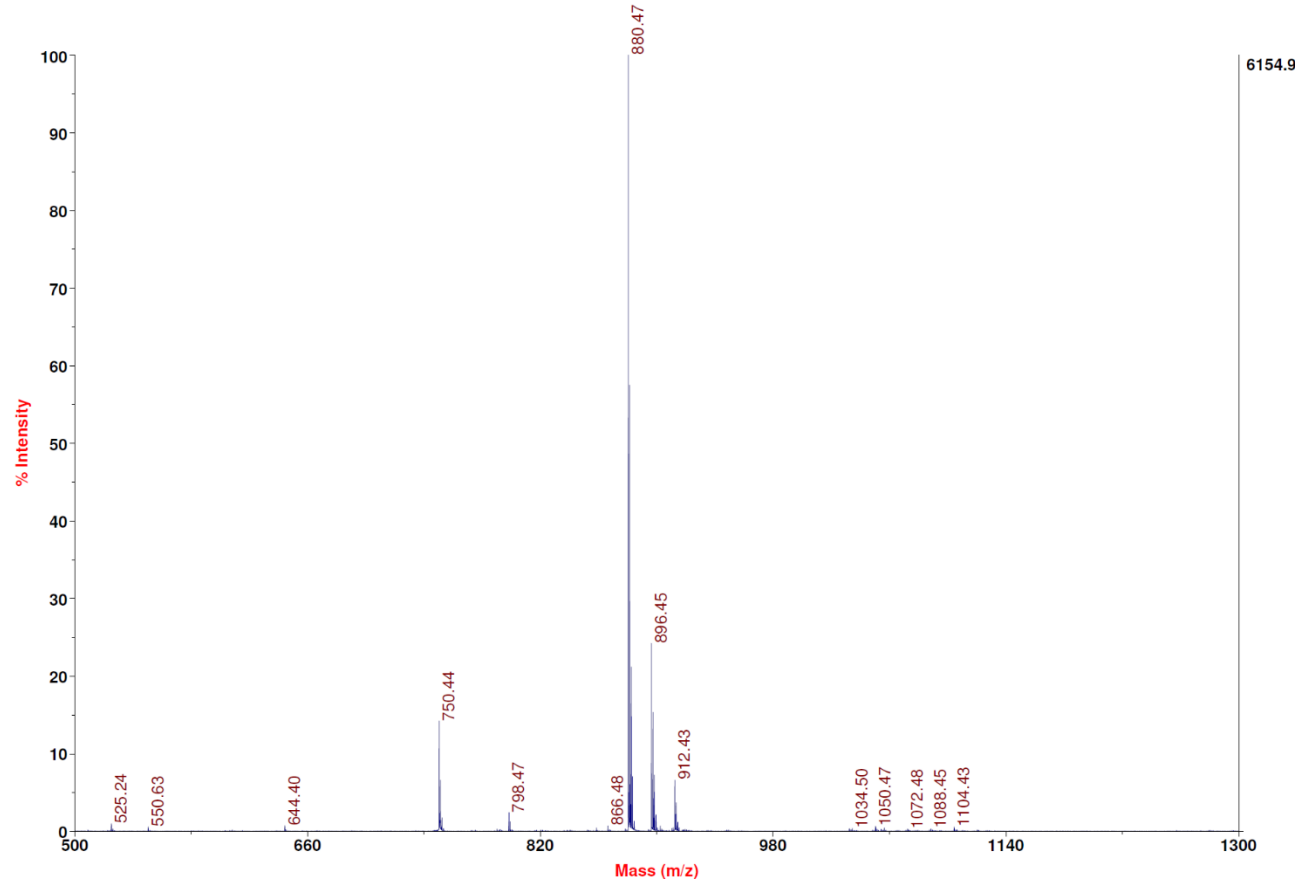

^{1}H NMR spectrum for compound **39** (500 MHz, DMSO-d_6)

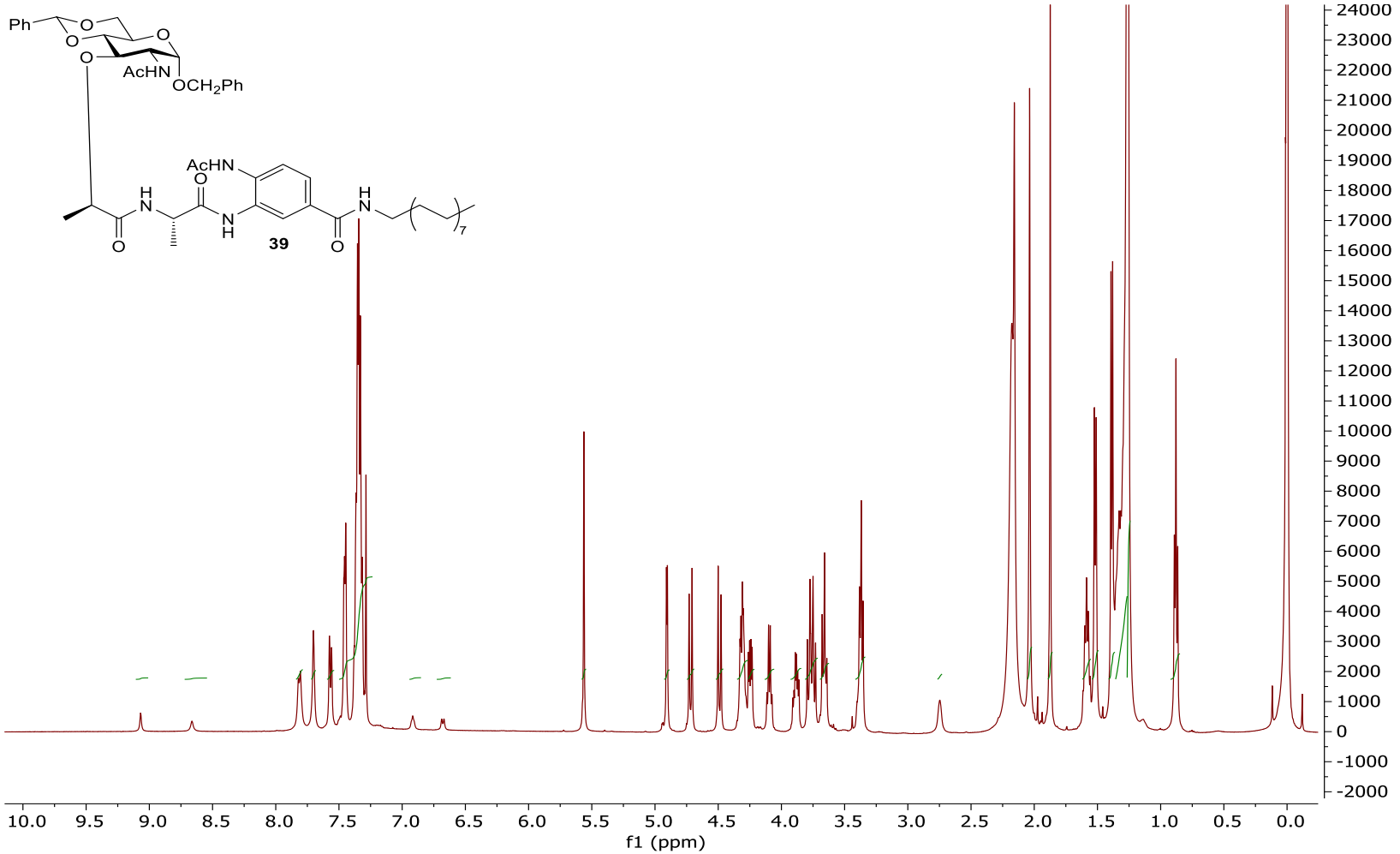

^{13}C NMR spectrum for compound **39** (126 MHz, DMSO-d_6)

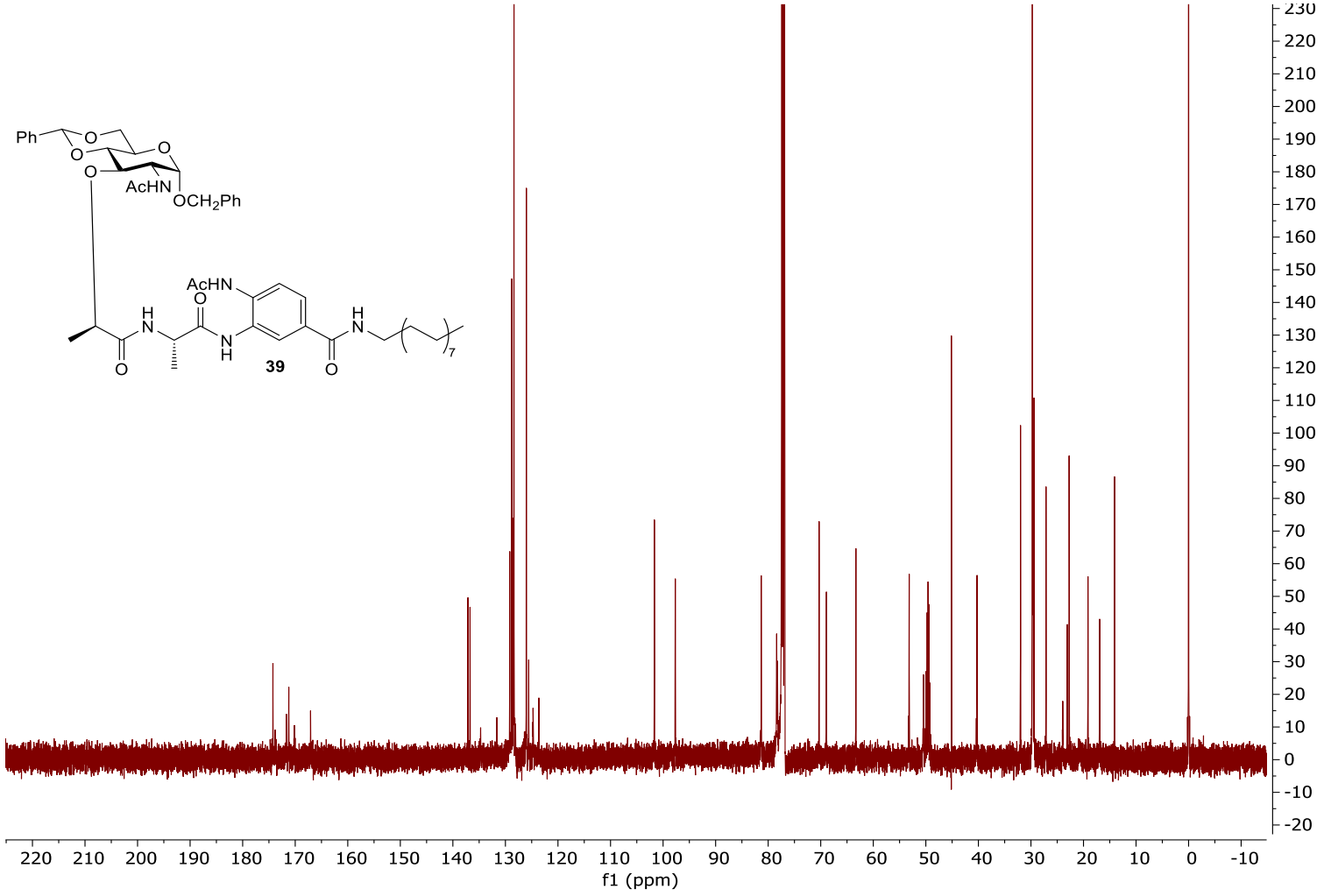

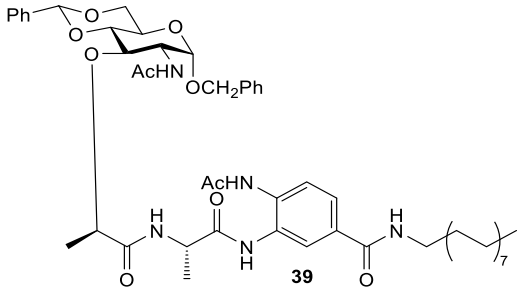

MALDI-MS m/z calcd for $C_{53}H_{75}N_5O_{10}$: 942.55; found: 964.54 [M+Na].

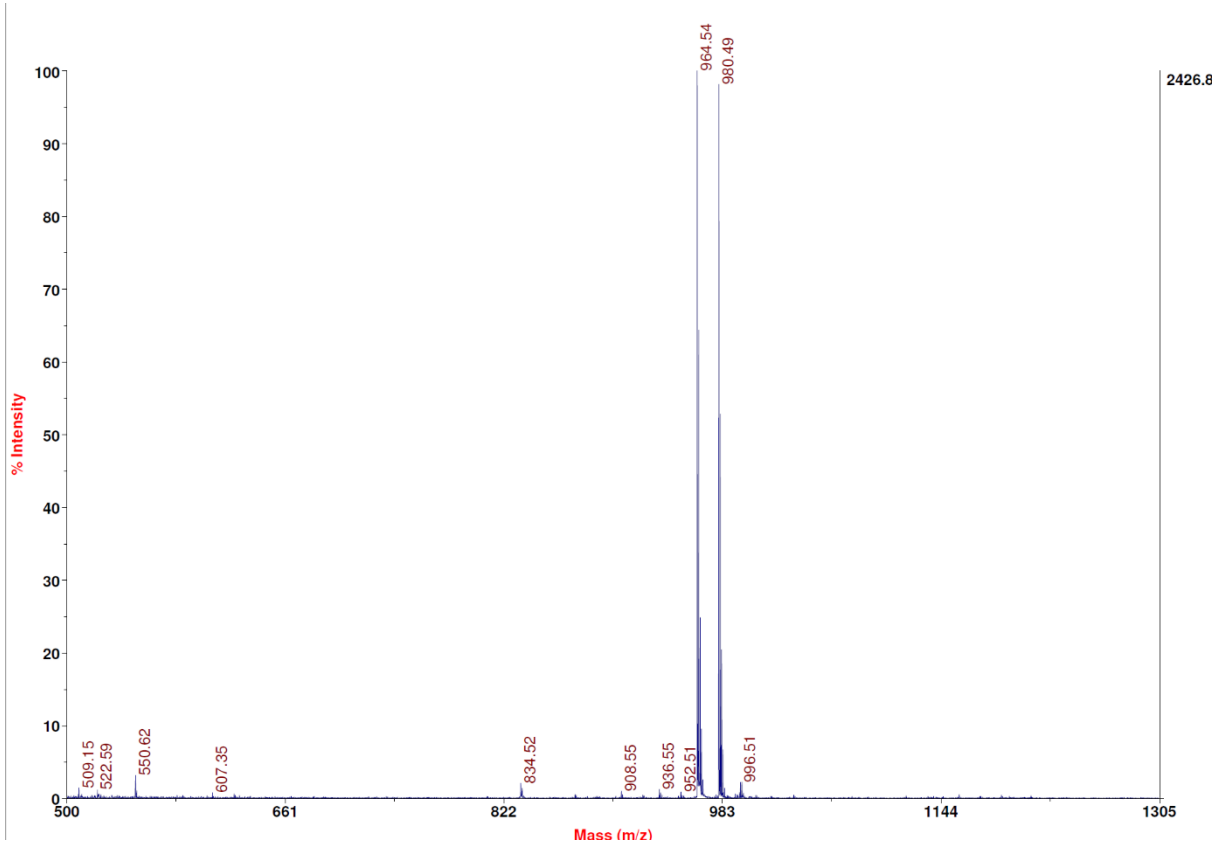

^{1}H NMR spectrum for compound **41** (500 MHz, chloroform-*d*)

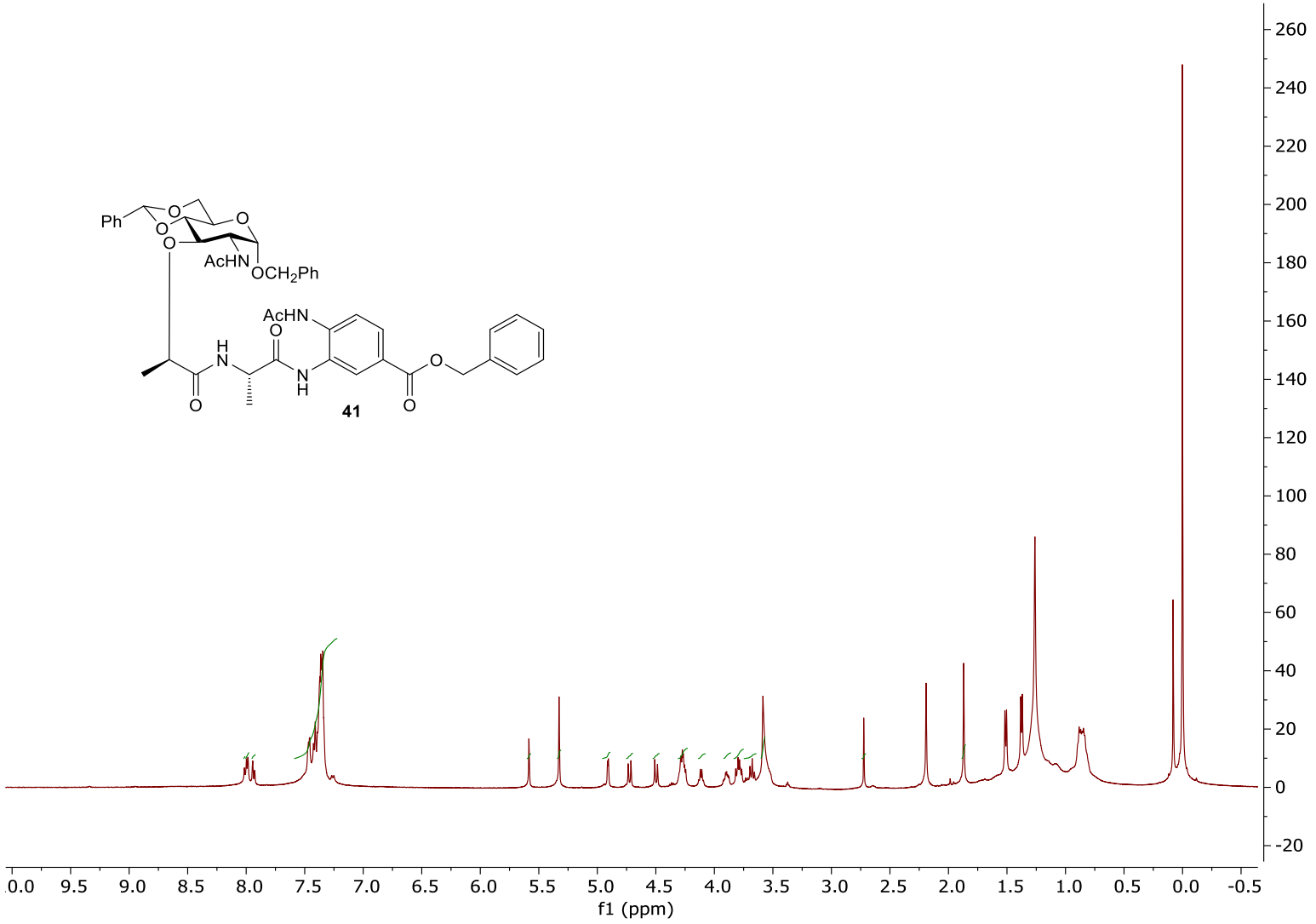

^{13}C NMR spectrum for compound **41** (126 MHz, chloroform-*d*)

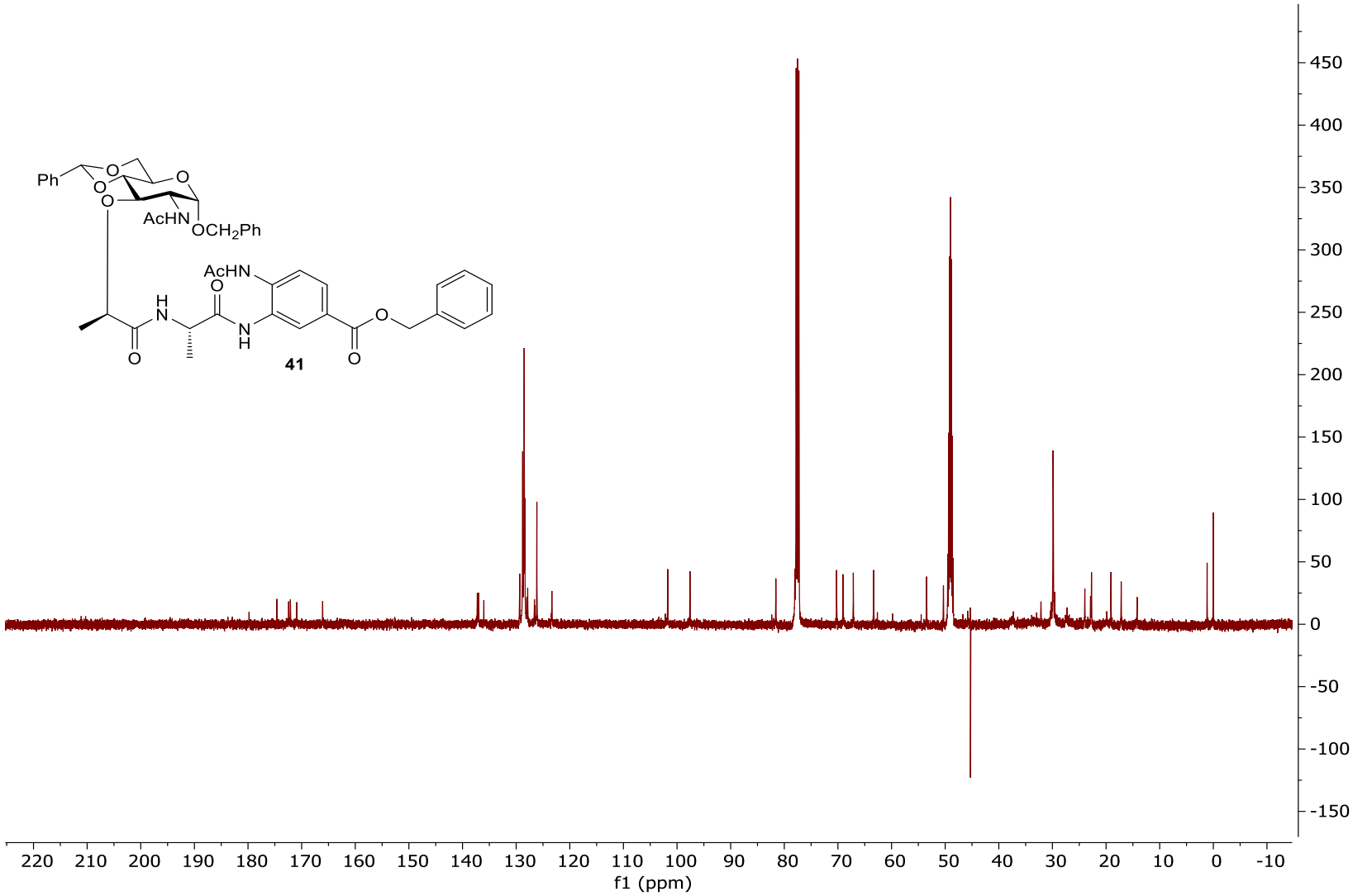

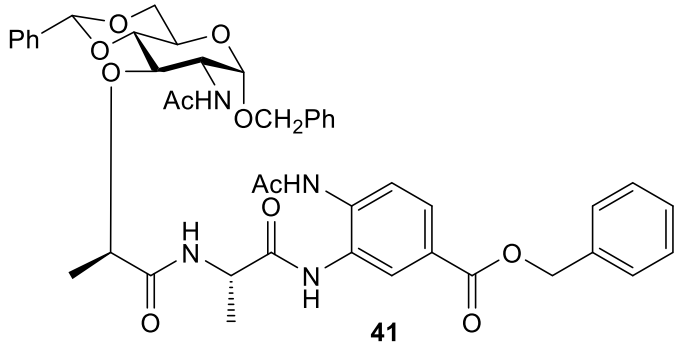

41

MALDI-MS m/z calcd for $C_{44}H_{48}N_4O_{11}$: 808.33; found: 831.33 [M+Na].

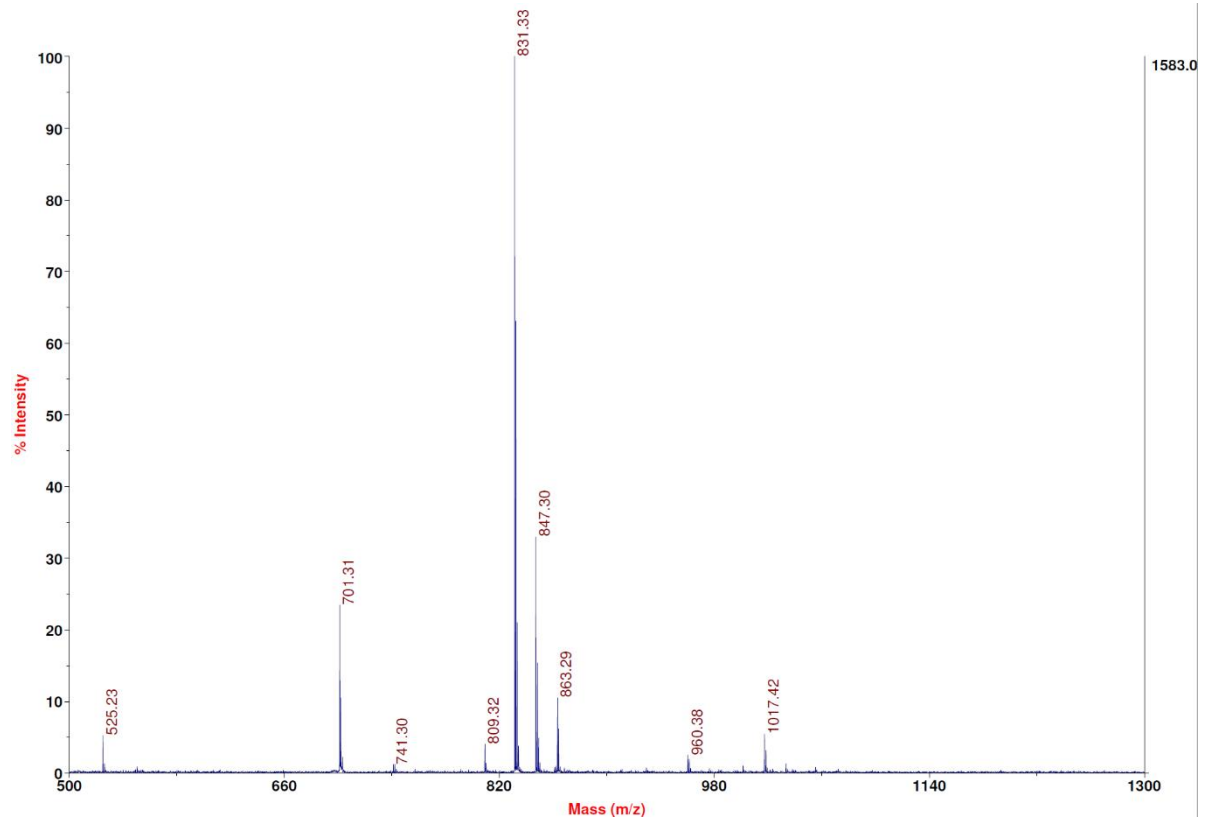

^{1}H NMR spectrum for compound **42** (500 MHz, methanol-d_4)

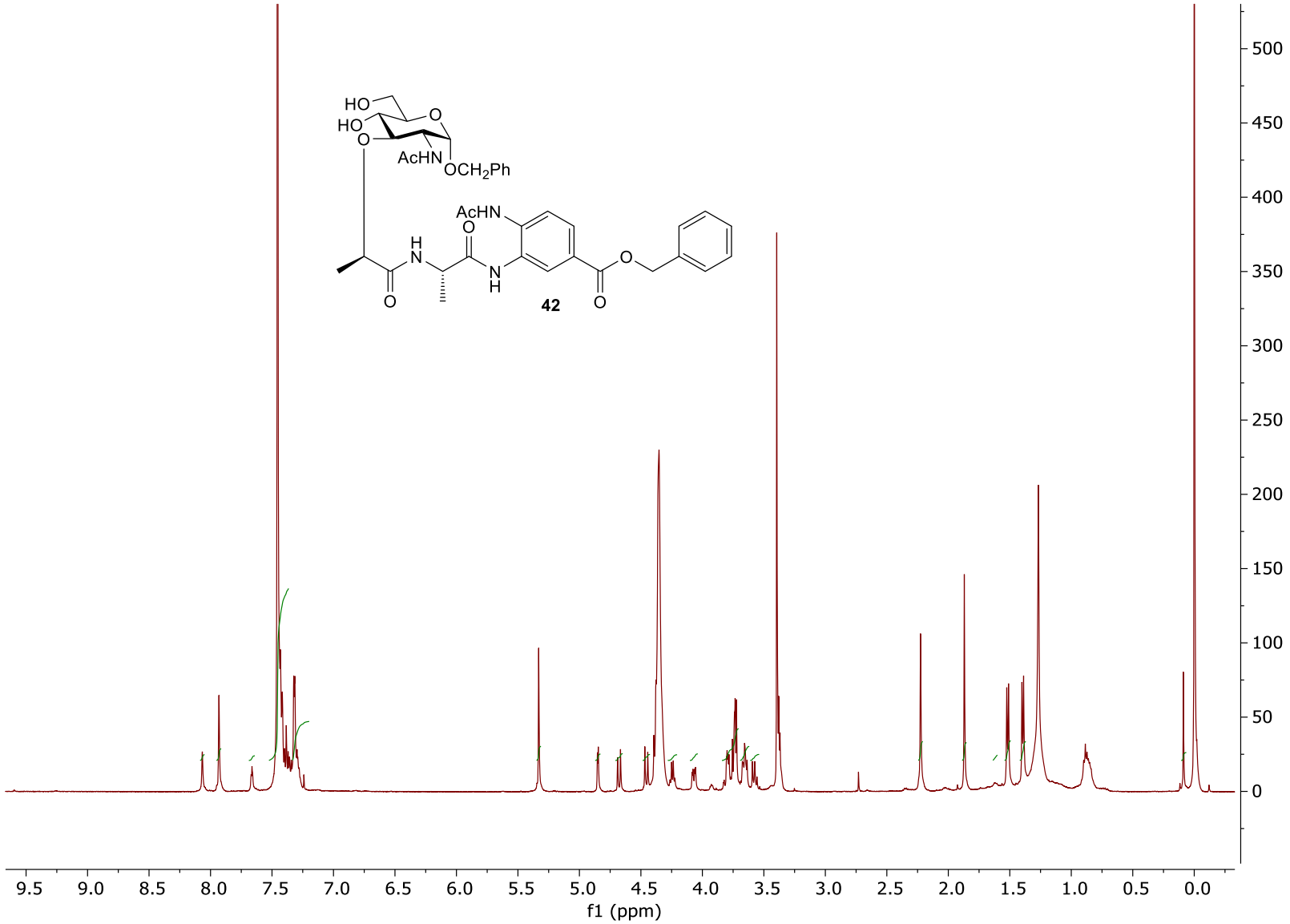

^{13}C NMR spectrum for compound **42** (126 MHz, chloroform-*d*/*methanol*-d_4)

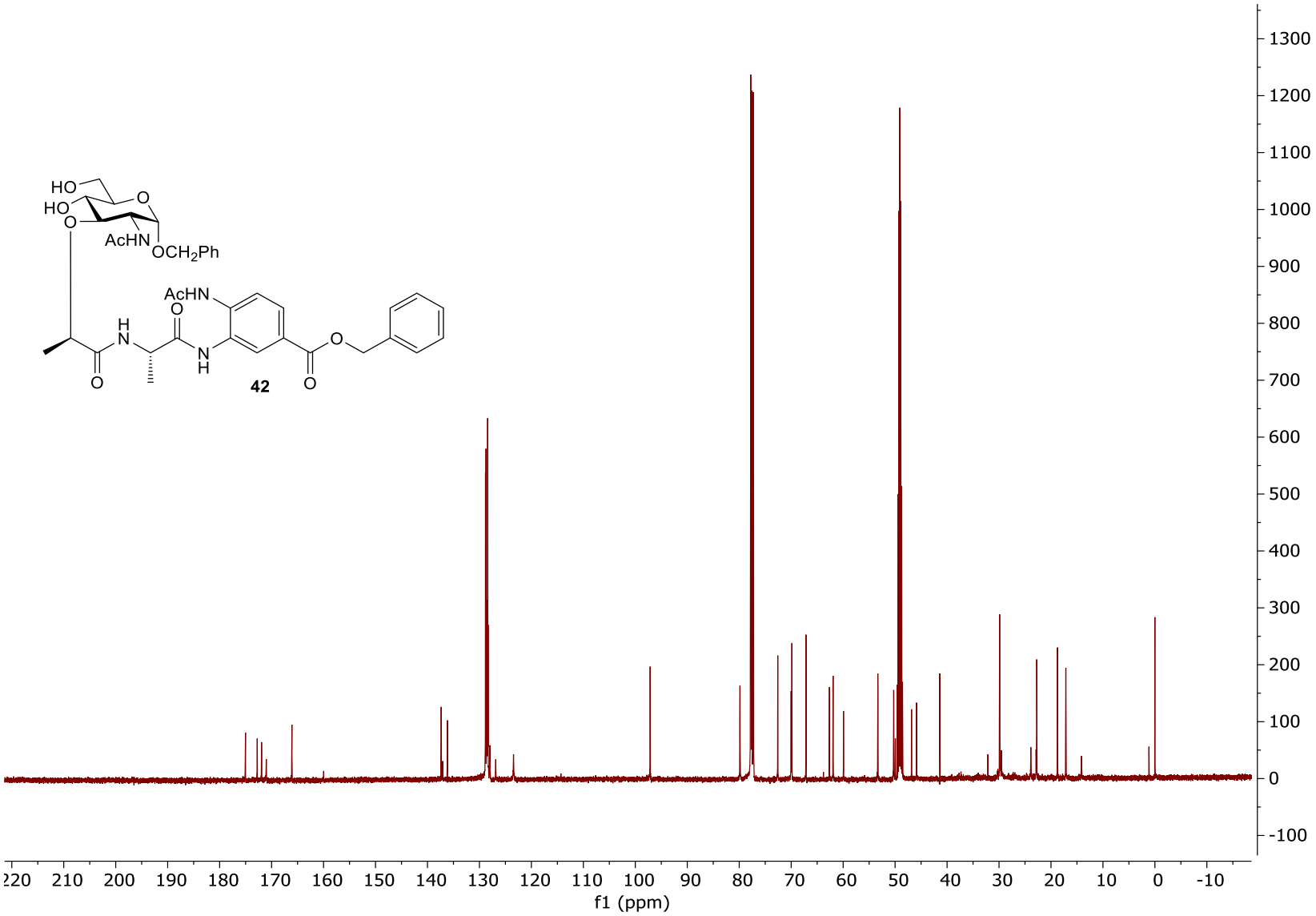

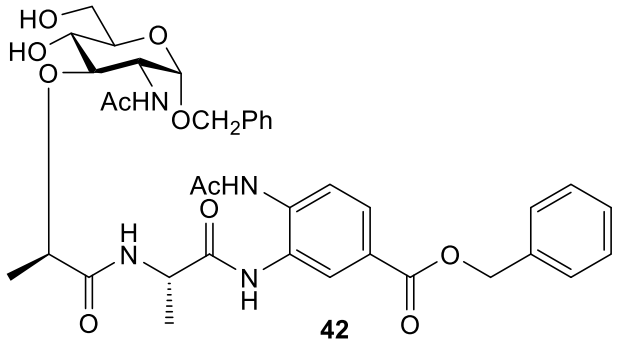

42

MALDI- MS m/z calcd for $C_{37}H_{44}N_4O_{11}$: 720.30; found: 721.33 [M+H], and 743.32 [M+Na].

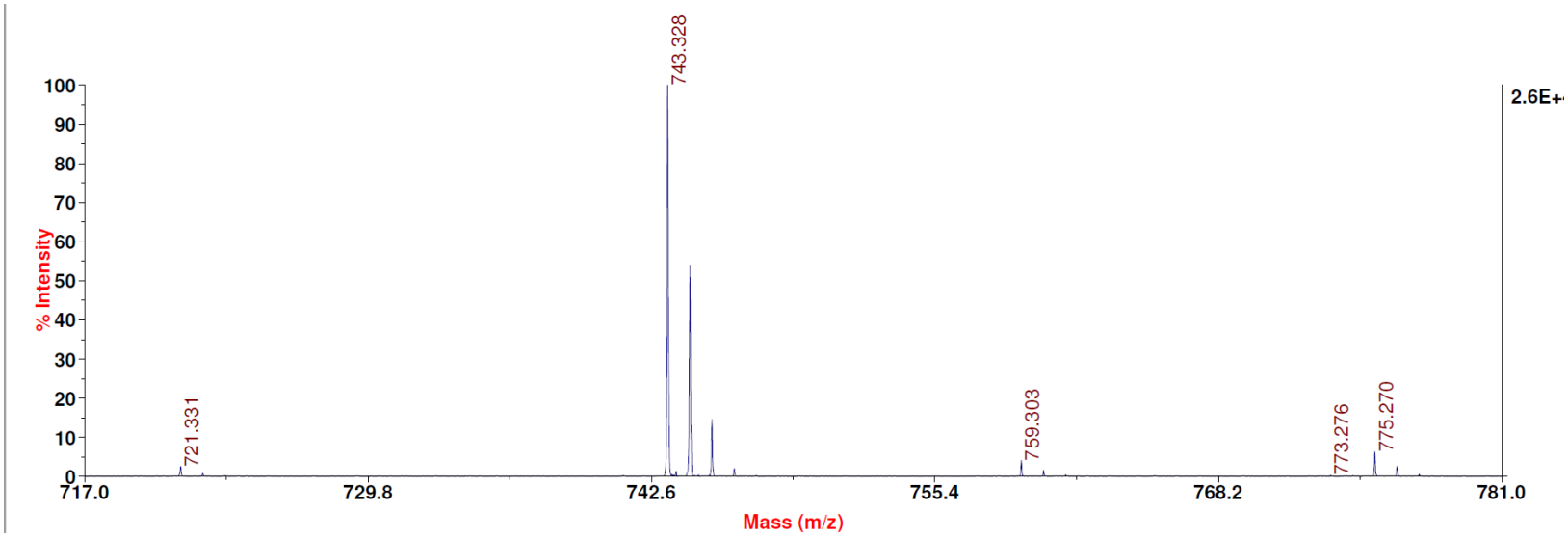

^{1}H NMR spectrum for the α-isomer of compound **4** (500 MHz, methanol-d_4)

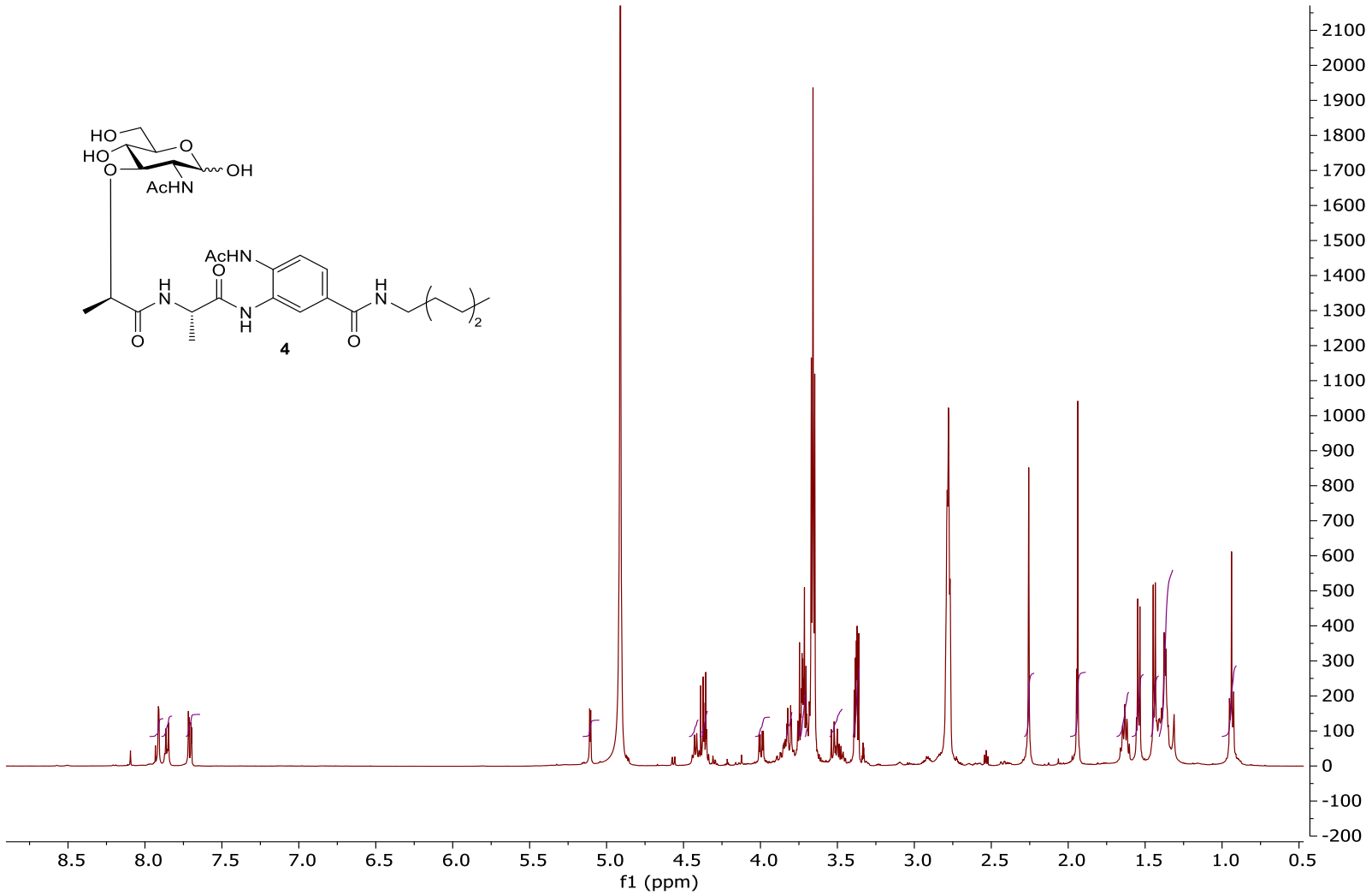

^{13}C NMR spectrum for the α-isomer of compound **4** (126 MHz, methanol-d_4)

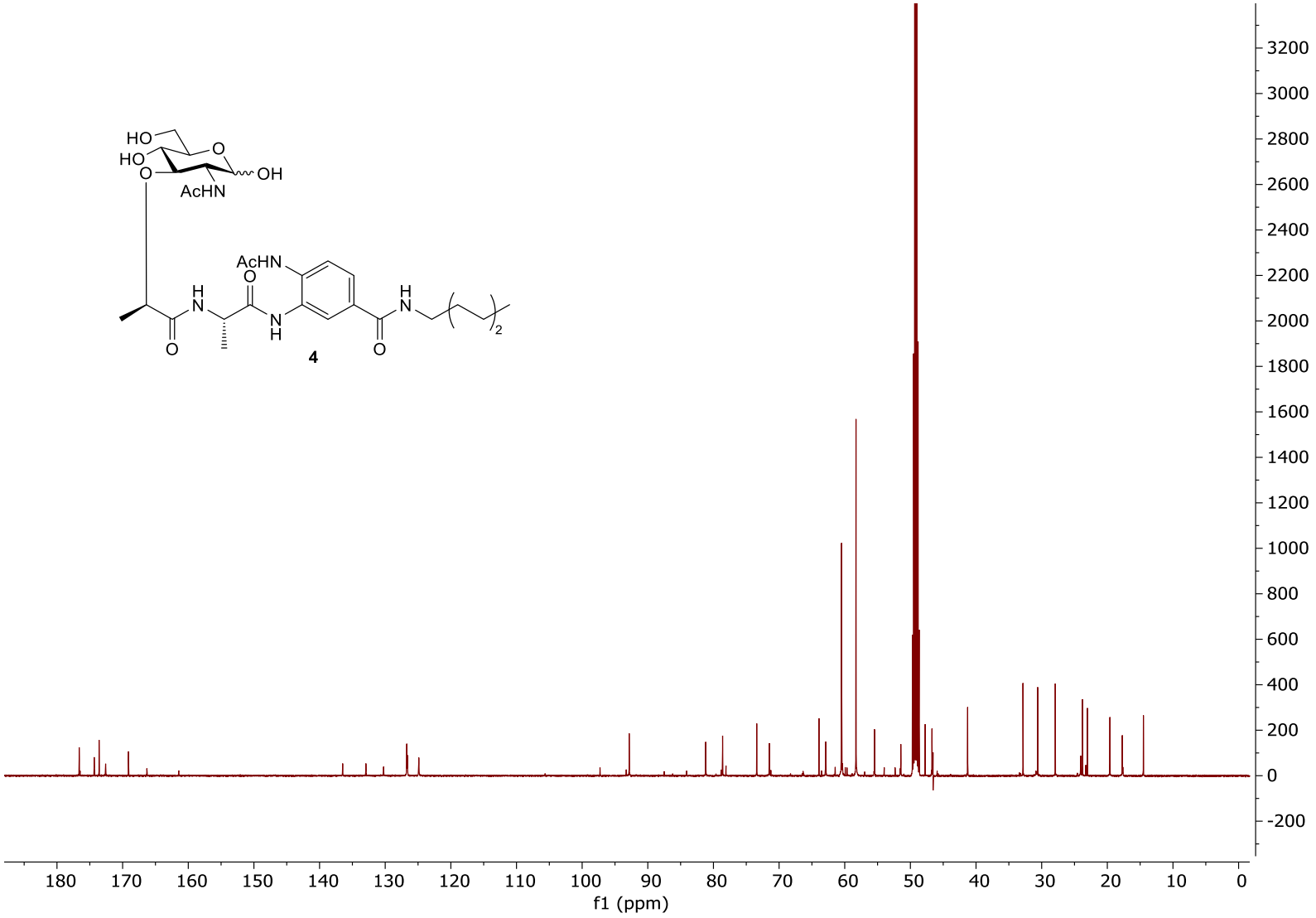

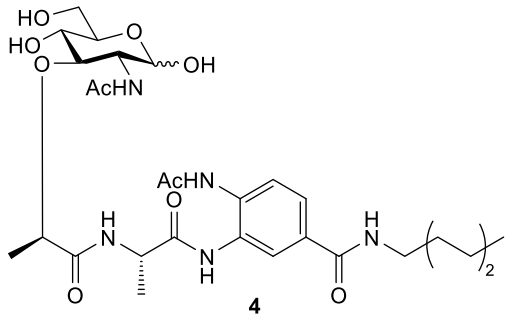

4

MALDI-MS m/z calcd for $C_{29}H_{45}N_5O_{10}$: 623.32; found: 646.33 [M+Na].

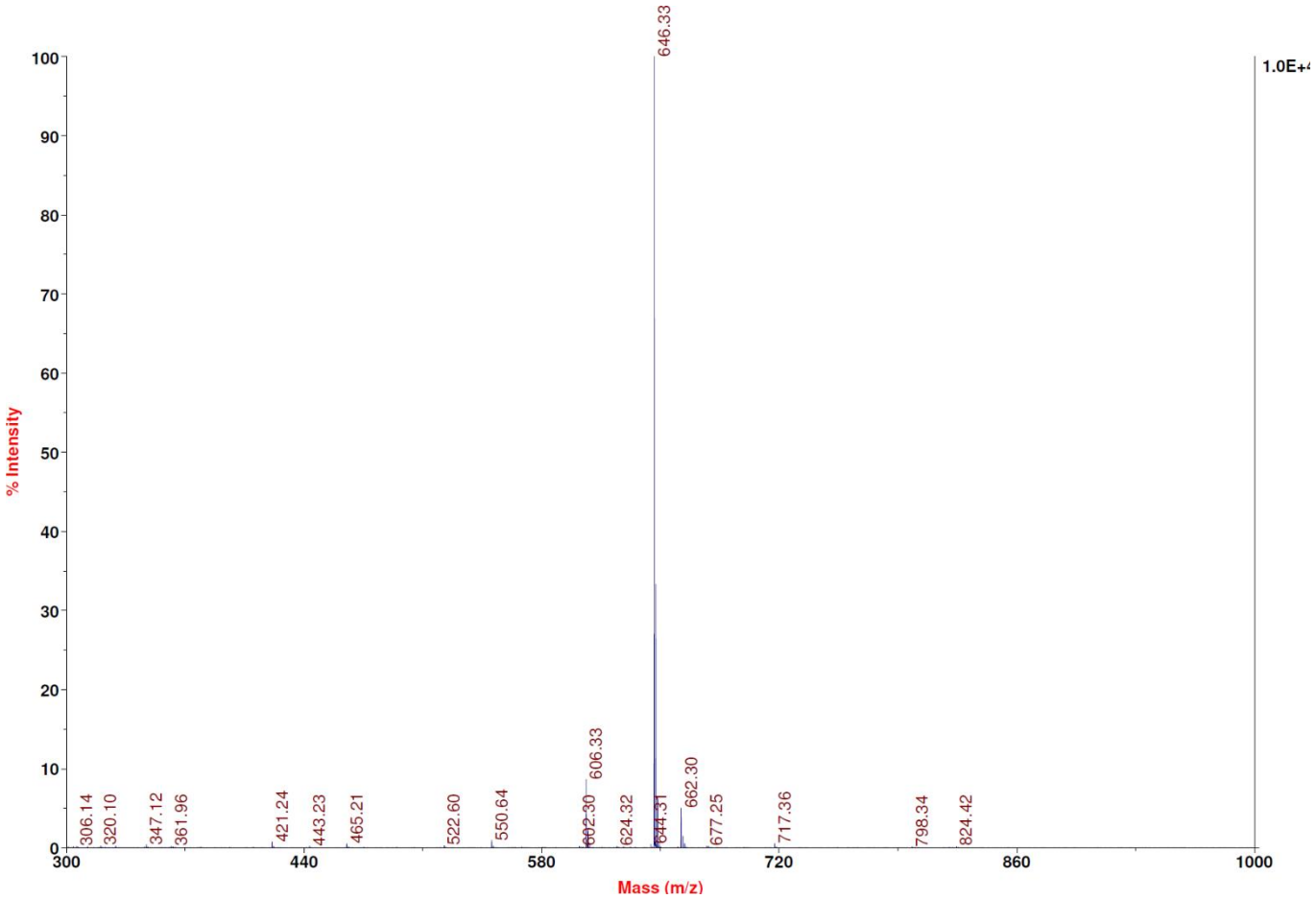

^{1}H NMR spectrum for the α-isomer of compound **5** (500 MHz, methanol-d_4)

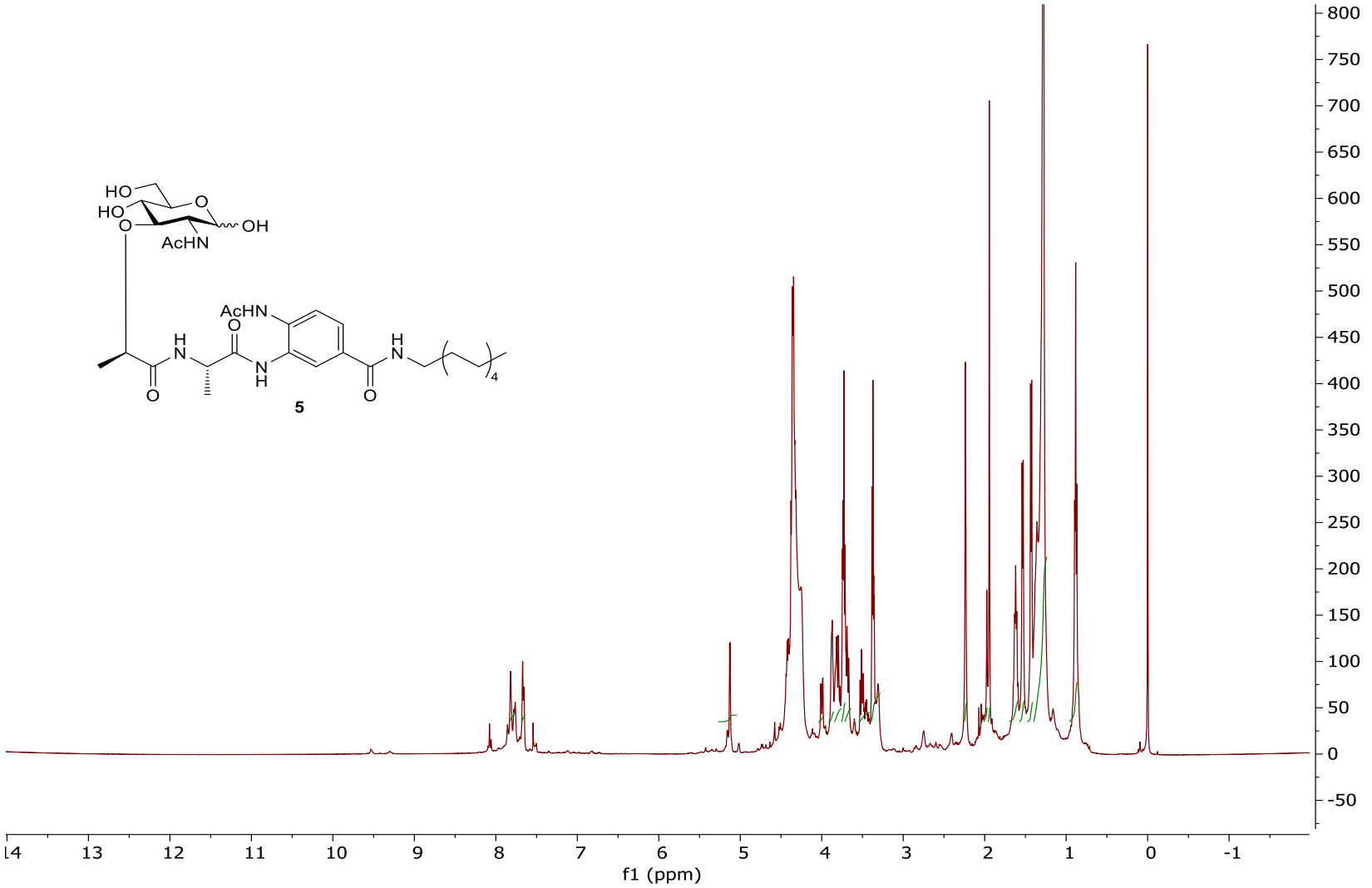

^{13}C NMR spectrum for the α-isomer of compound **5** (126 MHz, methanol-d_4)

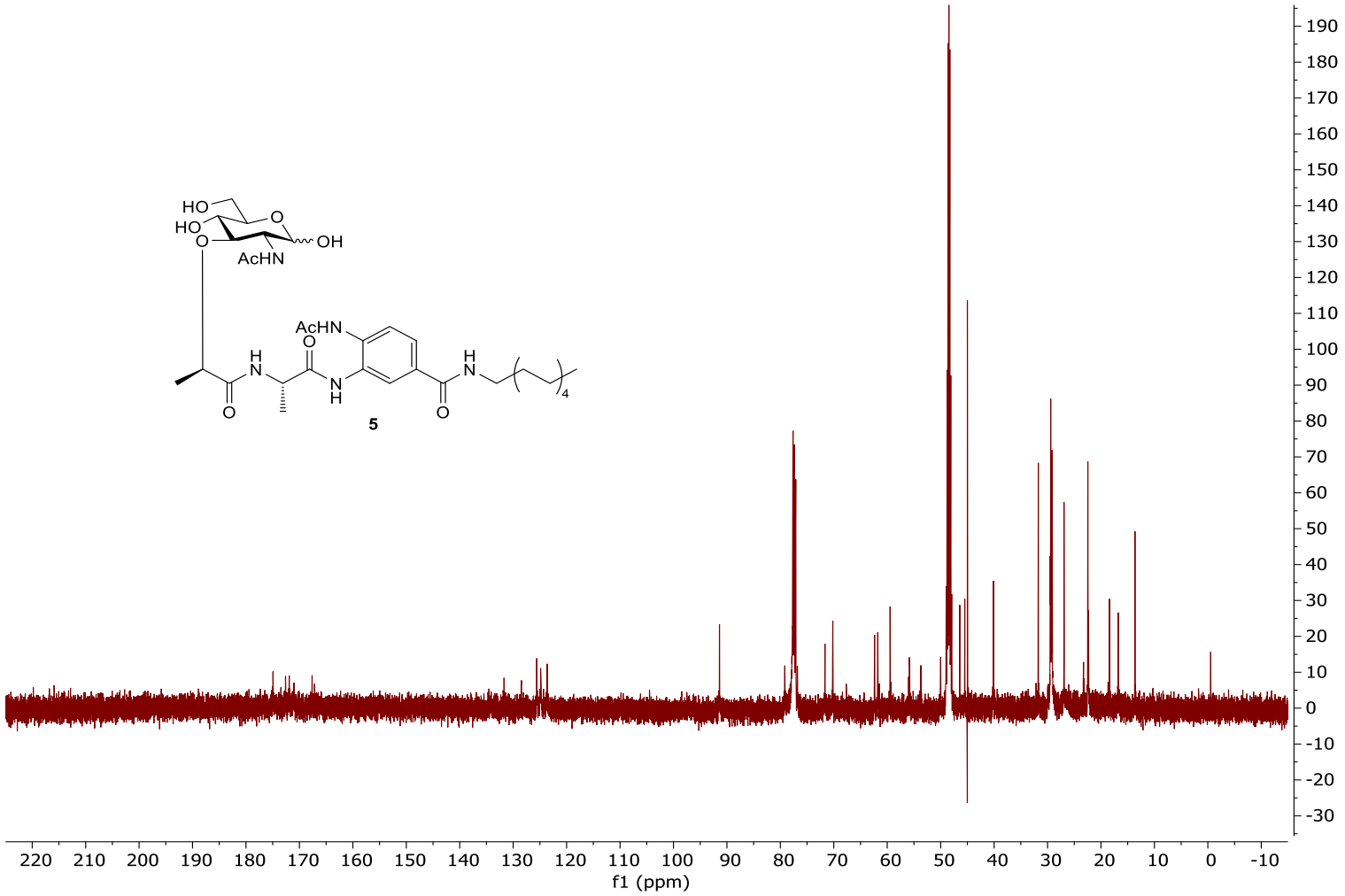

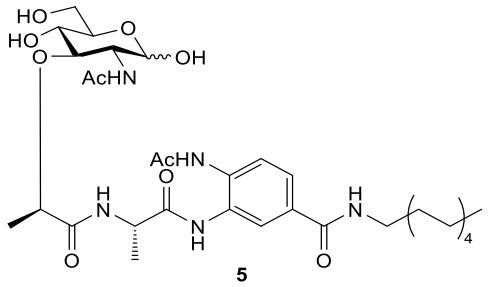

5

MALDI- MS m/z calcd for $C_{33}H_{53}N_5O_{10}$: 679.38; found: 702.39 [M+Na].

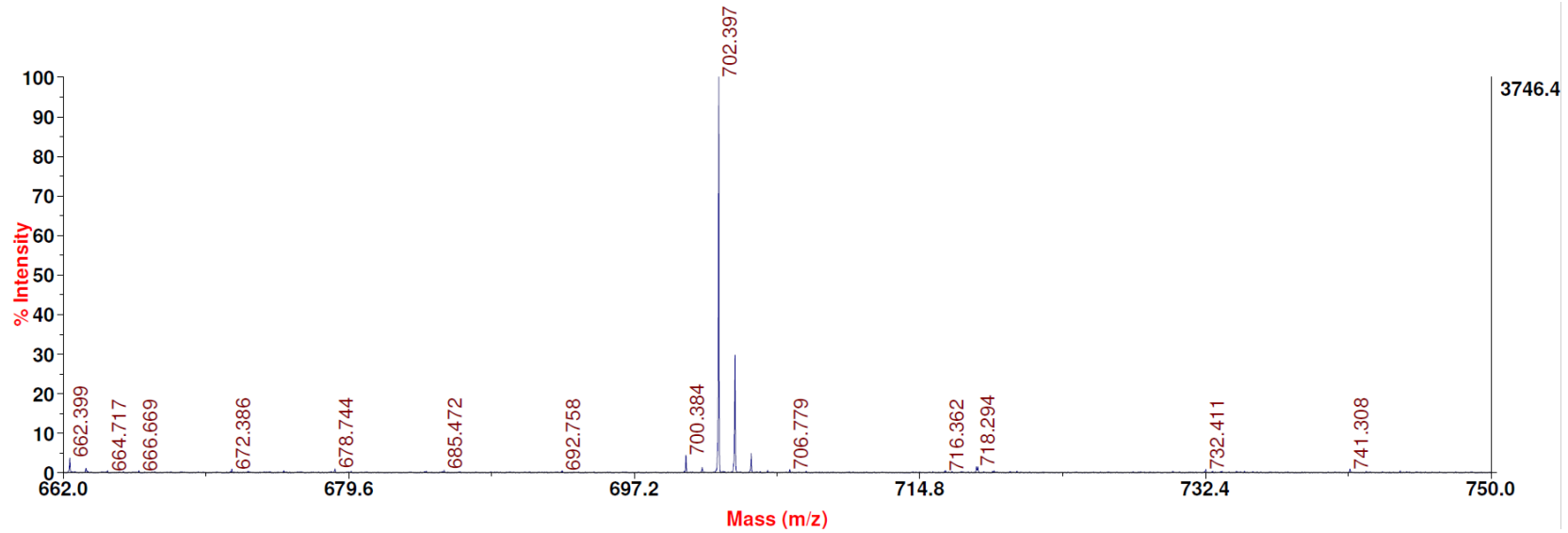

^{1}H NMR spectrum for the α-isomer of compound **6** (500 MHz, methanol-d_4)

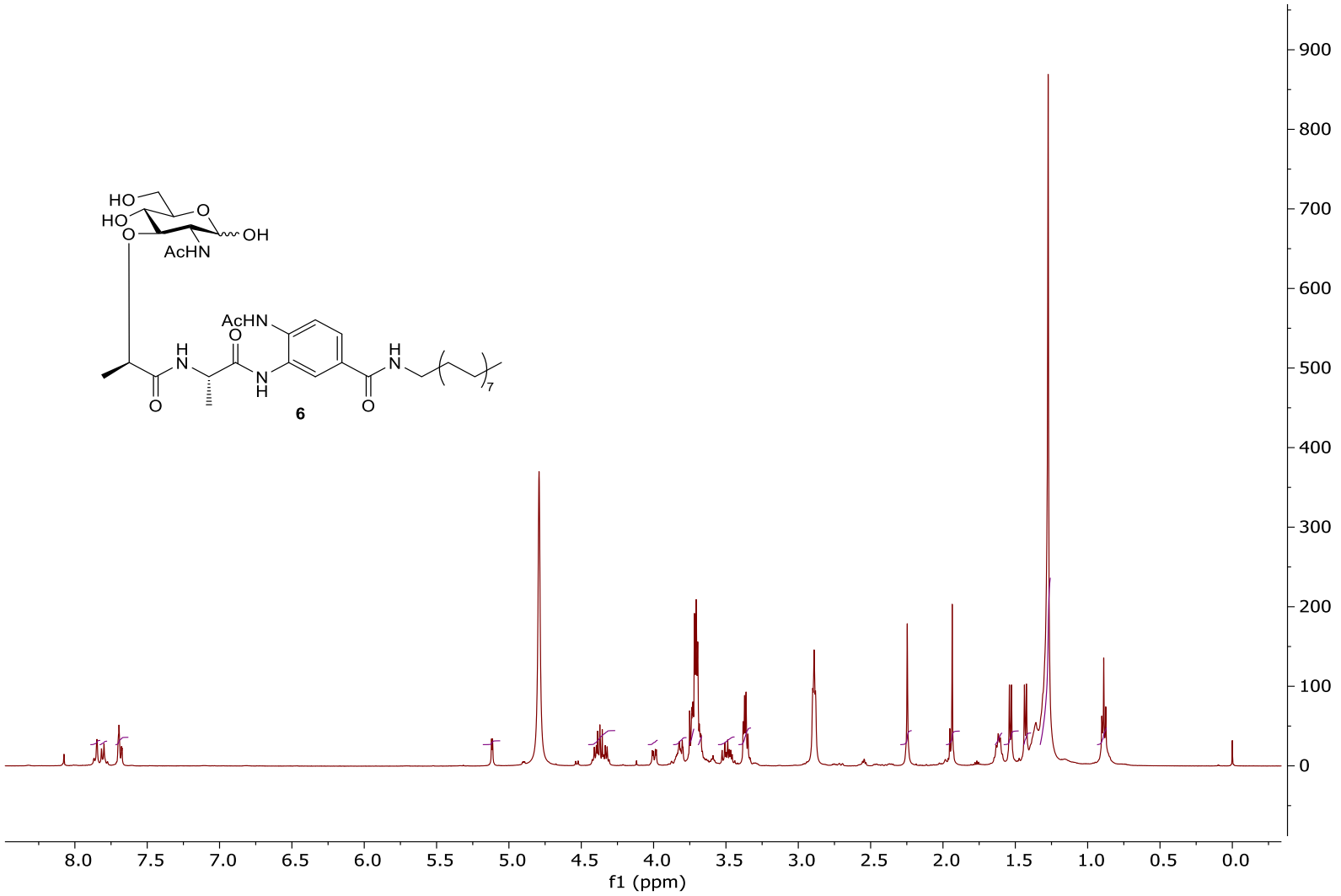

^{13}C NMR spectrum for the α-isomer of compound **6** (126 MHz, methanol-d_4)

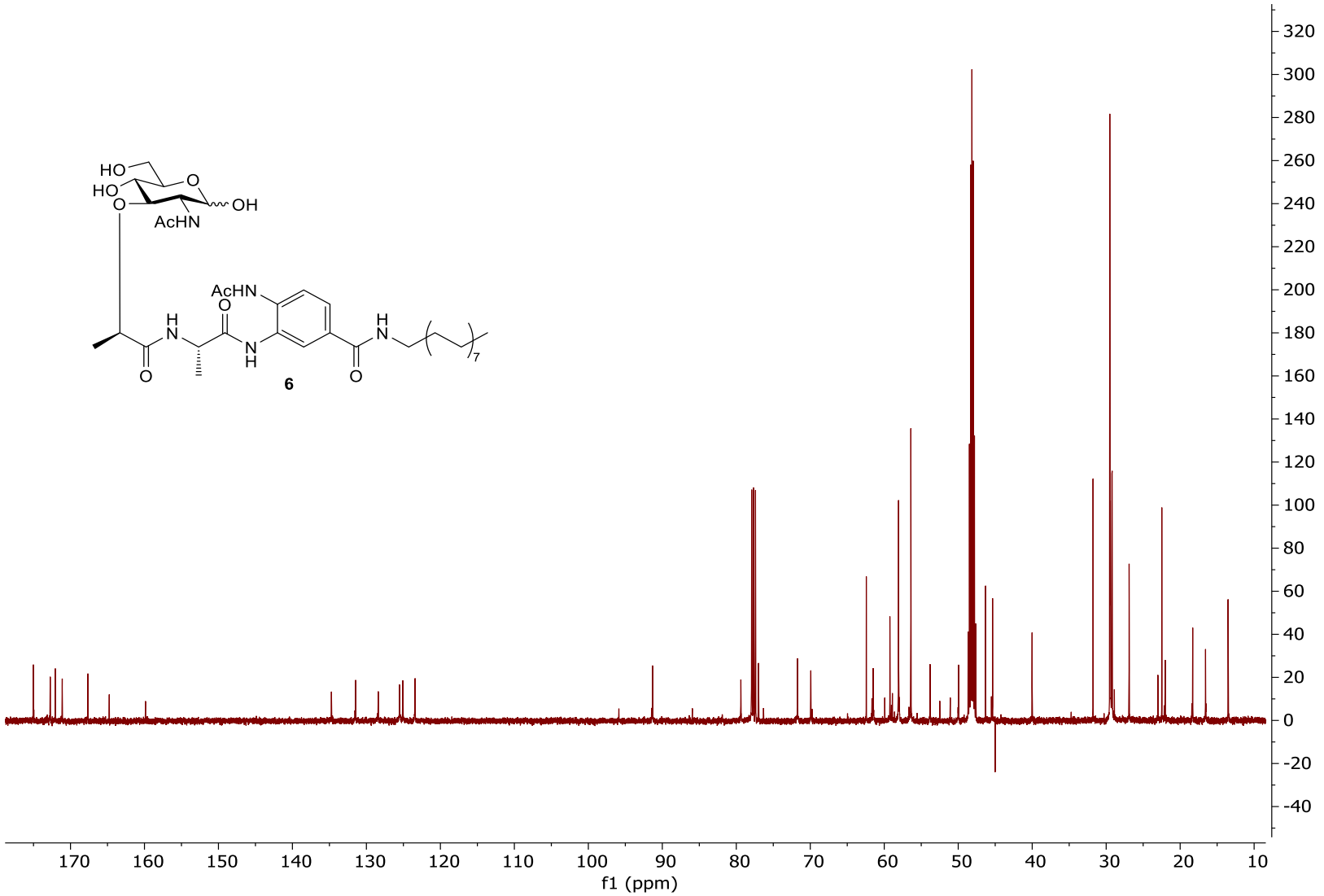

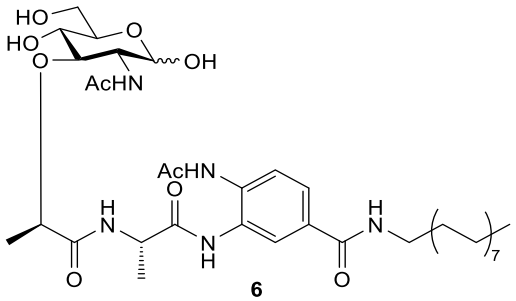

MALDI- MS m/z calcd for $C_{39}H_{65}N_5O_{10}$: 763.47; found: 786.49 [M+Na].

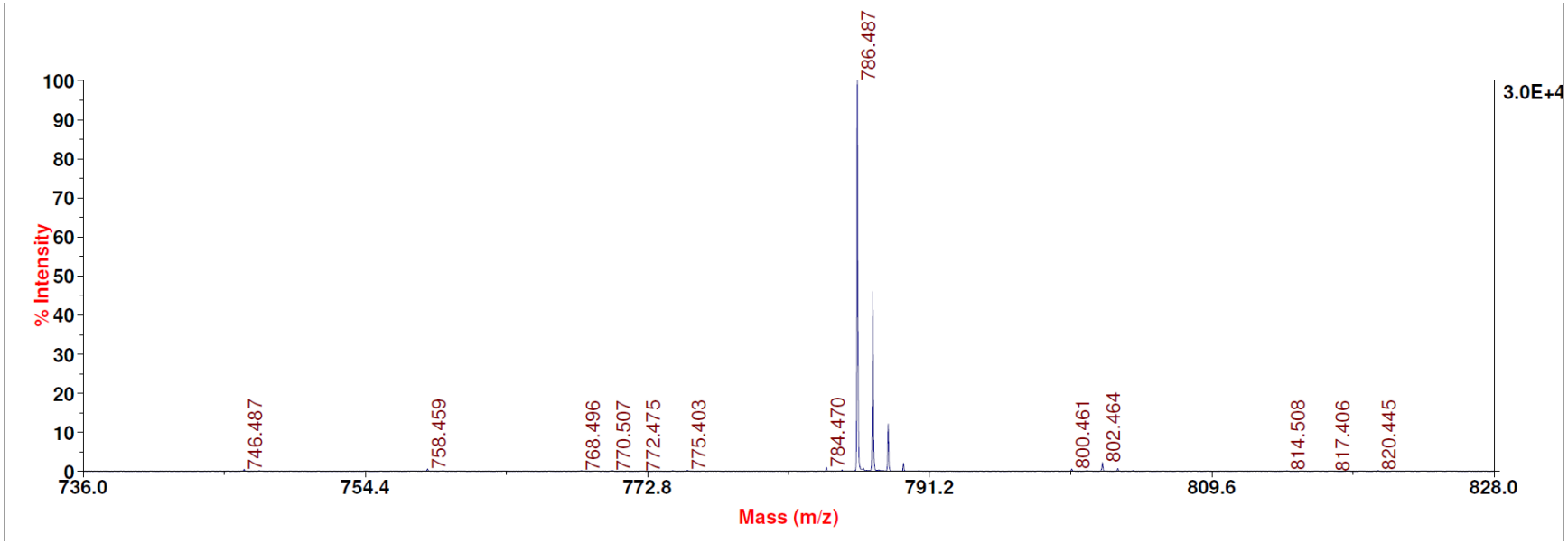

^{1}H NMR spectrum for compound **7** (500 MHz, methanol-d_4)

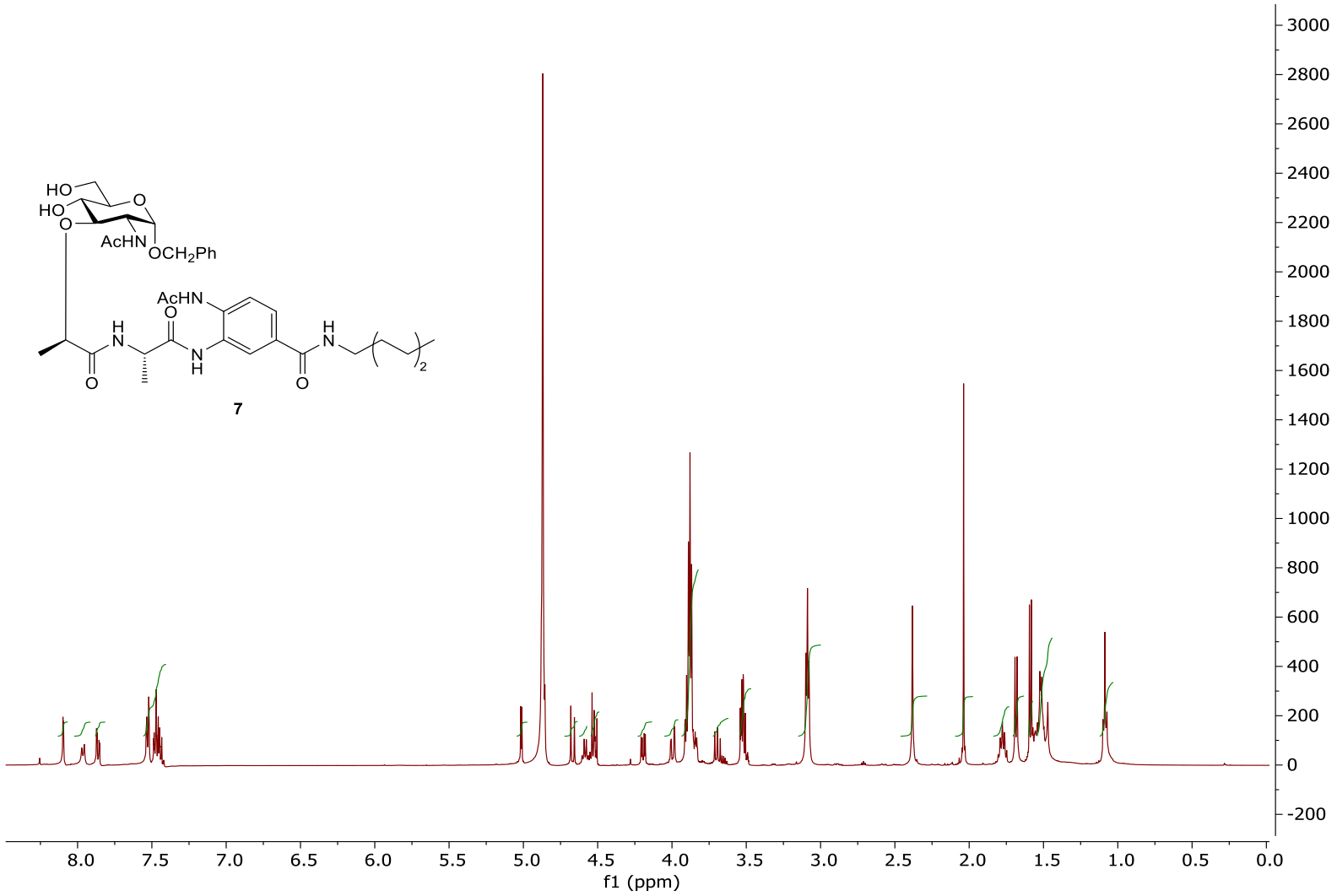

^{13}C NMR spectrum for compound **7** (126 MHz, methanol-d_4)

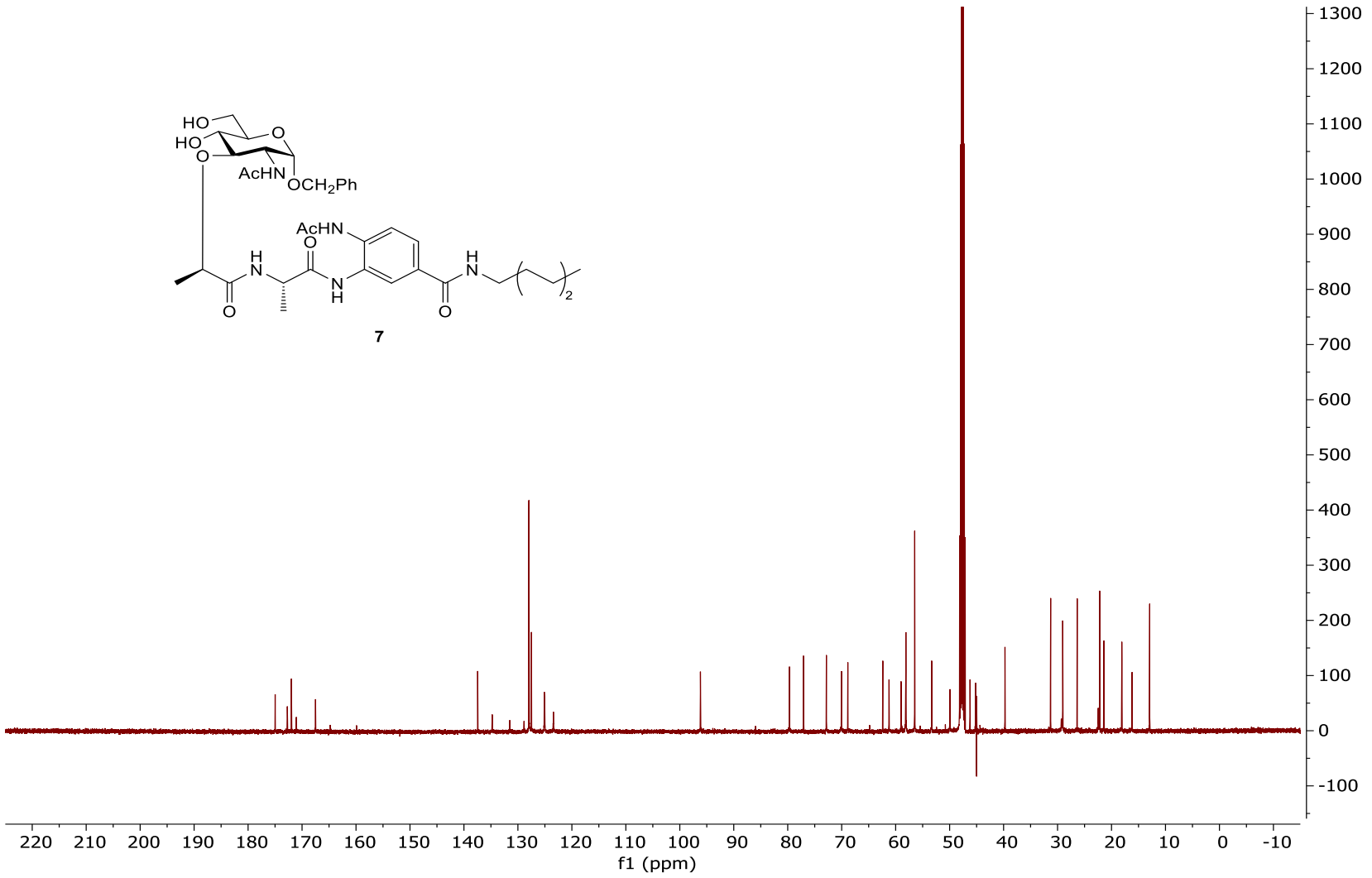

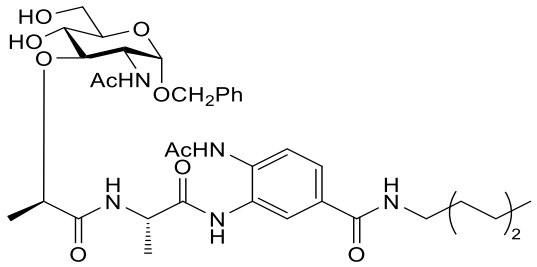

7

MALDI-MS m/z calcd for $C_{36}H_{51}N_5O_{10}$: 713.36; found: 736.35 [M+Na].

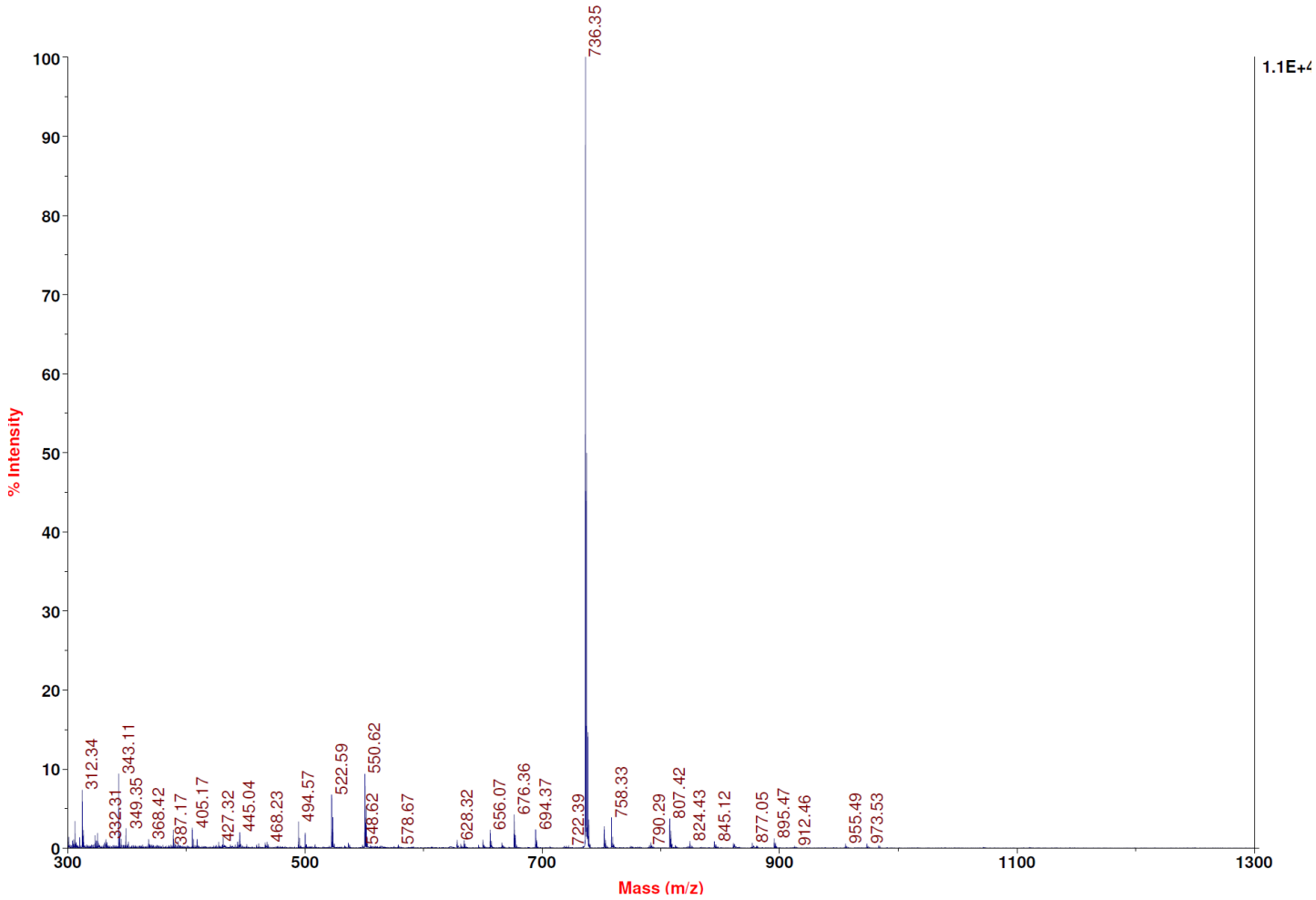

^{1}H NMR spectrum for compound **8** (500 MHz, Methanol-d_4)

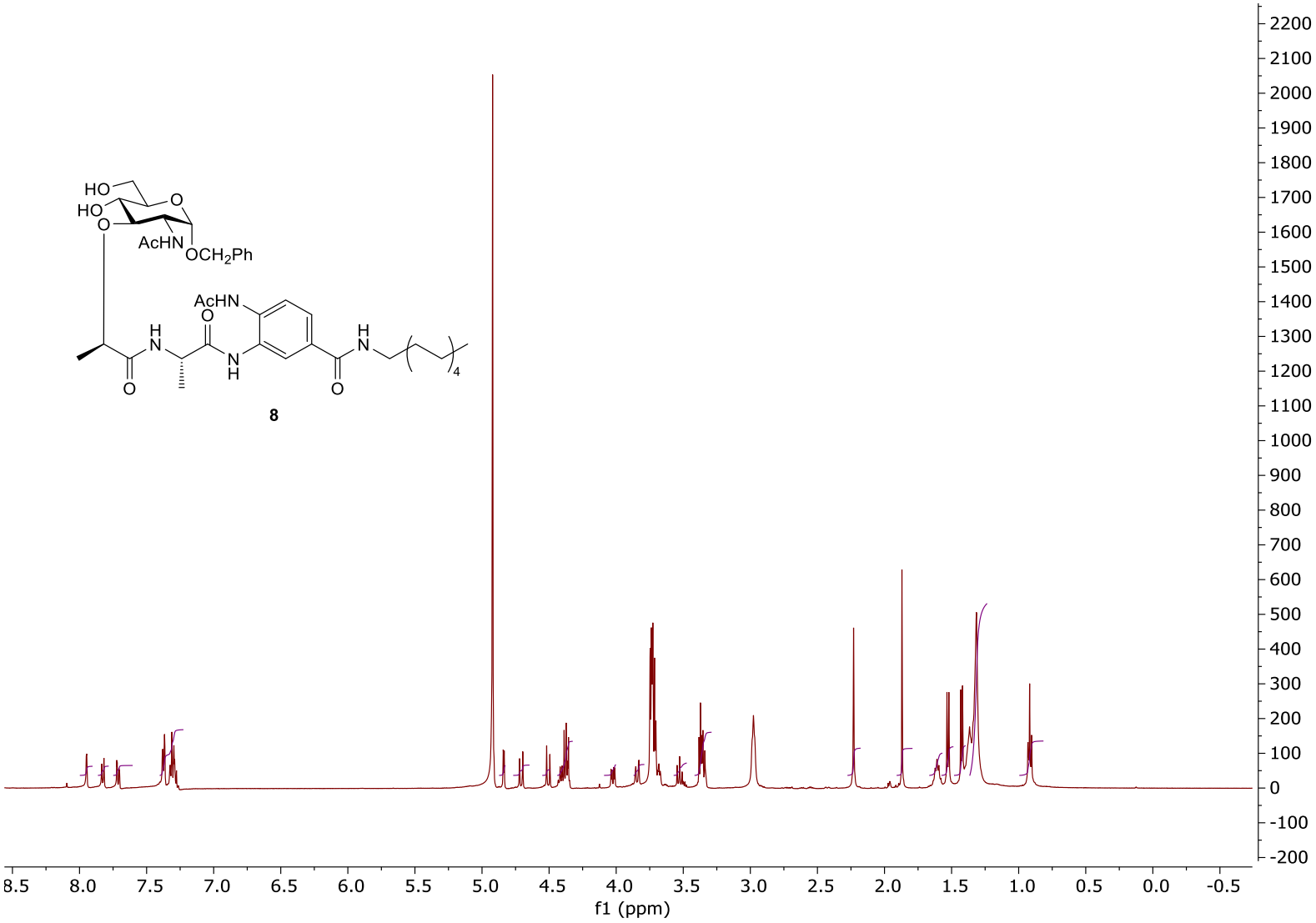

^{13}C NMR spectrum for compound **8** (126 MHz, Methanol-d_4)

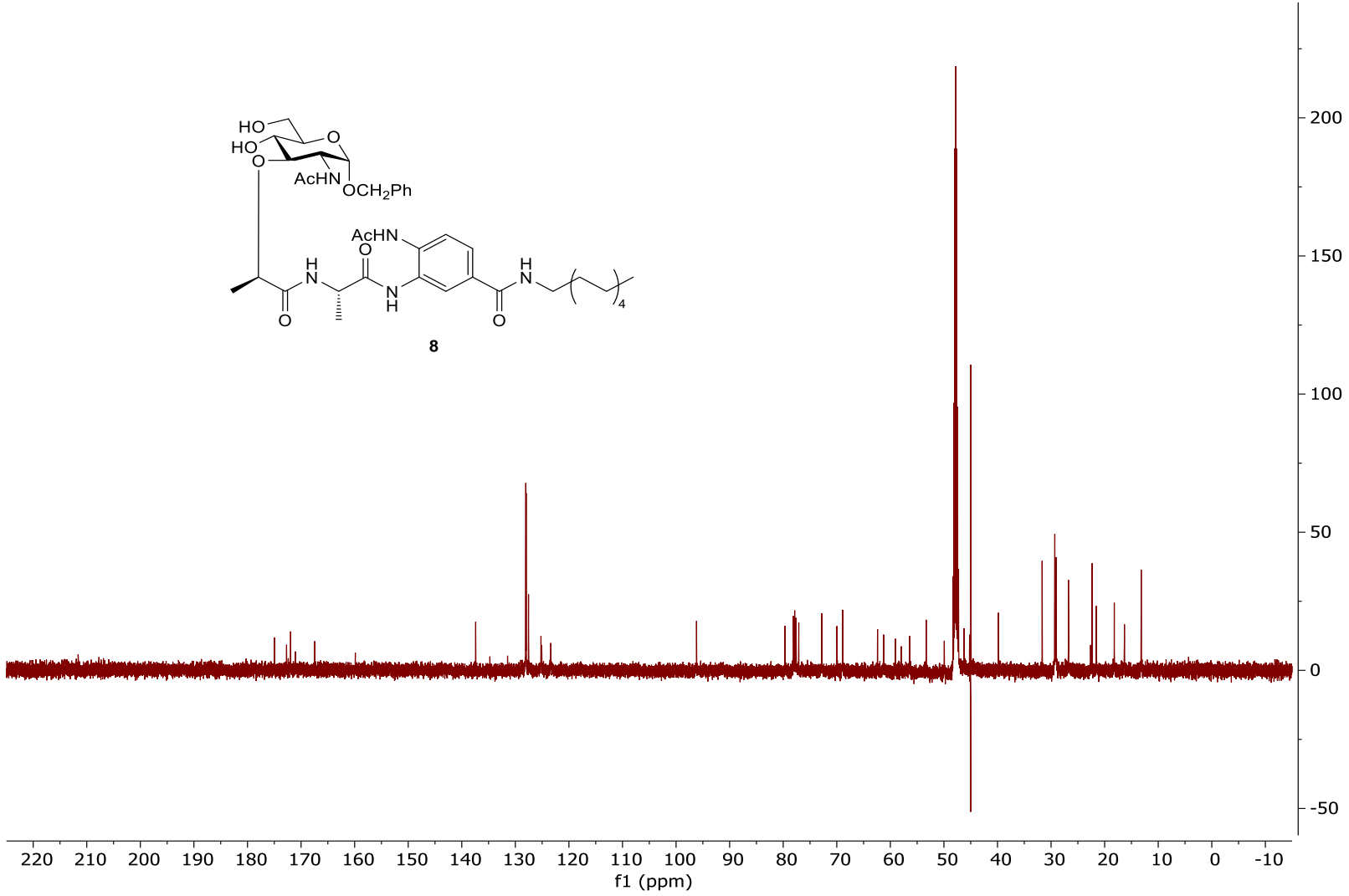

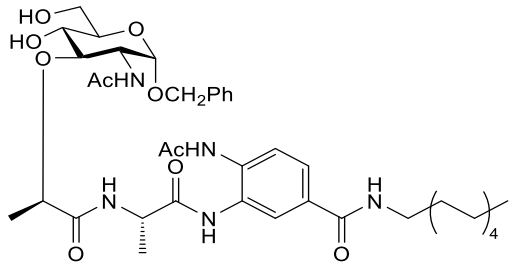

8

MALDI- MS m/z calcd for $C_{40}H_{59}N_5O_{10}$: 769.43; found: 792.44 [M+Na].

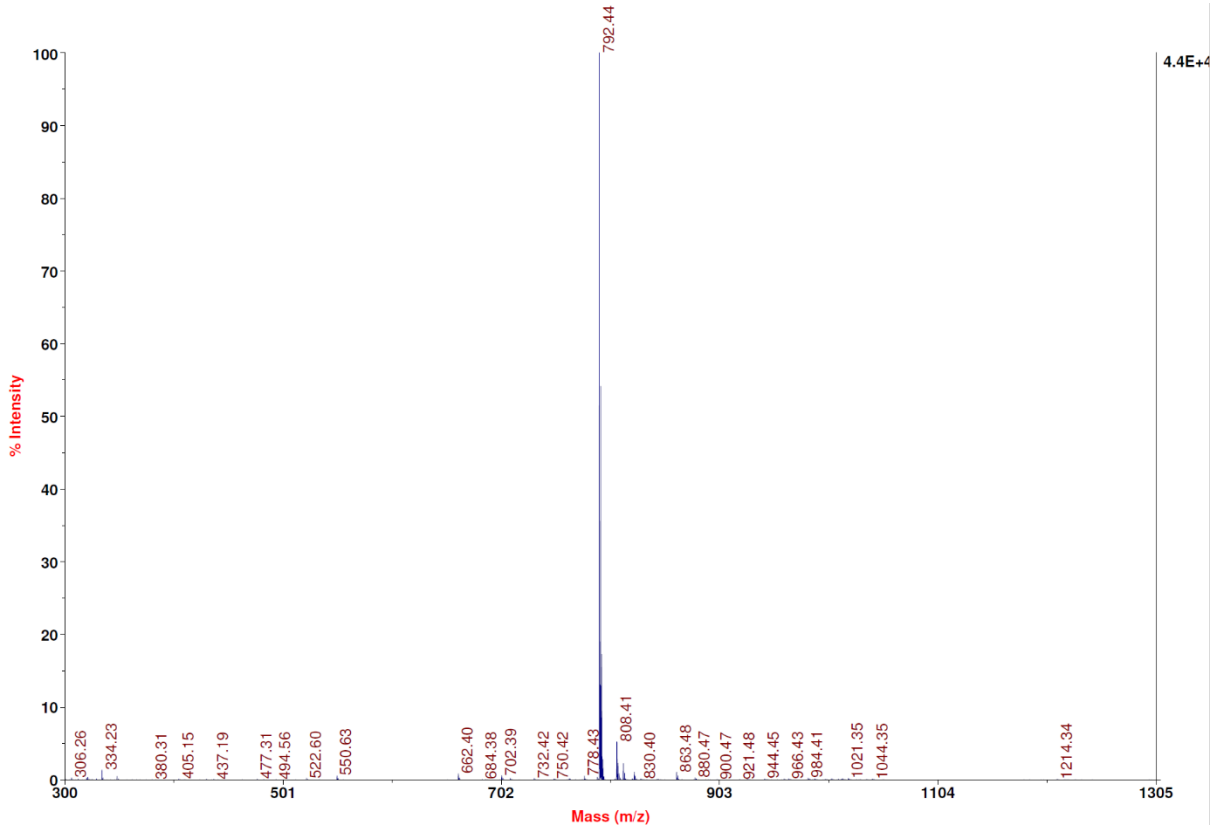

^{1}H NMR spectrum for compound **9** (500 MHz, methanol-d_4)

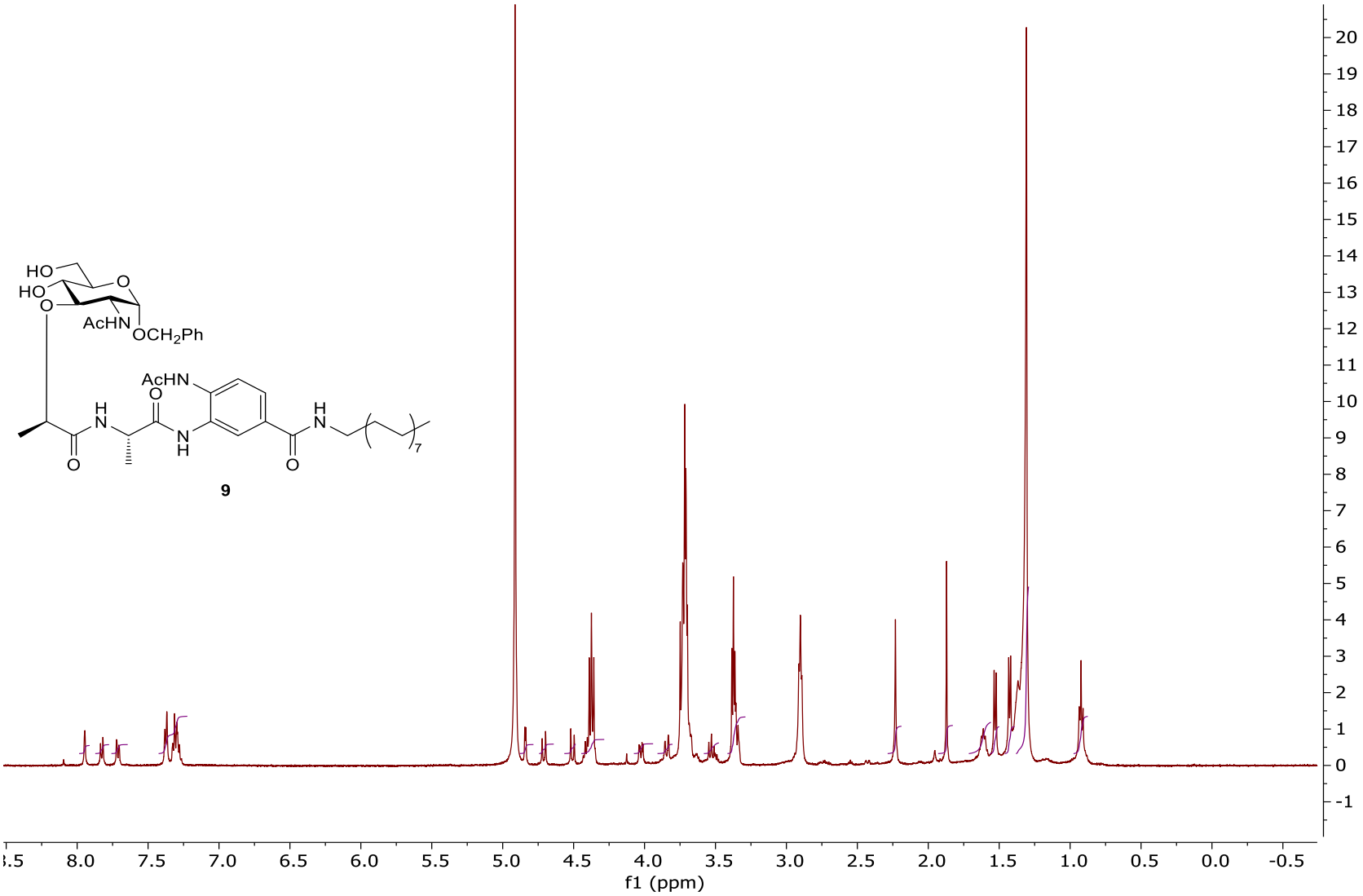

^{13}C NMR spectrum for compound **9** (126 MHz, methanol-d_4)

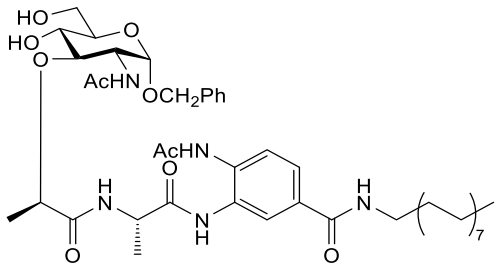

9

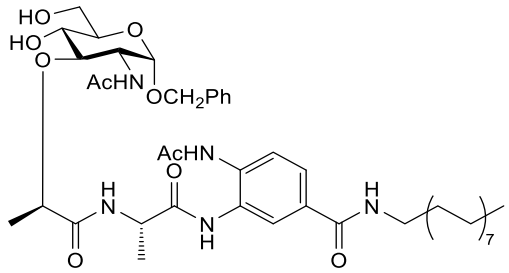

9

MALDI-MS m/z calcd for $C_{46}H_{71}N_5O_{10}$: 854.099; found: 876.52 [M+Na].